

Development of Advanced Methods for Evaluating Grid Stability Impacts by HVAC- and HVDC- Interconnected Offshore Wind Power Plants

Final Report

Prepared for:

National Offshore Wind Research and Development Consortium

Albany, NY

Julian Fraize

Program Manager

Prepared by:

NREL

Golden, CO

Vahan Gevorgian
Chief Engineer

Shahil Shah
Principal Engineer

Weihang Yan
Sr. Engineer

Pranav Sharma
Sr. Engineer

EPRI

Palo Alto, CA

S. Konstantinopoulos
EPRI Staff IV

S. Uppalapati
Sr. Project Engineer

A. Del Rosso
Program Manager

Notice

This report was prepared by NREL in collaboration with EPRI, in the course of performing work contracted for and sponsored by the National Offshore Wind Research and Consortium (NOWRDC), New York State Energy Research and Development Authority (NYSERDA), and the U.S. Department of Energy (hereafter the “Sponsors”). The opinions expressed in this report do not necessarily reflect those of the Sponsors or the State of New York, and reference to any specific product, service, process, or method does not constitute an implied or expressed recommendation or endorsement of it. Further, the Sponsors, the State of New York, and the contractor make no warranties or representations, expressed or implied, as to the fitness for particular purpose or merchantability of any product, apparatus, or service, or the usefulness, completeness, or accuracy of any processes, methods, or other information contained, described, disclosed, or referred to in this report. The Sponsors, the State of New York, and the contractor make no representation that the use of any product, apparatus, process, method, or other information will not infringe privately owned rights and will assume no liability for any loss, injury, or damage resulting from, or occurring in connection with, the use of information contained, described, disclosed, or referred to in this report.

NYSERDA makes every effort to provide accurate information about copyright owners and related matters in the reports it publishes. Contractors are responsible for determining and satisfying copyright or other use restrictions regarding the content of reports that they write, in compliance with NYSERDA’s policies and federal law. If you are the copyright owner and believe a NYSERDA report has not properly attributed your work to you or has used it without permission, please email print@nyserda.ny.gov.

Information contained in this document, such as web page addresses, is current at the time of publication.

Abstract

The main objective of this project was to develop advanced modeling, control, stability monitoring, and protection methods for the analysis and mitigation of dynamic stability problems in offshore wind power plants (WPPs) interconnected with onshore power systems via high-voltage alternating current (HVAC) or high-voltage direct current (HVDC) submarine transmission with strong and weak points of interconnections (POIs) to onshore power grids. This project is aimed at removing barriers for the reliable integration of large levels of offshore wind power. It uses the strategy of wide-scale dissemination of project results among all stakeholder groups, including reliability organizations, system operators, regulators, utilities, equipment vendors, project developers, and academia. The PSS/E-PSCAD co-simulation platform for offshore wind power analysis combined with the National Renewable Energy Laboratory's (NREL's) Grid Impedance Scan Tool (GIST) platform is instrumental for removing barriers to the reliable integration of large levels of offshore wind power. The tool application was demonstrated for various use cases using offshore WPP POIs in three different interconnections: PJM, New York Independent System Operator (NYISO), and Independent System Operator New England (ISO-NE). The tool can be used for HVDC- and HVAC-interconnected offshore WPPs and allows evaluating transient and dynamic behavior.

In this project, the NREL team developed a co-simulation platform that combines:

- PSS/E – positive-sequence transmission planning and analysis software by Siemens
- PSCAD – electromagnetic transient (EMT) simulation software
- E-TRAN – a software tool to interface positive-sequence phasor models in PSS/E of a large power system, such as the Eastern Interconnection, with the EMT models in PSCAD of power electronics generators, such as an offshore WPP with HVAC or HVDC transmission to the grid
- GIST – (PSCAD-based) developed by NREL.

The platform combines the strengths of three commercial software tools (PSS/E, PSCAD, and E-TRAN) and the NREL-developed GIST to accurately represent small-signal stability, dynamic and transient behavior, and instabilities and control interactions that can exist in offshore WPPs, between several WPPs, and between offshore WPPs and the onshore grid. The use of the platform was demonstrated in several cases for three independent system operators using models of offshore WPPs with HVAC and HVDC interconnection. POIs with low short-circuit ratios were selected for the model testing to demonstrate possible instabilities. Simulations conducted in this project are for demonstrating the capabilities of the co-simulation platform only and are not classified as integration studies. The platform can be used later by any stakeholder to conduct detailed integration studies for any offshore project or for studies to identify system-level reliability impacts of clusters of offshore WPPs using different transmission configurations.

The NREL team conducted testing on a utility-scale wind turbine generator installed at NREL's Flatirons Campus to demonstrate the feasibility of some of the controls and transient characteristics that were modeled using the co-simulation platform. The testing was conducted under controlled grid conditions using NREL's multi-megawatt, medium-voltage power electronic grid simulators, also known as the controllable grid interface. NREL also developed a model and tested the controls of modular multilevel converter HVDC converters used in HVDC-interconnected offshore WPPs.

This report provides a summary of the activities and results of a four-year research project led by NREL in collaboration with the Electric Power Research Institute and industry partners.

Keywords

Offshore wind power plants, HVAC transmission, HVDC transmission, transient stability, dynamic stability, co-simulation

Acknowledgments

This work was authored by the National Renewable Energy Laboratory, operated by Alliance for Sustainable Energy, LLC, for the U.S. Department of Energy (DOE) under awards by New York State Energy Research and Development Administration (NYSERDA) and Maryland Energy Administration (MEA). The views expressed in the report do not necessarily represent the view of DOE or the U.S. Government. The U.S. Government retains a nonexclusive, paid-up, irrevocable, worldwide license to publish or reproduce the published form of this work, or allow others to do so, for U.S. Government purposes. We would like to thank the National Offshore Wind Research and Development Consortium (NOWRDC), NYSERDA and MEA staff for their continuous support and guidance in this work. We also thank technical experts from PJM, New York ISO (NYISO) and ISO New England (ISO-NE) for their valuable contributions and support. We are also grateful to the DOE Wind Energy Technologies office for funding this project.

Table of Contents

Notice.....	i
Abstract	ii
Keywords	iii
Acknowledgments.....	iii
List of Figures.....	vi
List of Tables.....	ix
Acronyms and Abbreviations	x
Executive Summary	1
1 Modeling Challenges of Inverter-Based Resources	1
1.1 Key Issues for Maintaining Grid Reliability With Increased Variable Generation	1
1.2 Methods and Challenges of Modeling Inverter-Dominated Grids	1
1.3 Addressing Stability Problems in Inverter-Dominated Grids.....	2
1.4 Technology and Modeling Assumptions	3
2 Transferring Project Results to Industry	4
2.1 Commercial Utilization	4
2.2 ISO Engagement.....	5
2.3 How ISOs Can Use NREL’s Method.....	7
3 PSCAD-PSS/E Co-Simulation Platform.....	9
3.1 Co-Simulation Workflow	9
3.2 NREL’s Grid Impedance Scan Tool (GIST).....	10
3.3 Co-Simulation Workflow	10
3.4 Boundary Between PSCAD and PSS/E Models	13
3.5 Models of Offshore Wind Power Plants	14
3.6 Simulation Results for Type 3 and Type 4 Wind Power Plants.....	22
4 Examples of Stability Impacts of Onshore Wind Generation in NYISO, PJM, and ISO-NE ...	29
4.1 Simulations for NYISO POIs	29
4.2 Example of Impedance Analysis Using the Co-Simulation Platform Interfaced With GIST	38
4.3 Simulations for PJM POIs	40
4.4 Simulations for ISO-NE POIs	46
5 Simulation Results	52
5.1 Interactions Between HVAC- and HVDC-Interconnected Offshore Wind Power Plants.....	52
5.2 Sensitivity of an HVDC-Interconnected Wind Power Plant to the POI SCR.....	54
5.3 Sensitivity of an HVAC-Interconnected Wind Power Plant to POI SCR	57
5.4 Active Power Controls by HVDC-Interconnected Offshore Wind Power Plants	58
5.5 Active Power Controls by HVAC-Interconnected Offshore Wind Power Plants	60
5.6 Offshore Wind Power Participation in Automatic Generation Control	61

5.7	GFM Offshore Wind Power Plant	62
6	GFL and GFM Operation	64
6.1	Models of Offshore Wind Turbine Generators in GFL and GFM Modes.....	64
6.2	GFL and GFM Operation of Offshore Wind Power Plants.....	66
6.3	GFL and GFM Operation at Lower SCRs	69
6.4	GFM Operation in Islanded Mode	69
7	Testing Results	72
7.1	Description of Test Site	72
7.2	Test Platform.....	72
7.3	Voltage Fault Tests	73
7.4	Turbine Response to Frequency Variations	77
7.5	Emulation of HVDC Terminal	80
8	Summary and Conclusions.....	84
9	References.....	85

List of Figures

Figure 1. Concept of co-simulation	9
Figure 2. GIST general diagram	10
Figure 3. Co-simulation data flow	11
Figure 4. PSCAD model with buses 243441 and 243205	12
Figure 5. PSS/E model with bus 243441	13
Figure 6. Typical co-simulation response (PSS/E – left, PSCAD – right)	13
Figure 7. A two-area system model is used to evaluate the impact of the boundary between the PSCAD and PSS/E models on the accuracy of stability analysis.	14
Figure 8. Comparison of response for full PSS/E, full PSCAD, and EMT-phasor hybrid co-simulation (boundary at bus 1 and bus 7) during a transient event.	14
Figure 9. Type 4 wind turbine generator topology (direct-drive gearless)	15
Figure 10. Type 4 wind turbine model.....	16
Figure 11. Type 4 wind turbine control diagram	16
Figure 12. Inertia control implemented in PSCAD	17
Figure 13. Frequency droop control implemented in PSCAD	17
Figure 14. Voltage control implemented in PSCAD	17
Figure 15. Diagram of Type 3 wind turbine generator	18
Figure 16. HVAC-interconnected offshore WPP	18
Figure 17. Detailed PSCAD model of HVAC-interconnected offshore WPPs with Type 4 wind	18
Figure 18. HVDC-interconnected offshore WPP	19
Figure 19. Point-to-point HVDC transmission model (symmetric-monopole 320-kV DC, 1000 MW).....	20
Figure 20. HVDC MMC control diagram in GFL mode	20
Figure 21. HVDC MMC controls in GFM mode [14]	21
Figure 22. HVDC energization	22
Figure 23. HVDC fault ride-through.....	22
Figure 24. HVDC system diagram for a test system	22
Figure 25. Model of the Indian River POI with Type 3 and Type 4 HVAC-interconnected offshore	24
Figure 26. Three-phase low-voltage ride-through performance at the PJM Indian River POI (two Type 4 and single Type 3 WPPs, HVAC interconnection)	24
Figure 27. Single-phase low-voltage ride-through at the PJM Indian River POI (two Type 4 and single Type 3 WPPs, HVAC interconnection)	25
Figure 28. Response of PJM Indian River POI to SCR step change (two Type 4 and single Type 3 WPPs, HVAC interconnection)	26
Figure 29. Response of PJM Indian River POI to POI voltage phase angle 30deg jump (two Type 4 and single Type 3 WPPs, HVAC interconnection)	27
Figure 30. Type 4 and Type 3 offshore WPPs connected to the same offshore HVDC terminal	28
Figure 31. Instability observed during simultaneous operation of Type 3 and Type 4 WPPs connected to the same offshore HVDC terminal	28
Figure 32. Atlantic Offshore Wind Transmission Study 2030 SCR screening results for two dispatch conditions	29
Figure 33. Map of NYISO POIs	30
Figure 34. Impact of the POI SCR on Barrett stability	31
Figure 35. Balanced voltage fault ride-through for two different POI SCRs	31
Figure 36. Unbalanced voltage fault ride-through for two different POI SCRs	32
Figure 37. Increase in plant reactive power at the POI	32
Figure 38. Example of an NYISO co-simulation configuration: EMT models of three offshore WPPs interfaced with the PSS/E model of the interconnection through three different POIs.	34
Figure 39. NYISO co-simulation results: zero-voltage fault ride-through	35
Figure 40. NYISO co-simulation results: response to a 1,283-MW generation trip in NYISO	36

Figure 41. NYISO co-simulation results: response to a generation trip in Long Island	37
Figure 42. NYISO co-simulation results: response to simulated SCR degradation	38
Figure 43. GIST used between PSCAD model of an offshore WPP and PSS/E model of the grid ...	38
Figure 44. Wind power plant admittance	39
Figure 45. Power system admittance	39
Figure 46. Sequence impedance analysis	40
Figure 47. Indian River substation.....	41
Figure 48. Indian River three-phase and single-phase faults at two different SCRs (no voltage	
Figure 49. Indian River single-phase faults (SCR = 3). Left: undamped oscillation, plants have 5% voltage	
droop enabled. Right: stable recovery (with less aggressive droop and plant curtailment) .	42
Figure 50. Indian River single-phase faults (SCR = 3) with a Δ - Y_g substation transformer	43
Figure 51. Co-simulation example for PJM POIs	44
Figure 52. Response to 1000-MW generation trip in PJM.....	44
Figure 53. Response to 3000-MW generation trip in PJM.....	45
Figure 54. Response to a trip of one line connecting with the Indian River substation	45
Figure 55. 800 MW Vineyard Wind 1 project interconnected with W Barnstable bus.	47
Figure 56. Step changes in W Barnstable SCR	48
Figure 57. Zoomed-in view of Barnstable SCR switching from 9.4 to 2.4 level (no voltage droop) ..	48
Figure 58. Zoomed-in view of Barnstable SCR switching from 9.4 to 2.4 level (voltage droop	
Figure 59. 345-kV bus voltage as a function of SCR (left – no synchronous condenser, right – with	
100-MVA synchronous condenser)	49
Figure 60. EMT co-simulation region.....	50
Figure 61. PSCAD EMT interfaced with PSS/E model of ISO-NE system.....	50
Figure 62. Instability caused by tripping of two synchronous condensers (offshore WPP operates with voltage	
control)	51
Figure 63. Response of an offshore WPP with and without voltage control to the loss of one synchronous	
condenser	51
Figure 64. HVDC and HVAC wind plants interconnected with the onshore grid	52
Figure 65. Undamped oscillations in the Farragut and Gowanus POIs after SCR reduction.....	53
Figure 66. Stable performance provided by a 100-MVA synchronous condenser	53
Figure 67. Zero-voltage ride-through of an HVDC-interconnected plant	54
Figure 68. Zero-voltage ride-through of an HVDC-interconnected plant	55
Figure 69. SCR scan of an HVDC-interconnected plant (less aggressive current control gain).....	56
Figure 70. SCR scan of an HVDC-interconnected plant (more aggressive current control gain)	56
Figure 71. Low-voltage ride-through of an HVAC-interconnected Type 4 plant with a synchronous condenser	
.....	57
Figure 72. HVAC-interconnected plant ride-through 200-ms L-to-G fault, SCR=3 (no synchronous condenser	
– left, with synchronous condenser – right).....	57
Figure 73. SCR scan of HVAC-interconnected plant for different configurations	58
Figure 74. Provision of frequency responsive services by an HVDC-interconnected offshore plant	
.....	58
Figure 75. Plant frequency response with Option 1 controls.....	59
Figure 76. Plant frequency response with Option 2 controls.....	60
Figure 77. Frequency responsive controls of an HVAC-interconnected WPP.....	61
Figure 78. Offshore plant following automatic generation control set points	62
Figure 79. Offshore WPP with GFM Type 4 wind turbine	63
Figure 80. Transition to islanded operation.....	63
Figure 81. Model of an offshore wind turbine generator operating in GFL mode.....	65
Figure 82. Model of an offshore wind turbine generator operating in GFM mode.....	65
Figure 83. Model of an offshore WPP connected to the onshore grid	66
Figure 84. Simulated response of a GFL WPP to a 30° phase jump in a 345-kV grid (right – no voltage droop	
control, left – 5% voltage droop control enabled). Plant response is shown for 345-kV bus.	67

Figure 85. Simulated response of GFM WPP to a 30° phase jump	68
Figure 86. Simulated response of an offshore WPP to a 10% step increase in voltage in a 345-kV grid (left – GFL operation, right – GFM operation)	68
Figure 87. 345-kV POI voltage dependence on SCR (GFL – left, GFM – right)	69
Figure 88. Transition to islanded operation during system separation (GFM wind plant – left, GFL wind plant – right)	70
Figure 89. Islanded operation of a GFM wind plant under variable load and wind conditions	71
Figure 90. NREL test site with GE wind turbine and CGI	72
Figure 91. NREL experimental platform	73
Figure 92. Turbine ride-through during a 300-ms, 40% voltage fault (5% SCR)	74
Figure 93. Turbine ride-through during a 300-ms, 50% voltage fault	75
Figure 94. Turbine ride-through during the 40%, 625-ms long-recovery fault and subsequent	
Figure 95. Turbine ride-through during the 90%, 1-s rectangular fault and subsequent turbine trip	76
Figure 96. Turbine inability to ride-through zero-voltage fault	77
Figure 97. Provision of frequency responsive services by an HVDC-interconnected offshore plant	78
Figure 98. Turbine response: inertial control only	79
Figure 99. Turbine response: combination of inertial and primary frequency response	79
Figure 100. Diagram of MMC-HVDC real-time simulation	80
Figure 101. RSCAD modeling diagram of MMC-HVDC in real-time simulation	81
Figure 102. Real-time simulation of MMC-HVDC with AC fault at MMC terminal 1	81
Figure 103. Real-time simulation of MMC-HVDC with AC fault at MMC terminal 1	82
Figure 104. Monitoring of converter capacitor voltages	82
Figure 105. RTDS system at NREL Flatirons Campus for MMC-HVDC real-time simulation	83

List of Tables

Table 1. List of POIs used for model testing 6
Table 2. List of NYISO POIs used for model testing 7
Table 3. List of ISO-NE POIs used for model testing 7
Table 4. List of NYSO offshore plants 11
Table 5. List of ISO-NE projects 11
Table 6. Spring light load case: short circuit results 41
Table 7. ISO-NE POIs 46
Table 8. Grid strengths for the 2031 multiregional modeling working group summer case (results from NREL-PNNL Atlantic offshore wind study) 46

Acronyms and Abbreviations

Δ	delta winding configuration
CGI	controllable grid interface
FACTS	flexible AC transmission system
GFL	grid following
GFM	grid forming
GIST	Grid Impedance Scan Tool
GTSOC	Giga Transceiver System on a Chip
GW	gigawatt
HVAC	high-voltage alternating current
HVDC	high-voltage direct current
Hz	hertz
IBR	inverter-based resource
ISO	independent system operator
ISO-NE	Independent System Operator New England
kV	kilovolt
MEA	Maryland Energy Administration
mH	millihenry
MMC	modular multilevel converter
ms	millisecond
MW	megawatt
NREL	National Renewable Energy Laboratory
NYISO	New York Independent System Operator
NYSERDA	New York State Energy Research and Development Authority
POI	point of interconnection
PV	photovoltaic
SCR	short-circuit ratio
STATCOM	static compensator
WPP	wind power plant
Y_g	star-grounded winding configuration

Executive Summary

Maintaining bulk system reliability requires balancing the supply of electricity with demand at all timescales. With high shares of variable wind and solar generation, maintaining reliability presents issues that can be summarized into three general categories: (1) responding to the short-term variability of wind and solar generation; (2) ensuring enough generation to meet demand during all hours of the year; and (3) maintaining stability in the event of a grid disturbance. Increasing penetrations of power electronics-based renewable energy resources such as wind and solar photovoltaic (PV) plants—along with the application of high-voltage direct current (HVDC) and flexible AC transmission system (FACTS) devices in utility power systems—have resulted in many system integration problems. This has increased the importance of modeling power electronic converters to understand, analyze, and mitigate the resonance and stability problems arising in power systems with high penetrations of power electronic converters.

Modeling approaches for power electronic converters can be broadly classified into time-domain and frequency-domain modeling methods. The objective of the time-domain modeling methods is to simplify the dynamic model of a converter while retaining the dynamics of interest. This usually involves the application of perturbation techniques, such as some form of averaging, to the ODE-based dynamic model of a converter to remove the time dependency in the model. The time dependency is generally introduced by switching action and/or time-varying periodic inputs to the converter. Frequency-domain modeling is applied to the simplified dynamic model obtained using the time-domain modeling methods. The objective of the frequency-domain modeling is to linearize the converter dynamic model and find a Laplace transfer function-type relationship between the selected input and output variables. The transfer function models are useful for control design and for the analysis of interactions between a converter and the networks at its terminals.

During this project, we developed advanced modeling, control, stability monitoring, and protection methods for the analysis and mitigation of dynamic stability problems in offshore wind power plants (WPPs) interconnected with onshore power systems via high-voltage alternating current (HVAC) or high-voltage direct current (HVDC) submarine transmission connected to strong and weak points of interconnections (POIs) in onshore power grids. The PSS/E-PSCAD co-simulation platform for offshore wind power analysis combined with the National Renewable Energy Laboratory's (NREL's) Grid Impedance Scan Tool (GIST) platform is instrumental for removing barriers to the reliable integration of large levels of offshore wind power. The tool application was demonstrated for various use cases using offshore WPP POIs in three different interconnections: PJM, New York Independent System Operator (NYISO), and Independent System Operator New England (ISO-NE). The tool can be used for HVDC- and HVAC-interconnected offshore WPPs and allows evaluating transient and dynamic behavior.

In this project, the NREL team developed a co-simulation platform that combines:

- PSS/E – positive-sequence transmission planning and analysis software by Siemens
- PSCAD – electromagnetic transient (EMT) simulation software
- E-TRAN – a software tool to interface positive-sequence phasor models in PSS/E of a large power system, such as the Eastern Interconnection, with the EMT models in PSCAD of power electronics generators, such as offshore WPP with HVAC or HVDC transmission to the grid
- GIST – (PSCAD-based) developed by NREL.

The platform combines the strengths of three commercial software tools (PSS/E, PSCAD, and E-TRAN) and the NREL-developed GIST to accurately represent small-signal stability, dynamic and transient behavior, and instabilities and control interactions that can exist in offshore WPPs, between several WPPs, and between offshore WPPs and the onshore grid. The use of the platform was demonstrated in several cases for three ISOs using models of offshore WPPs with HVAC and HVDC interconnection. POIs with low short-circuit ratios (SCRs) were selected for the model testing to demonstrate possible instabilities.

Simulations conducted in this project are for demonstrating the capabilities of the co-simulation platform only and are not classified as integration studies. The platform can be used later by any stakeholder to conduct detailed integration studies for any offshore project or for studies to identify system-level reliability impacts of clusters of offshore WPPs using different transmission configurations.

S.1 Description of Co-Simulation Platform

The concept of the co-simulation platform is explained in Figure S. 1. To represent onshore grids, we use the PSS/E positive-sequence power simulator software, which is an adequate software tool for simulating the dynamics of large, interconnected power systems with a library of standard sub-models for generation and loads. Custom models can be developed in PSS/E as well. PSS/E is widely used by ISOs, utilities, and developers; however, PSS/E capabilities are not sufficient to investigate stability problems in inverter-dominated grids, as described earlier in this report. PSCAD software offers superior capability for more accurate representation of wind, PV, HVDC, static compensators (STATCOM), battery energy storage systems, synchronous condensers, and protection models to investigate various stability aspects and transient performance in power grids with high levels of inverter-based resources. Models of both HVAC- and HVDC-interconnected offshore WPPs have been developed for this project by the NREL and Electric Power Research Institute (EPRI) teams. The PSCAD model is enhanced with the NREL-developed GIST, which is a small-signal stability tool (described later in this section) allowing analysis of potential stability issues and control interactions within offshore WPPs, between offshore WPPs and the onshore grid, and between two or more offshore WPPs interacting through the onshore grid. Commercial E-TRAN software tools are used to interface the PSS/E and PSCAD models.

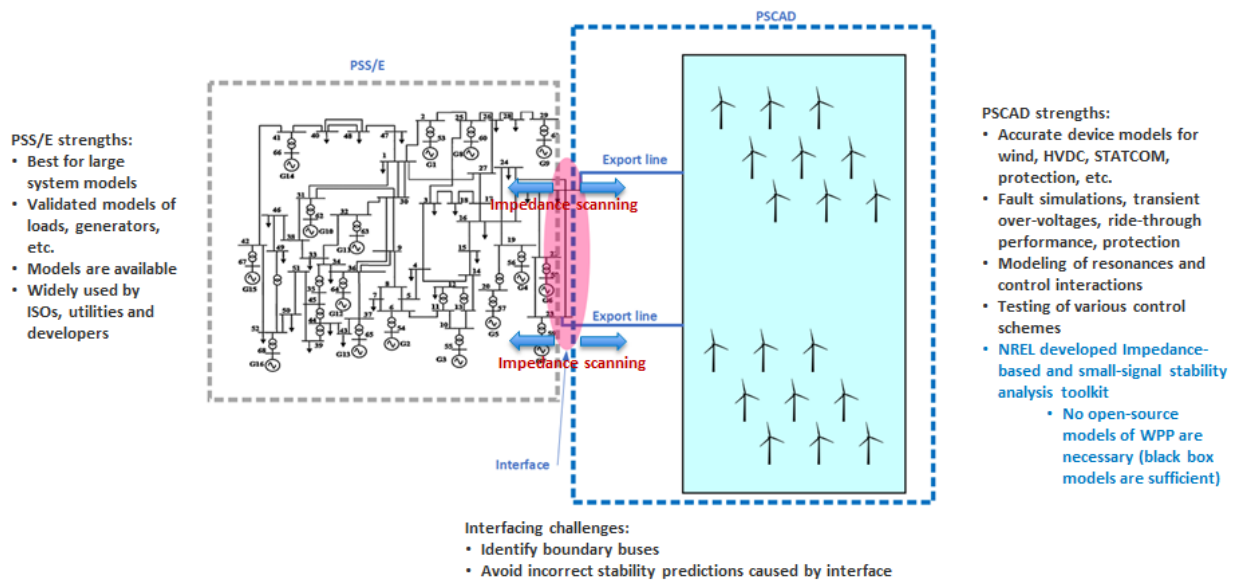


Figure S. 1. Concept of the co-simulation

S.2 Models of Offshore WPPs

The full WPP models implemented in PSCAD for HVAC- and HVDC-interconnected offshore WPPs consisting of type 3 and 4 wind turbine generators of +10-MW capacity are shown in Figure S. 2 and Figure S. 3, respectively. Both models use a 66-kV collector system with 10- to 15-MW Type 4 wind turbines. An HVAC-interconnected plant is modeled with a 30-mile, 230-kV submarine export cable with shunt compensation. Models of a STATCOM, battery system (either grid forming or grid following), or synchronous condensers can be added to the onshore substation. A model of the battery energy storage of the desired power and energy rating can be added to the onshore substation as well.

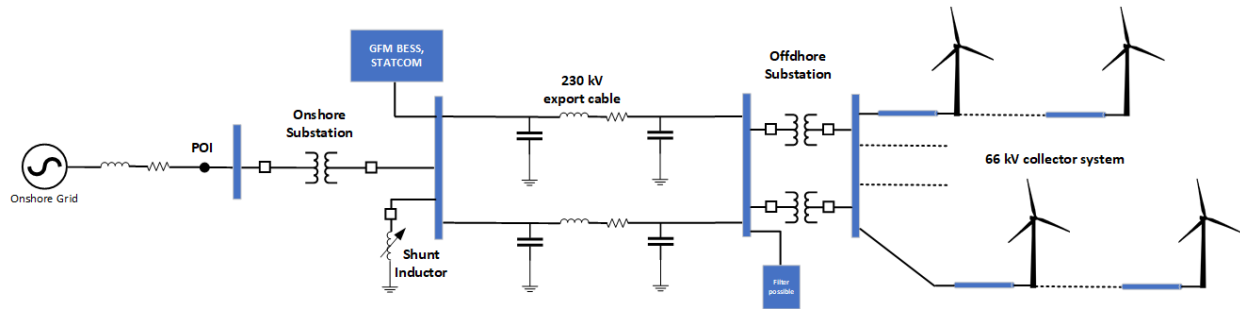


Figure S. 2. HVAC-interconnected offshore WPP

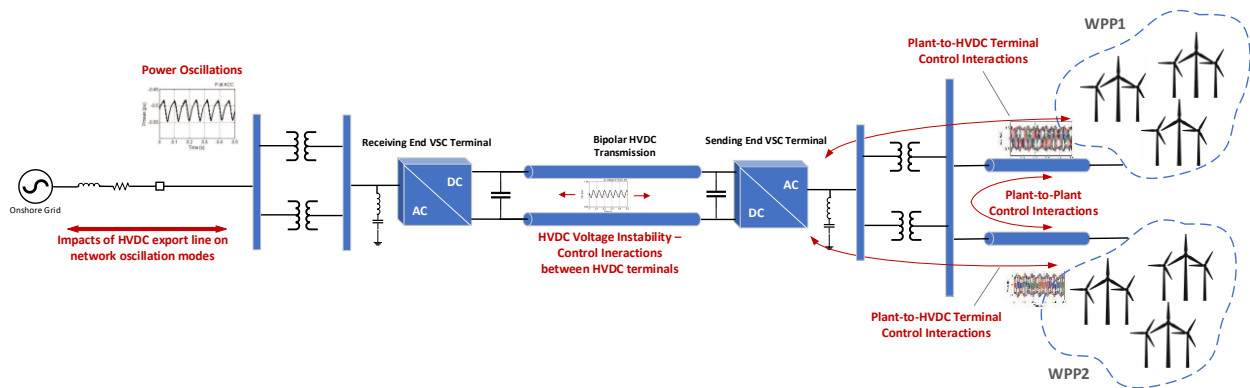


Figure S. 3. HVDC-interconnected offshore WPP

S.3 Examples of Co-Simulation Results

The NREL-developed PSCAD model of a large HVAC-interconnected offshore WPP was configured and used in simulations to evaluate the stability impacts on sample POIs located in the PJM, NYISO, and ISO-NE systems. The selection of POIs was based on SCR screening for all planned projects for the 2030 system (summer and winter peak load cases) using the results of the analysis conducted under NREL's Atlantic Offshore Wind Transmission Study [9]. Of 24 POIs considered for the 2030 system, only 9 can be classified as strong ($SCR > 5$), 3 as moderate ($3 < SCR < 5$), and 17 as weak ($SCR < 3$). Similar screening was conducted for 2030 planning cases with 30 GW of offshore wind under conditions selected from the nodal production cost modeling for three typical days representing summer peak, winter peak, and spring off-peak seasons. In this case, of 24 POIs, only 5 can be classified as strong, 5 as moderate, and 14 as weak. These results from the Atlantic Offshore Wind Transmission Study were used for selecting the weakest POIs for conducting simulations using the co-simulation platform developed in this project.

The Barrett 138-kV substation located in the Long Island Power Authority territory was selected to test the model of a 1000-MW, Type 4 offshore WPP (Empire Offshore Wind LLC) connected with the Barrett POI via a 30-mile, 230-kV export cable with shunt compensation in both ends. The Barrett substation is located at the southeastern tip of Long Island, as shown in Figure S. 4. The POI was modeled with different SCR values to emulate different grid strengths identified in the PSS/E simulations.

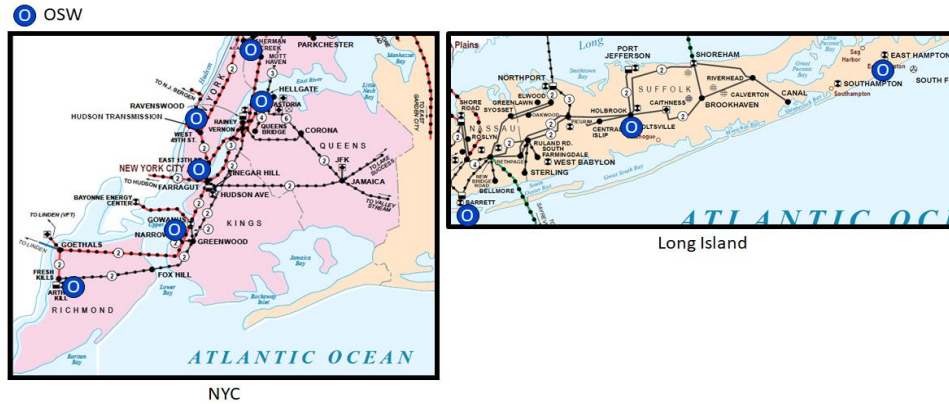


Figure S. 4. Map of NYISO POIs

Simulations were conducted using the PSCAD model to demonstrate the impact of POI SCR on the stability of the interconnection. In the case of the weaker interconnection ($SCR < 3$), the plant may exhibit unstable behavior depending on the impedance characteristics of the POI and the offshore plant itself (combined impedance of export cables with compensation, offshore transformers, collector system, and turbines). Figure S. 5 shows the results of steady-state plant operation when the POI SCR has a small change (the plant is operating with a 5% voltage droop setting). The plant goes unstable during an extremely small change in SCR (at around $SCR = 2.44$). This result is specific to the turbine models, cable/transformer parameters, and level of compensation used in the model. Nevertheless, it demonstrates the impact of small changes in SCR on interconnection stability. In the case of onshore transmission trips and other faults in the onshore network, the POI SCR may drop dramatically, causing a significant stability impact. In such a case, the plant controller needs to curtail its power to maintain stability. Simulations need to be conducted for each offshore project using accurate parameters of all components and accurate turbine models to evaluate the stability issues and mitigation measures for each project.

The ability of the modeled plant to provide low-voltage ride-through was also tested for different POI strengths for three-phase and single-phase voltage faults occurring in the 138-kV network, as shown in Figure S. 6 and Figure S. 7, respectively. The plant is able to ride through both types of faults under weaker and stronger POI conditions.

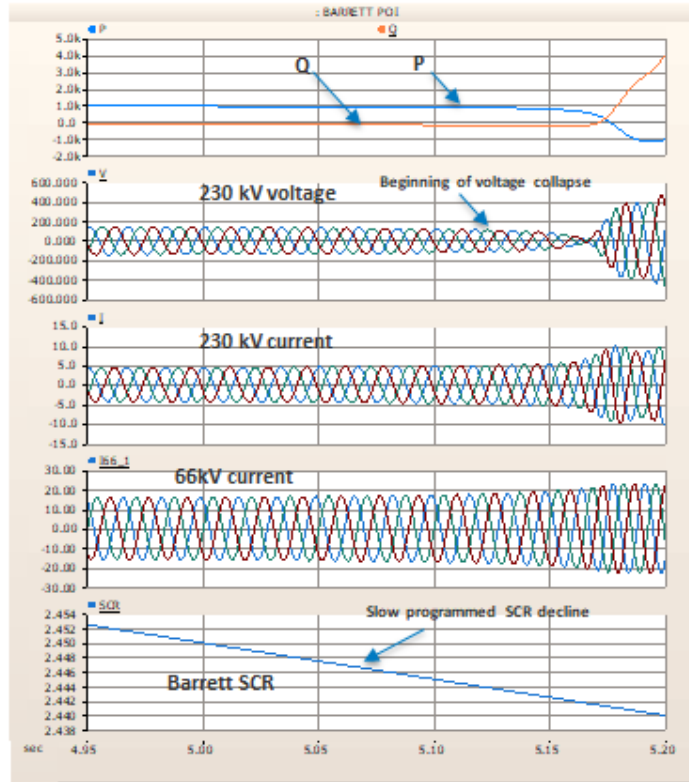


Figure S. 5. Impact of the POI SCR on Barrett substation stability

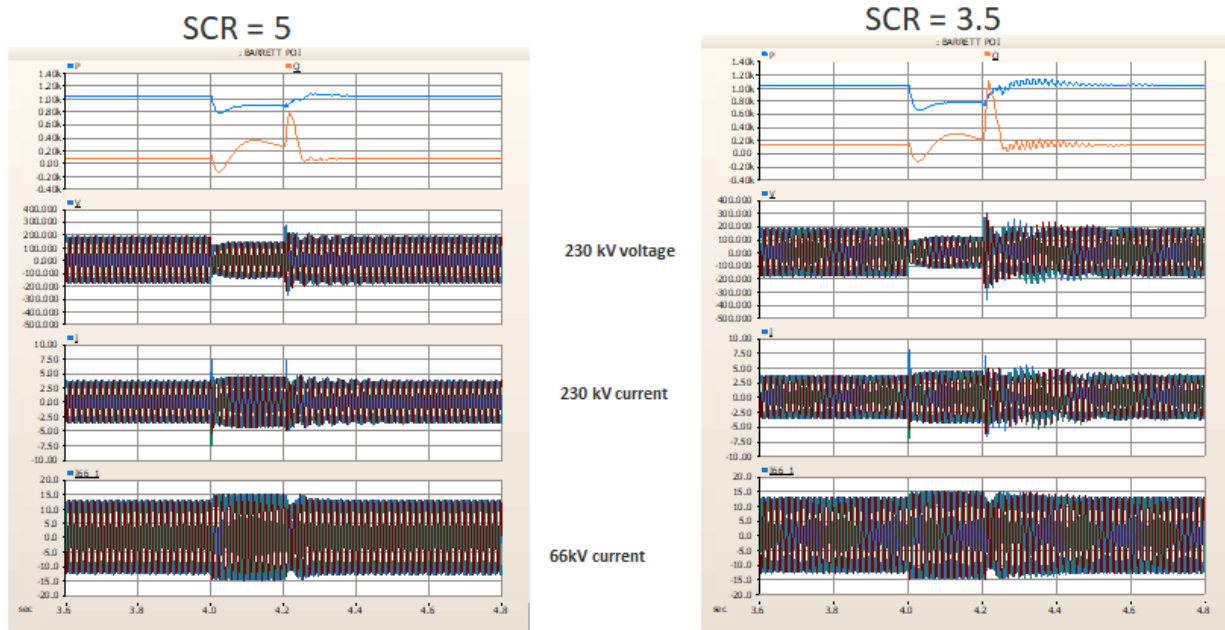


Figure S. 6. Balanced voltage fault ride-through for two different POI SCRs

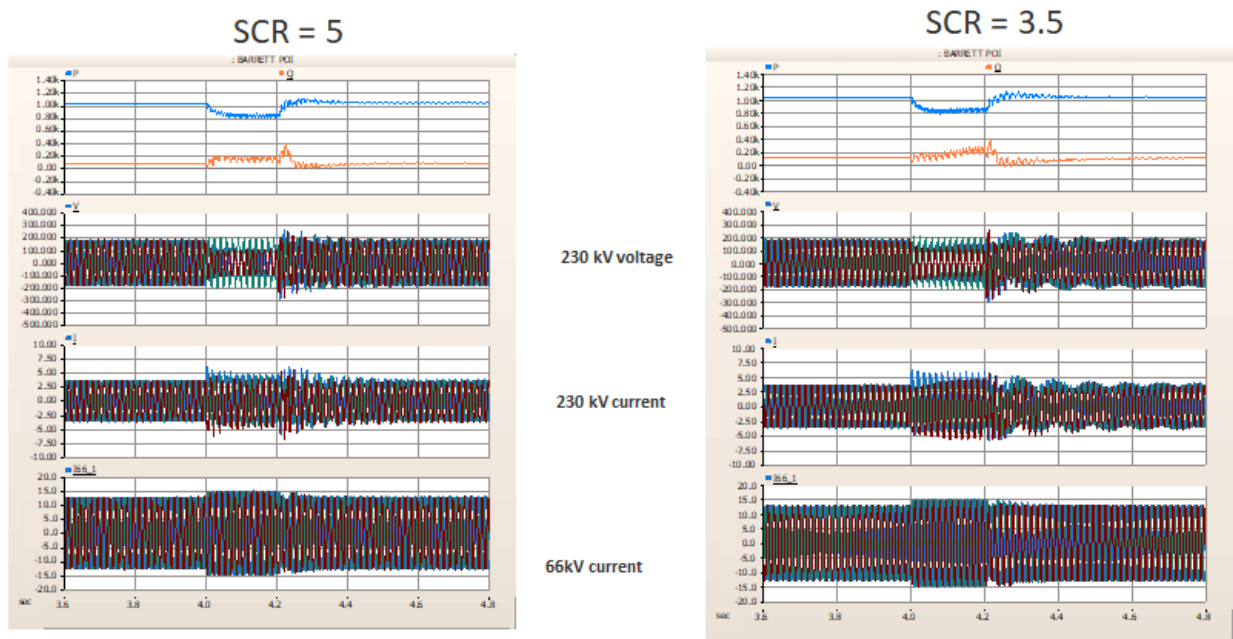


Figure S. 7. Unbalanced voltage fault ride-through for two different POI SCRs

It is important to consider the ability of offshore WPPs to provide short-circuit current during faults at levels that are adequate for protection systems. In some cases, the use of synchronous condensers at the POI may be justified to provide an adequate level of fault currents. Additional benefits of synchronous condensers include their ability to increase grid strength as well as provide voltage controls and real rotating inertia to the system.

Offshore WPPs can provide volt/volt ampere reactive (VAR) support at POIs. Such capability is important for maintaining voltage stability in onshore networks when other conventional generators are not online. This is important for the New York City–eastern Long Island area, where voltage stability constraints exist and spinning reserves inside New York City load pockets are dispatched to provide voltage support. Wind can replace such spinning reserves and provide volt/VAR in those areas to respect existing voltage stability constraints.

The co-simulation platform was demonstrated for the NYISO system for different transient and dynamic cases. One example of a co-simulation configuration is shown in Figure S. 8 with three offshore projects (Holbrook 840 MW, Barret 1000 MW, and Ruland 816 MW) modeled in PSCAD and then interfaced with a PSS/E model of the NYISO system with three different POIs (three POIs in total). The response of the system to a 150-ms, zero-voltage fault in the Long Island grid is shown in Figure S. 9, demonstrating successful ride-through for all three offshore WPPs.

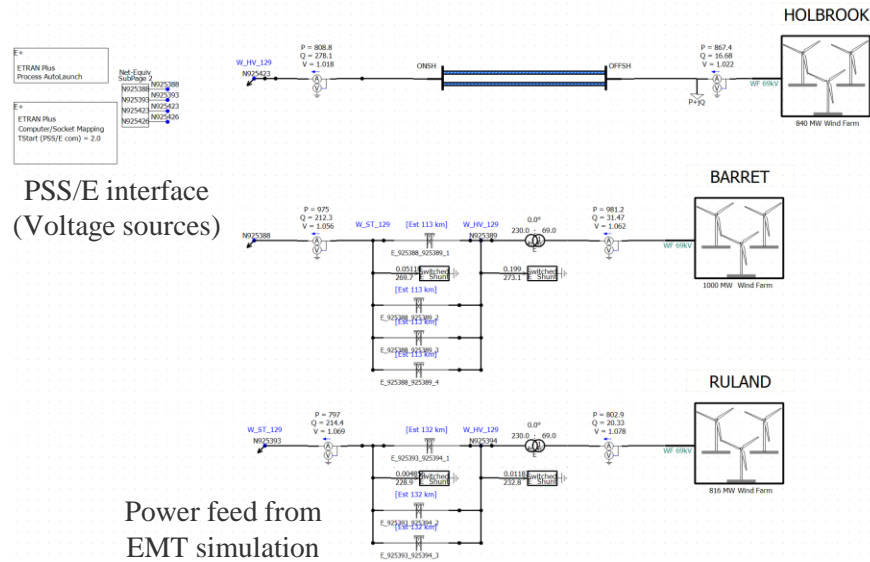


Figure S. 8. Example of NYISO co-simulation configuration: EMT models of three offshore WPPs interfaced with PSS/E model of the interconnection through three different POIs

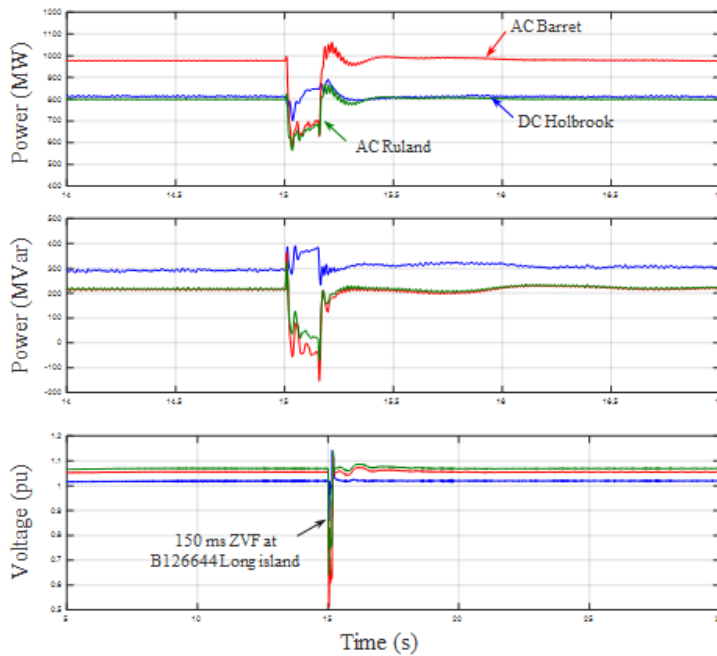


Figure S. 9. NYISO co-simulation results: zero-voltage fault ride-through

S.3 Summary and Conclusions

During this project, we developed advanced modeling, control, stability monitoring, and protection methods for the analysis and mitigation of dynamic stability problems in offshore WPPs interconnected with onshore power systems via HVAC or HVDC submarine transmission connected to strong and weak points of interconnections in onshore power grids. The PSS/E-PSCAD co-simulation platform for offshore wind power analysis combined with NREL's GIST platform is instrumental for removing barriers to the reliable integration of large levels of offshore wind power. The tool application was demonstrated for various use cases using offshore WPP POIs in three different interconnections: PJM, NYISO, and ISO-NE. The tool can be used for HVDC- and HVAC-interconnected offshore WPPs to evaluate transient and dynamic behavior.

In this project, the NREL team developed a co-simulation platform that combines:

- PSS/E – positive-sequence transmission planning and analysis software by Siemens
- PSCAD –EMT simulation software
- E-TRAN – a software tool to interface positive-sequence phasor models in PSS/E of a large power system, such as the Eastern Interconnection, with the EMT models in PSCAD of power electronics generators, such as offshore WPP with HVAC or HVDC transmission to the grid
- GIST – (PSCAD-based) developed by NREL.

The platform combines the strengths of three commercial software tools (PSS/E, PSCAD, and E-TRAN) and the NREL-developed GIST to accurately represent small-signal stability, dynamic and transient behavior, instabilities, and control interactions that can exist in offshore WPPs, between several WPPs, and between offshore WPPs and the onshore grid. The use of the platform was demonstrated in several cases for three ISOs using models of offshore WPPs with HVAC and HVDC interconnection. POIs with low SCR were selected for the model testing to demonstrate possible instabilities. Simulations conducted in this project are for demonstrating the capabilities of the co-simulation platform only and are not classified as integration studies. The platform can be used later by any stakeholder to conduct detailed integration studies for any offshore project or for studies to identify system-level reliability impacts of clusters of offshore WPPs using different transmission configurations.

The NREL team conducted testing on a utility-scale wind turbine generator installed at NREL's Flatirons Campus to demonstrate the feasibility of some of the controls and transient characteristics that were modeled using the co-simulation platform. The testing was conducted under controlled grid conditions using NREL's multi-megawatt, medium-voltage power electronic grid simulators, also known as the controllable grid interface. NREL also developed a model and tested the controls of modular multilevel converters used in HVDC-interconnected offshore WPPs.

1 Modeling Challenges of Inverter-Based Resources

1.1 Key Issues for Maintaining Grid Reliability With Increased Variable Generation

Maintaining bulk system reliability requires balancing the supply of electricity with demand at all timescales. With high shares of variable wind and solar generation, maintaining reliability presents issues that can be summarized into three general categories: (1) responding to the short-term variability of wind and solar generation; (2) ensuring enough generation to meet demand during all hours of the year; and (3) maintaining stability in the event of a grid disturbance [1]. Many studies have addressed various aspects of grid reliability impacts with increased levels of inverter-based resources (IBRs) up to 100% of demand [2], [3], [4]. With appropriate measures to change grid planning and operations, a desired level of reliability can be achieved for different contributions from renewable generation. These measures can be categorized as:

1. Managing short-term variability and uncertainty in variable generation by increasing grid flexibility in the most cost-effective way
2. Using a portfolio approach to meet electricity demand during all hours of the year by aggregating variable generation with dispatchable sources, such as energy storage
3. Expanding and reinforcing transmission networks
4. Using capabilities of IBRs to provide all essential reliability and stability services to the grid.

The fourth category is very important when applied to grids dominated by IBRs, such as grids in the U.S. East Coast region with planned integration of tens of gigawatts of high-voltage alternating current (HVAC)- and high-voltage direct current (HVDC)-interconnected offshore wind power plants (WPPs) in the coming decades. New stability challenges may evolve in such grids because of low inertia, degraded grid strength, fast controls by IBRs, diversity of controls, possible control interactions, and more complex dynamics in the system. Unavailability of proprietary dynamic and transient models of IBRs makes it difficult to evaluate such impacts through simulations.

1.2 Methods and Challenges of Modeling Inverter-Dominated Grids

Increasing penetrations of power electronics-based renewable energy resources such as wind and solar photovoltaic (PV) plants—along with the application of HVDC and flexible AC transmission system (FACTS) devices in utility power systems—have resulted in many system integration problems. This has increased the importance of modeling power electronic converters to understand, analyze, and mitigate the resonance and stability problems arising in power systems with high penetrations of power electronic converters.

Modeling approaches for power electronic converters can be broadly classified into time-domain and frequency-domain modeling methods. The objective of the time-domain modeling methods is to simplify the dynamic model of a converter while retaining the dynamics of interest. This usually involves the application of perturbation techniques, such as some form of averaging, to the ODE-based dynamic model of a converter to remove the time dependency in the model. The time dependency is generally introduced by switching action and/or time-varying periodic inputs to the converter. Frequency-domain modeling is applied to the simplified dynamic model obtained using the time-domain modeling methods. The objective of the frequency-domain modeling is to linearize the converter dynamic model and find a Laplace transfer function-type relationship between the selected input and output variables. The transfer function models are useful for control design and for the analysis of interactions between a converter and the networks at its terminals [7].

Power converters are highly nonlinear systems with time-varying dynamics because of high-frequency switching modulations and lower-frequency closed-loop controls. The stability of converter-based power systems is studied using small- and large-signal stability analysis methods, such as:

- Eigenvalue-based stability and sensitivity small-signal analysis
- Impedance-based small- and large-signal stability analysis
- Time-domain small-signal and transient stability analysis.

In this work, we focus on impedance-based stability analysis using a National Renewable Energy Laboratory (NREL)-developed software tool kit combined with small-signal stability analysis for the PSCAD environment and time-domain simulations for large-signal stability analysis, such as system response to N-1 and N-2 contingencies and voltage faults. The modeling tools being developed under this project are described in this report.

1.3 Addressing Stability Problems in Inverter-Dominated Grids

Simplicity of operation and control has made voltage source converters a preferred class of converter topologies for interfacing AC and DC power systems in applications ranging from wind turbines and PV inverters to FACTS and high-power HVDC transmission. Fast control dynamics of voltage source converters within the range of electromagnetic dynamics of networks at the voltage source converter terminals can result in undesired interactions between them, manifesting as either instability or sustained oscillations (resonance). Such stability issues often occur in weaker grids or grids with series-compensated transmission lines. They can be caused by interactions of voltage source converters with the torsional mode of conventional generators as well as by interactions with HVDC and FACTS systems [11].

Variable wind power is one of the fastest-growing energy generation technologies, harnessing the energy of wind both on land and at sea. During the past decade, the global share of wind generation has grown tremendously and is evolving into a major contributor to electricity supplies in many countries. With this trend, wind is also becoming a source of reliability services to the grid, which has required grid-supporting functions originally provided by synchronous generators, enabling very high levels of instantaneous penetration (within the range of 60%–70% in some power systems). These challenges in grids with very high shares of IBRs can be grouped into a few main categories:

- 1) The impact of degrading grid strength and short-circuit current levels on stability, transient performance (fault ride-through), and adequacy of protection
- 2) Impacts of degrading system inertia on the stability of power system frequency
- 3) Increasing number of stability issues caused by control interactions, oscillations, and resonances in IBR-dominated grids
- 4) Uncertainty about what is forming the grid in the absence of synchronous generators
- 5) Concerns about how to jump-start the grid after blackouts and how to operate it when it is broken into many smaller islands.

In this work, we focus on the first three of these challenges and provide some insights about grid-forming (GFM) operation by wind power.

The rapid transformation of conventional power systems with high-damping, high short-circuit current levels, and high inertia to converter-dominated systems with limited damping, low short-circuit current levels, and degrading inertia can result in instabilities if not properly investigated. Offshore wind power, like any converter-based resource, creates stability challenges, such as small- and large-signal stability, in both sub-synchronous and harmonic frequency ranges.

Power converters of wind turbines are using multi-timescale control loops to control active and reactive power, current limiting, and the provision of various grid services (such as inertial response, fast frequency response, primary frequency response, participation in frequency regulation, voltage control, and transient

ride-through controls).

Low-frequency instabilities manifest as frequency-coupling oscillations in AC currents and voltages around fundamental frequency caused by active power/voltage control loops and phase-locked loops used for synchronization. Phase-locked loops are used in grid-following (GFL) inverters employed in all modern wind turbine generators. Under certain conditions, phase-locked loops may introduce negative damping that will lead to growing system instabilities, especially in weaker grids. High-frequency instabilities have resulted from interactions between inner current and voltage control loops on the inverter, with the grid also causing negative damping that may result in high-frequency oscillations because of resonances.

Offshore WPPs that are interconnected with the onshore power grid through long HVAC and HVDC submarine transmission systems can become a source of both low-frequency and high-frequency instabilities if not addressed properly:

- In the planning stage, potential instability issues can be addressed by proper modeling and simulations using valid dynamic and transient models of offshore WPPs, the transmission system, and the onshore grid. This approach requires the availability of specific wind turbine models from turbine manufacturers (either open-source or black-box). In the case of HVDC-interconnected plants, a specific HVDC system model is also needed from vendors.
- In the operational stage, instability issues can be addressed by adaptive controls to introduce additional damping to suppress instabilities. Valid models are also needed for this purpose.

1.4 Technology and Modeling Assumptions

The following assumptions have been used to build a simulation model of offshore WPPs for this study. These assumptions were discussed and agreed upon with the project advisory board:

- Single turbine capacity: +10 MW
- Turbine type: Type 4 electric topology, direct-drive permanent magnet generators (no gearboxes)
- Collector system: Radial string topology
- Distance between turbines: 1 nautical mile
- Collector system voltage: 66 kV
- HVAC transmission: 230-kV export cable for distances shorter than 50–60 miles
- HVDC transmission: The main configuration is symmetric—monopole 320-kV modular multilevel converter (MMC) HVDC (monopole 525-kV DC possible)
- Model includes wind turbine-level controls: inertial response, voltage/reactive power/power factor control
- Model includes plant-level controls: primary frequency response, automatic generation control, provision of spinning reserve, plant-level voltage control
- Dynamic reactive compensation in the form of STATCOM (in addition to shunt compensation) can be achieved with short-term battery energy storage at an onshore POI.
- Synchronous condensers are considered in this work as grid-strength-enhancing devices.

2 Transferring Project Results to Industry

This project is aimed at removing barriers to reliable integration of large levels of offshore wind power, using the strategy of wide-scale dissemination of project results among all stakeholder groups, including reliability organizations, system operators, regulators, utilities, equipment vendors, project developers, and academia. The main objectives of this project are (1) to develop advanced modeling, control, stability monitoring, and protection methods for the analysis and mitigation of dynamic stability problems in offshore WPPs interconnected with onshore power system via HVAC or HVDC submarine transmission connected to strong and weak points of interconnections and (2) conduct demonstration testing at NREL.

This project is complementary to the recent New York Power Grid Study conducted for the New York State Public Service Commission [5]. Findings of the New York Power Grid Study, recommendations for future New York grid upgrades and enhancements, and solutions for integrating 6 GW of offshore wind generation into the New York City grid are used in development of simulation scenarios in this work. The project described in this report is also complementary to the Atlantic Offshore Wind Transmission Study. We used some of this transmission study's results on grid strength analysis when selecting sites to show how our co-simulation platform can be used in integration studies. Our project was designed to develop a new advanced simulation platform that can help address reliability and stability barriers that prevent the U.S. offshore wind industry, system operators, and utilities from fully integrating offshore wind power generation into onshore grids. The project has developed and tested new ways to co-simulate the detailed transient models of offshore wind power and dynamic models of large onshore grids.

The NREL-Electric Power Research Institute (EPRI) team is implementing the following approach to transfer project results to industry:

- Dissemination activities: Use the project report, conference papers and presentations, and webinars to broadcast results of this project to all segments of the stakeholder community— regulators, NERC, ISOs, utilities, offshore project developers, plant owners and operators, manufacturers, equipment vendors, and academia.
- Training activities: Collaborate with ISOs, utilities, project developers, and offshore plant operators to demonstrate the use of the PSS/E-PSCAD co-simulation platform, and train designated personnel on conduction co-simulations to identify potential stability issues and control interactions between offshore WPPs and the onshore grid.
- Technical assistance: Provide assistance to ISOs and utilities to develop use cases for additional simulation scenarios, depending on their needs, specific offshore projects, and their POIs.

2.1 Commercial Utilization

The co-simulation platform developed under this project is an open-source software model that can be used by any member of the industry. However, it is important to note that the PSS/E portion of onshore grid models are not “free access” by anyone. The use of PSS/E models must be authorized by ISOs. Any user that is intended to use the platform needs to have software licenses for:

- PSCAD (version 4.8.2 or higher)
- E-TRAN
- PSS/E (version 35 or higher)

NREL can provide initial assistance to future users (ISOs, utilities, project developers, equipment vendors, academia) in setting up the models and conducting simulations.

Another component of the platform is the NREL-developed PSCAD-based GIST.

Details about this tool will be provided later in this report. To be included in the co-simulation platform, the tool requires a separate licensing agreement between NREL and end-user.

Commercial use of the method involves the following steps:

- The NREL method is not designed for licensing and sale to end users. To use it for commercial purposes, users need to purchase their own licenses of PSS/E, E-TRAN, and PSCAD.
- Once having all software licenses in place, NREL can provide ISOs, utilities, project developers, and plant operators with written guidance on how to set up a co-simulation platform using models of onshore grid for any desired planning year, offshore WPP(s), types of export cables (AC or DC), description of impedance scan tools, etc.
- NREL can also assist during initial runs of the model to ensure the simulation process and interpretation of results are correct.
- The tool can be used to estimate stability impacts of commercial offshore projects on the onshore grid for all parts of the U.S. East Coast region.
- The same platform can be used for evaluating stability impacts of offshore plants in the Gulf of Mexico and the U.S. West Coast region. For these cases, it is necessary to use models of the Electric Reliability Council of Texas and U.S. Western Interconnection onshore grids in PSS/E, respectively.
- Since NREL does not expect any financial gain from the developed method, it can be used by third parties to perform integration studies for commercial “for-profit” projects, with no royalties, fees, or licensing payments to NREL or EPRI.
- The NREL and EPRI teams are planning several joint dissemination activities (conference papers, webinars, direct contacts with ISOs and utilities) to promote commercial adaptation of the method developed under this project.

Some ISOs have already requested NREL to license the GIST to them to for long-term use. We are working with the NREL Technology Transfer Office to finalize the licensing agreements for transferring the software to the interested ISOs. This is one example of a commercialization path, since ISOs will be using this tool in interconnection studies and stability assessments for offshore WPPs in their regions.

2.2 ISO Engagement

The NREL-EPRI team has been working with three ISOs: PJM, New York Independent System Operator (NYISO), and Independent System Operator New England (ISO-NE) as part of the advisory board for this project.

PJM expressed strong interest in this project based on the following actions:

1. Participating in project advisory board. Engineers from the PJM Transmission Planning division (Aaron Berner and Byuongkon Choi) have been engaged in industry advisory board meetings, project approach and scenario discussions. They have provided detailed information about operation of their system, planned transmission reinforcements, planned offshore projects, and POIs.
2. The PJM team provided their 2026 light load case dynamic PSS/E model with offshore WPPs integrated with the Indian River substation in Maryland as well as a number of WPPs integrated with substations in New Jersey.
3. The PJM team provided a set of ISO documents and reports related to their own integration studies, identified challenges and system limitations, and planned upgrades and reinforcements.

4. PJM worked with the EPRI team (EPRI is a subcontractor to NREL in this project) to refine the PSS/E models and modify dispatch to reflect planned shares of offshore wind power in their system.
5. The ISO team expressed their interest in using the NREL-developed tool in future integration studies since it provides a unique platform for evaluating stability impacts on the onshore grid.

The list of POIs for five offshore projects for which PJM provided information and full support is shown in Table 1.

Table 1: List of POIs used for model testing

No	Name	kV level of interconnection	MW size	MVA size	69 kV cables	POI kV cables
1	Oyster Creek	230 kV	719	748.9583	9	3
2	BL England	138 kV	381	396.875	4	2
3	Cardiff	230 kV	1,510	1572.917	15	*4
4	Smithburg	500 kV	1,148	1195.833	12	*3
5 (Maryland)	Indian River	230 kV	800	833.3333	9	3

NYISO expressed strong interest in this project based on the following actions:

1. Participating in project advisory board. A NYISO representative (Michael Swider, senior market and technologies strategist) has been engaged in the industry advisory board meetings, project approach and scenario discussions and has provided detailed information about NYISO’s system operation, planned transmission reinforcements, planned offshore projects, and POIs.
2. The NYISO team provided their 2026 light load case dynamic PSS/E models with 11 offshore WPPs integrated with onshore substations in the New York City and Long Island area.
3. The NYISO team provided a set of ISO documents and reports related to their own integration studies, identified challenges and system limitations, and planned upgrades and reinforcements.
4. NYISO worked with the EPRI team to refine the PSS/E models and modify dispatch to reflect planned shares of offshore wind power in their system.
5. NYISO emphasized the importance of volt/VAR support by offshore WPPs to address the Central-East voltage stability constraints in the New York City–Long Island area, which can be modeled by our co-simulation platform.
6. The NYISO team expressed their interest in using the NREL-developed tool in future integration studies since it provides a unique platform for evaluating stability impacts on the onshore grid.

A list of POIs for 11 offshore projects for which NYISO provided information and full support is shown in Table 2.

Table 2. List of NYISO POIs used for model testing

Queue Pos.	Owner/Developer	Project Name	Plant Size (MW)	POI Name	Region	Utility	Approx. Cable Distance to Shore (miles)	Connection Types
0612	Deepwater Wind South Fork, LLC	South Fork Wind Farm	96	East Hampton 69kV	LI	LIPA	40	AC
0695	Deepwater Wind, LLC	South Fork Wind Farm II	40					
0737	Empire Offshore Wind LLC	El Sunset Park	816	Gowanus Substation 345kV	NY	ConEd	30	AC
0766	Bay State Wind LLC	NY Wind Holbrook (Sunrise)	880	Holbrook 138kV	LI	LIPA	80	VSC-HVDC
1016	Beacon Wind LLC	El Steinway 1	1300	Astoria West 138 kV	NY	ConEd	120	VSC-HVDC
0958	Empire Offshore Wind LLC	El Oceanside	1000	Barrett 138 kV Substation	LI	LIPA	30	AC
0767	Bay State Wind LLC	NY Wind Gowanus	1200	Farragut 345kV (previously @ Gowanus 345 kV)	NY	ConEd	110	VSC-HVDC
0790	Atlantic Shores Offshore Wind Project 2, LLC (EDF)	Atlantic Shores Offshore Wind 9	880	Fresh Kills 345kV	NY	ConEd	70	VSC-HVDC
0738	Empire Offshore Wind LLC	El Melville	816	Ruland Rd. Substation 138kV	LI	LIPA	35	AC
1066	Bay State Wind	NY Wind - Mott Haven	1272	Mott Haven 345kV	NY	ConEd	110	VSC-HVDC
0679	Anbaric Development Partners, LLC	New York City Offshore Wind	1200	W. 49 St 345kV (previously @ Gowanus 345 kV)	NY	ConEd	50	VSC-HVDC

ISO-NE expressed strong interest in this project based on the following actions:

1. Participating in project advisory board. An ISO-NE representative (Xiaochuan Lua, Technical manager) has been engaged in industry advisory board meetings, project approach and scenario discussions and has provided detailed information about operation of their system, planned transmission reinforcements, planned offshore projects, and their POIs.
2. ISO-NE provided their 2026 light load case dynamic PSS/E models with three offshore WPPs integrated with onshore substations in Rhode Island and Massachusetts.
3. ISO-NE team provided a set of ISO documents and reports related to their own integration studies, identified challenges and system limitations, and planned upgrades and reinforcements.
4. The ISO team expressed their interest in using the NREL-developed tool in future integration studies since it provides a unique platform for evaluating stability impacts on the onshore grid.
- 5.

A list of POIs for three offshore projects for which ISO-NE provided information and full support is shown in Table 3.

Table 3. List of ISO-NE POIs used for model testing

Project	Capacity	POI	POI capacity
Vineyard Wind 1	800 MW	Davisville (RI)	871 MW capacity
Revolution Wind	704 MW	Barnstable	800 MW
Park City Wind	804 MW	West Barnstable	2, 576 MW

2.3 How ISOs Can Use NREL’s Method

A PSS/E-based traditional modeling approach used by ISOs for reliability and planning studies is not sufficient to investigate new, evolving stability problems in grids with high shares of IBRs such as offshore WPPs (both HVAC- and HVDC-interconnected). The PSCAD software offers superior capability for more accurate representation of wind power, solar PV, battery energy storage, HVDC transmission, STATCOM systems, and protection models to investigate various stability aspects and transient performance in power grids with high levels of IBRs. The PSCAD model enhanced with NREL-developed impedance-scanning and small-signal stability tools allows analysis of potential stability issues and control interactions within

offshore WPPs, between offshore WPPs and onshore grid, and between two or more offshore WPPs interacting through the onshore grid. Commercial E-TRAN software tools are used to interface PSS/E and PSCAD models. All three tools linked through NREL's impedance-scanning tool create a powerful stability assessment platform for ISOs, utilities, and project developers. The intended uses of the platform are listed below:

- Identify risks of different types of dynamic interactions between offshore WPPs, submarine HVAC and HVDC tie-lines, and the onshore network with different POI characteristics and develop impedance-based design guidelines using impedance models of offshore wind plants
- Investigate control interactions and stability issues for HVAC- and HVDC-interconnected offshore WPPs
- Investigate operation and control of large Type 4 WTGs connected to the onshore power grid through a voltage source converter–HVDC transmission system
- Explore various active damping schemes through the HVDC converter controls.
- Perform analysis of GFM operation and black start services by offshore WPPs.

3 PSCAD-PSS/E Co-Simulation Platform

3.1 Co-Simulation Workflow

A co-simulation platform that NREL team developed for this project is a combination of three software tools:

- PSS/E – positive-sequence transmission planning and analysis software by Siemens
- PSCAD – electromagnetic transient (EMT) simulation software
- E-TRAN – a software tool to interface positive-sequence phasor models in PSS/E of a large power system, such as the Eastern Interconnection, with the EMT models in PSCAD of power electronics generators, such as offshore WPP with HVAC or HVDC transmission to the grid
- GIST – (PSCAD-based) developed by NREL.

The concept of co-simulation platform is explained in Figure 1. To represent onshore grids, we use PSS/E positive-sequence power simulator software, which is an adequate software tool for simulating dynamics of large, interconnected power systems with a library of standard sub-models for generation and loads. Custom models can be developed in PSS/E as well. PSS/E is widely used by ISOs, utilities, and developers. However, PSS/E capabilities are not sufficient to investigate stability problems in inverter-dominated grids as described earlier in this report. PSCAD software offers superior capability for more accurate representation of wind, PV, HVDC, STATCOM, battery energy storage, synchronous condensers, and protection models to investigate various stability aspects and transient performance in power grids with high levels of IBRs. Models of both HVAC- and HVDC-interconnected offshore WPPs have been developed for this project by the NREL and EPRI teams. The PSCAD model is enhanced with the NREL-developed GIST, which is a small-signal stability tool (described later in this section) allowing analysis of potential stability issues and control interactions within offshore WPPs, between offshore WPPs and the onshore grid, and between two or more offshore WPPs interacting through the onshore grid. Commercial E-TRAN software tools are used to interface PSS/E and PSCAD models.

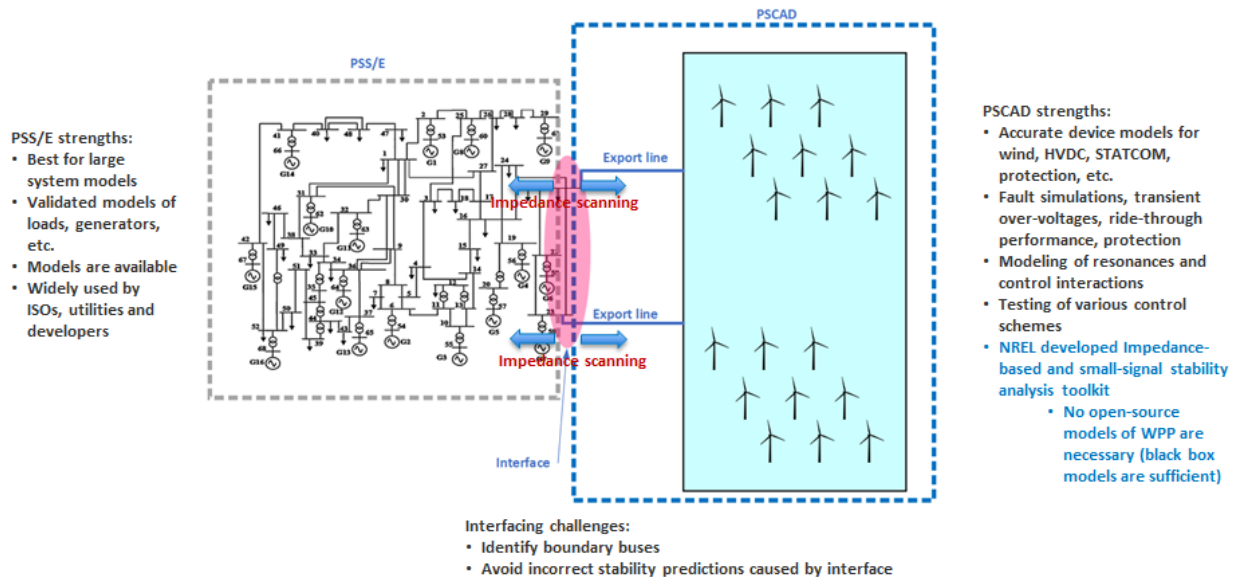


Figure 1. Concept of co-simulation

3.2 NREL's Grid Impedance Scan Tool (GIST)

NREL's GIST, developed earlier under other DOE-funded projects, has recently emerged as an award-winning, trusted, and unique solution to identify and prevent grid oscillations anywhere [8]. GIST scans the electrical behavior of any network and grid devices at different frequencies to discover problematic electrical interactions. GIST can scan black-box models of devices in a software version, or the physical device itself in-the-loop with simulated grid networks. This is analogous to spectroscopy for the power system to determine how it behaves at different frequencies. To date, GIST has helped grid operators and manufacturers worldwide avoid multimillion-dollar curtailments of renewable energy. GIST is the basis for several interconnection standards, and as partners attest, is an essential tool for reducing grid instabilities.

For this project, GIST became an integral part of the PSS/E-PSCAD co-simulation platform, making the whole NREL approach unique and very useful for identifying and mitigating oscillations that may be present in IBR-dominated grids. A general diagram explaining the GIST application is shown in Figure 2. Main capabilities of GIST include:

- Scans IBR and grid impedances in PSCAD across wide range of frequencies
- Evaluates the impact of IBRs on grid stability using impedance scans
- Conducts fully automated scans at POIs in both directions; scans a PSCAD model of IBRs (offshore WPPs in this case) and a PSS/E model of the whole interconnection
- Produces scan results when the fundamental frequency is not stationary (deviates from 60 Hz)
- Outputs in all reference frames, including stationary, rotating (d-q), and power-domain.

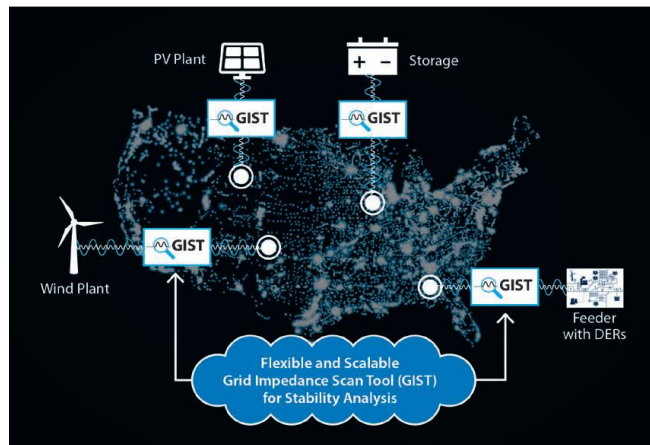


Figure 2. GIST general diagram

3.3 Co-Simulation Workflow

NREL has developed an algorithm for combining the PSS/E and PSCAD models for co-simulation files as described in Figure 3. Original PSS/E power flow and dynamic cases of the whole U.S. Eastern Interconnection are updated to include offshore wind plant models to verify the dispatches and adequate power flow and dynamic performance of the system under various contingencies. NREL-developed PSCAD models of offshore WPPs are then converted into a format suitable for hybrid co-simulation using the E-TRAN conversion tool.

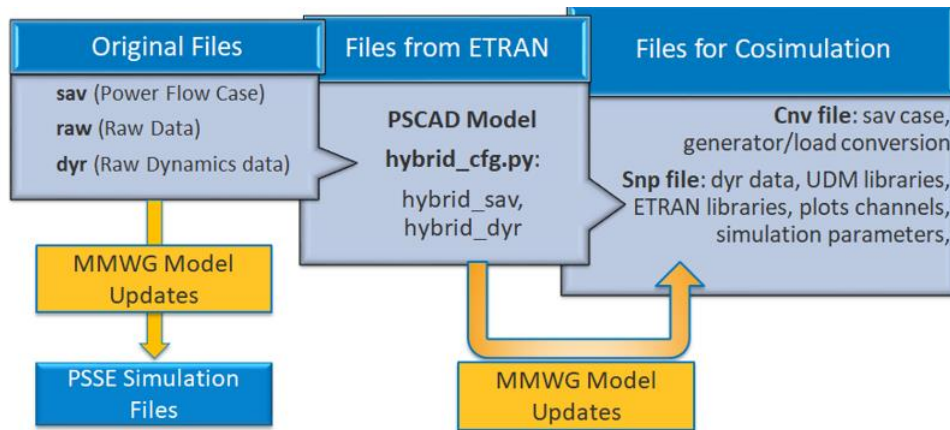


Figure 3. Co-simulation data flow

EPRI updated the original 2025 light load PSS/E cases of the Eastern Interconnection (developed by the Eastern Interconnection Planning Committee and referred to as multiregional modeling working group models) to include offshore WPPs interconnected to the PJM and NYISO grids. NREL did the same for the ISO-NE grid. In total, six offshore wind plants were integrated with the PSS/E model for NYISO (Table 4), three for ISO-NE (Table 5), and one for PJM (Indian River POI).

Table 4. List of NYISO offshore plants

Queue Pos.	Owner/Developer	Project Name	Plant Size (MW)	POI Name	Region	Utility
0612	Deepwater Wind South Fork, LLC	South Fork Wind Farm	96	East Hampton 69kV	LI	LIPA
0695	Deepwater Wind, LLC	South Fork Wind Farm II	40	East Hampton 69kV	LI	LIPA
0737	Empire Offshore Wind LLC	EI Sunset Park	816	Gowanus Substation 345kV	NYC	ConEd
0766	Bay State Wind LLC	NY Wind Holbrook (Sunrise)	880	Holbrook 138kV	LI	LIPA
1016	Beacon Wind LLC	EI Steinway 1	1300	Astoria West 138 kV	NYC	ConEd
0958	Empire Offshore Wind LLC	EI Oceanside	1000	Barrett 138 kV Substation	LI	LIPA
0767	Bay State Wind LLC	NY Wind Gowanus	1200	Farragut 345kV (previously @ Gowanus 345 kV)	NYC	ConEd
0790	Atlantic Shores Offshore Wind Project 2, LLC (EDF)	Atlantic Shores Offshore Wind 9	880	Fresh Kills 345kV	NYC	ConEd
0738	Empire Offshore Wind LLC	EI Melville	816	Ruland Rd. Substation 138kV	LI	LIPA
1066	Bay State Wind	NY Wind - Mott Haven	1272	Mott Haven 345kV	NYC	ConEd
0679	Anbaric Development Partners, LLC	New York City Offshore Wind	1200	W. 49 St 345kV (previously @ Gowanus 345 kV)	NYC	ConEd

Table 5. List of ISO-NE projects

Project name	Plant size (MW)	POI name	Buses
Vineyard Wind 1	800	Barnstable, West Barnstable	111365, 111367
Revolution Wind	704	Davisville	117539, 117542, 117551, 117554
Park City Wind	804	Barnstable, West Barnstable	111389, 111390

Once the PSS/E cases with offshore WPPs were established, the next step was to replace some of the offshore WPP models (including models of offshore transmission) by detailed PSCAD models to evaluate impacts of offshore wind generation on grid stability. First, the NREL team demonstrated co-simulation

between a PSS/E model of a simple 39-bus system and a PSCAD model of an offshore WPP. When using the PSS/E model of the whole Eastern Interconnection, the NREL team encountered several simulation errors. These errors were related to interfacing the PSS/E model of the whole Eastern Interconnection with the PSCAD model because the programs developed by Eastern Interconnection Planning Commission to set parameters of user-defined models in the multiregional modeling working group models were not compatible with the PSS/E models of Eastern Interconnection generated by E-TRAN software tool after removing the part of the network modeled inside PSCAD.

The NREL team had to come up with a solution to many co-simulation errors that occurred when generating files for hybrid co-simulation and trying to establish communication between PSS/E and PSCAD in boundary buses. This was a long debugging process based on communication with E-TRAN tech support that took much longer than originally planned. This process slowed down the progress in this reporting period. Eventually, all these issues were resolved, and the team is now all set to conduct co-simulations in an error-free environment.

Example of a valid co-simulation response is explained here. The PSCAD Model with Eastern Interconnection buses 243441 and 243205 is shown in Figure 4, where bus 243205 is the boundary bus with the PSS/E model. Eastern Interconnection PSS/E model with Bus 243441 (Figure 5) is disabled from the network, and an hybrid bus generator is added at boundary bus 243205 to communicate with the PSCAD part of the system. The hybrid bus generator model is added by the E-TRAN software tool, and it communicates with the PSCAD part of system at every time step.

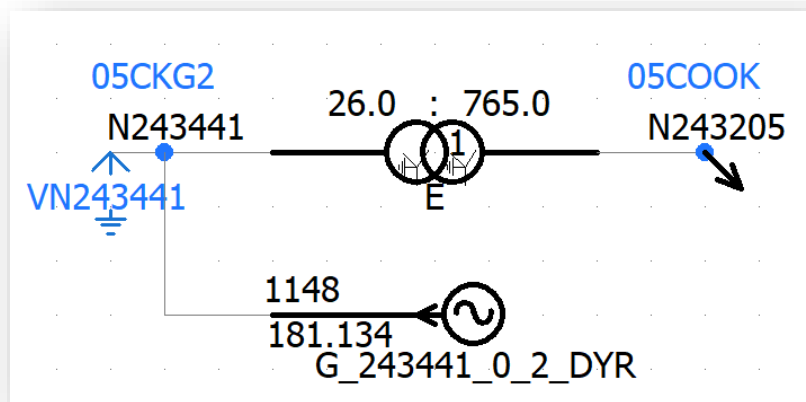


Figure 4. PSCAD model with buses 243441 and 243205

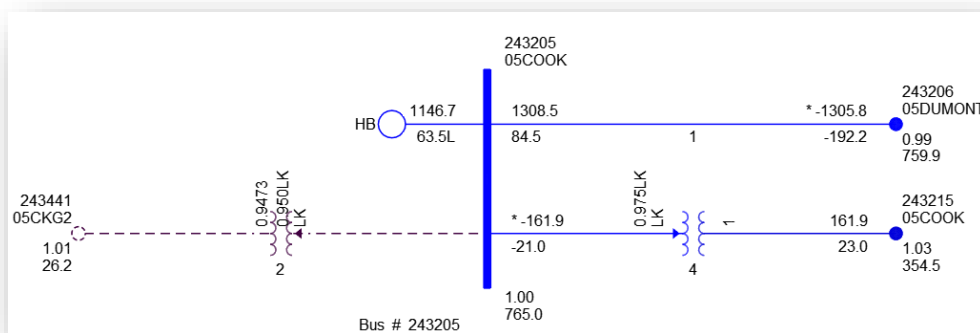


Figure 5. PSS/E model with bus 243441

Dynamic simulations were performed to verify that co-simulation of the whole Eastern Interconnection model in PSS/E with a PSCAD model is working in a desired manner. In one example, a three-phase fault is applied at bus 129421 at $t = 3\text{s}$ for 150ms. Voltage response at the faulted bus and the PSCAD-PSS/E boundary bus can be observed from the PSCAD simulation results shown in Figure 6. Note that the faulted bus 129421 represents the Holbrook substation in NYISO territory, which will be used as a point of interconnection with an 800 MW offshore wind plant connected by an HVDC transmission line.

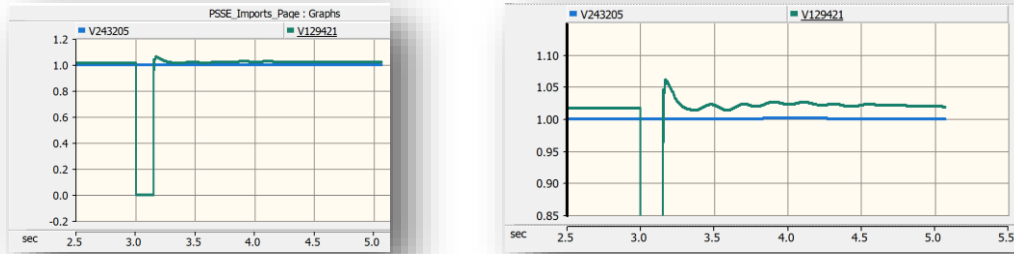


Figure 6. Typical co-simulation response (PSS/E – left, PSCAD – right)

The project team has successfully established co-simulation between the PSS/E model of the whole Eastern Interconnection with PSCAD models of offshore WPPs. As a next step, we used the co-simulation platform to connect the PSCAD models of all offshore wind plants with the Eastern Interconnection PSS/E model at POIs to evaluate the impact of offshore wind on onshore grid stability in the NYISO, ISO-NE, and PJM grids.

3.4 Boundary Between PSCAD and PSS/E Models

NREL is using the E-TRAN+ co-simulation module from Electranix for establishing and designing the interface between the EMT-PSCAD models of offshore WPPs and the positive-sequence PSS/E models of the onshore bulk power system. Two parallel efforts are being undertaken in the co-simulation.

First, the co-simulation task focused on using small test cases to evaluate the impact of partitioning a power system into the EMT and phasor models. The impact of partitioning the system—the boundary between the PSS/E and PSCAD models—on accuracy is being studied by performing transient simulations, comparing different selection of boundaries, and using the impedance scan tool. The approach for selecting the boundary using the GIST is to compare the impedance response of the network seen by an offshore WPP for different boundaries between PSS/E and PSCAD models set in terms of distance measured as the number of buses from the POI. If the impedance response from the POI stops changing when the boundary of PSS/E is pushed further away from the POI of an offshore WPP, it indicates that there is no further gain in including a further part of the network in PSCAD, which is computationally more intensive.

The project team evaluated the impact of partitioning a power system model into PSCAD and PSS/E. Figure 7 shows a simple two-area system model used to evaluate the selection of a boundary between the PSS/E and PSCAD models. Figure 8 compares the response of the output

of a generator at bus 3 when the load at bus 9 is increased by 30 MW for full PSS/E, full PSCAD, and EMT-phasor hybrid co-simulation models. The co-simulation model considers the boundary at two places. For the first case, everything on the left of bus 1 is kept inside PSCAD and the rest of the system is modeled in PSS/E. For the second case, everything on the left of bus 7 is modeled in PSCAD and the rest of the system is modeled in PSS/E. Clearly all simulation models—full EMT, full positive-sequence, and hybrid co-simulation cases—give similar results. As the next steps in the report, we used the impedance scan tool to evaluate the selection of the boundary between the PSCAD and PSS/E models for larger systems.

The second part of the co-simulation task was focused on preparing PSS/E models of the onshore grid in PJM and NYISO territory for co-simulation with the high-fidelity EMT-PSCAD models of the offshore network including offshore WPPs, transmission cables, and onshore and offshore substations. Co-simulations for POIs in the PJM, NYISO, and ISO-NE territories are discussed later in this report.

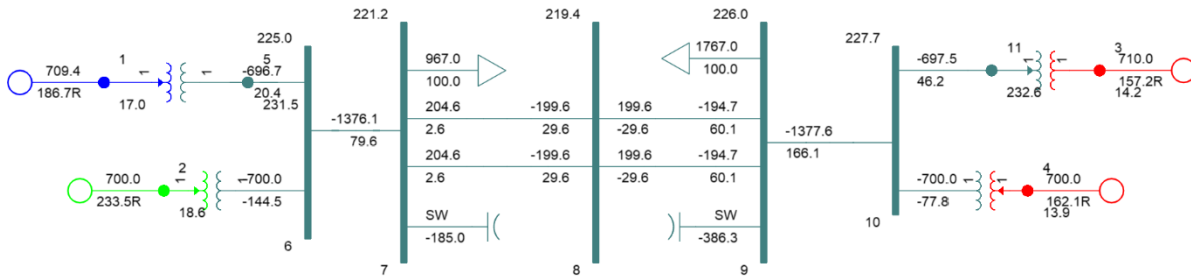


Figure 7. A two-area system model is used to evaluate the impact of the boundary between the PSCAD and PSS/E models on the accuracy of stability analysis.

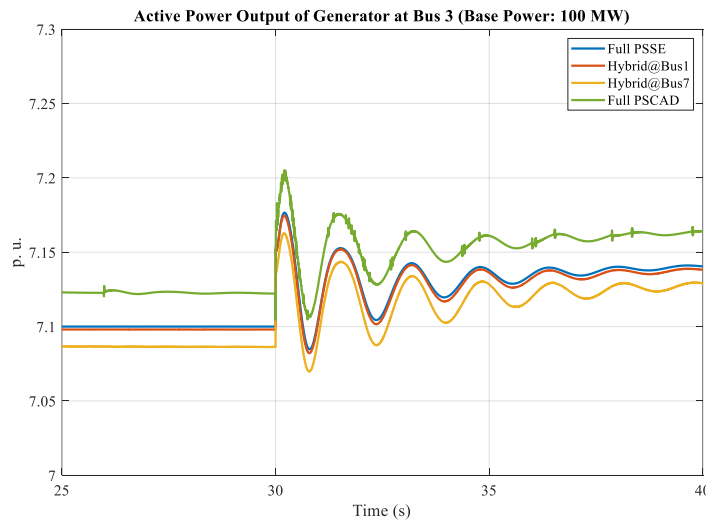


Figure 8. Comparison of response for full PSS/E, full PSCAD, and EMT-phasor hybrid co-simulation (boundary at bus 1 and bus 7) during a transient event.

3.5 Models of Offshore Wind Power Plants

Type 4 wind turbines use a full-scale power converter, which acts as interface between generator stator

windings and the grid. The Type 4 turbine can be geared or gearless as shown in Figure 9 where a permanent magnet, low- speed synchronous generator is coupled directly with a wind rotor without a gearbox. The turbine converter operates at 690 VAC voltage level (in most turbine models). A step-up transformer is used to bring this voltage up to 66 kV collector system voltage level.

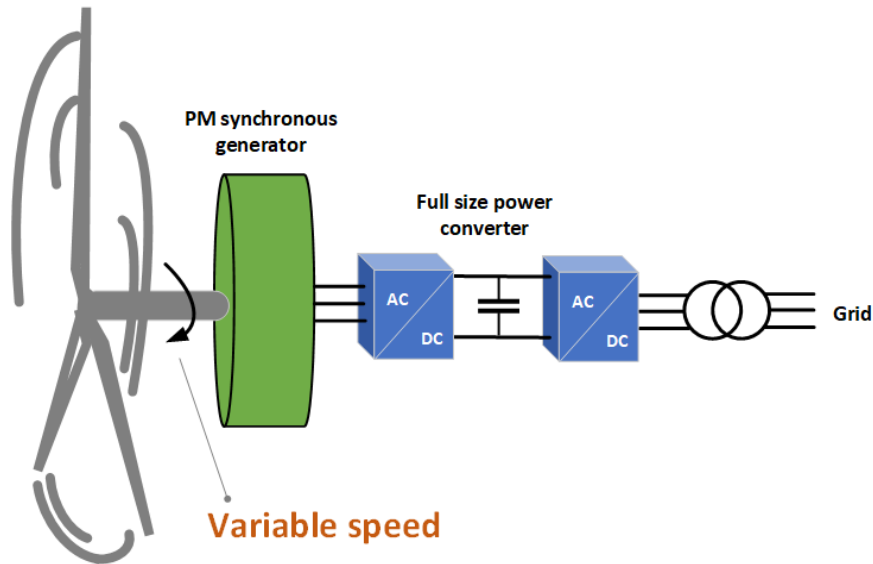


Figure 9. Type 4 wind turbine generator topology (direct-drive gearless)

The following turbine- and plant-level active and reactive power controls have been implemented in the model using commercially available GE WPP control products [12]:

- Turbine-level inertial control—ability of a single turbine to provide inertial response
- Plant-level frequency droop control—ability of the plant to provide frequency droop response (tested in “plant-of one” configuration)
- Plant-level active power control—ability of the plant to follow active power set point (tested in “plant-of one” configuration)
- Plant-level reactive power/voltage/power factor control (tested in “plant-of one” configuration)

All of the above controls have also been fully tested and validated at an NREL test site using a 1.5-MW GE wind turbine generator.

The Type 4 wind turbine model with detailed controls is established in PSCAD simulation, which is illustrated Figure 10. The mechanical components, including the turbine shaft train, are simulated. The turbine torque controller determines the maximum power set point based on turbine rotor speed. Pitch controllers will be enabled during high wind speed conditions in order to prevent the overspeed of the turbine rotor. The model of the permanent magnet synchronous generator and the control of the machine side converter are simplified as a controllable DC current source. By ignoring the power loss at the machine side, the power set point P_{ref} derived from torque control can be used to calculate the current reference of DC current source. The power flow into the grid-side converter is considered as electromagnetic power of the permanent magnet synchronous generator. The grid-side converter and associated controls are modeled in detail to better study possible control interactions. To better simulate system dynamics of a wind plant, 8 wind turbines are connected in a string using current scaling. The control diagram of the torque controller, pitch controller, and grid-side converter controller is presented in Figure 11.

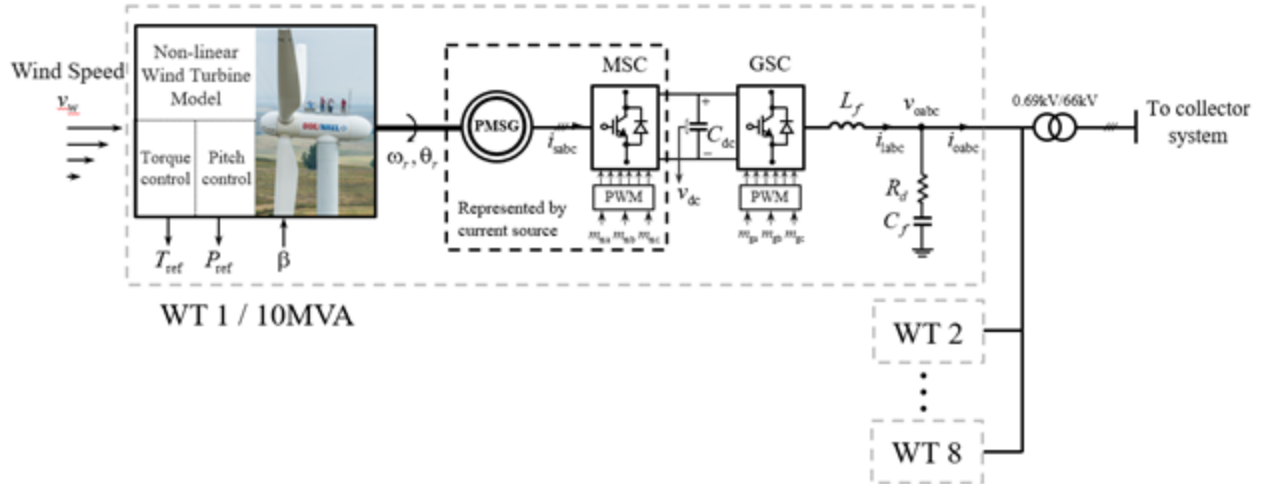


Figure 10. Type 4 wind turbine model

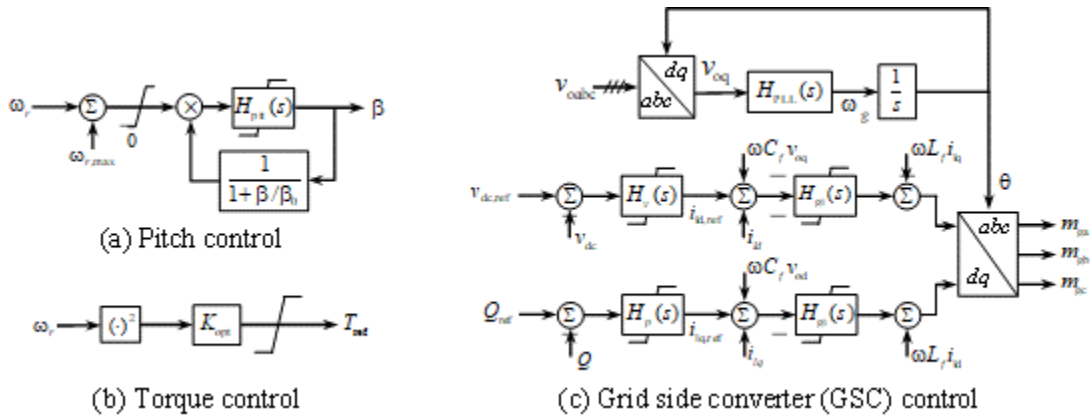


Figure 11. Type 4 wind turbine control diagram

Controls for various types of grid services have been implemented in the NREL PSCAD model, including inertial response (Figure 12), primary frequency, frequency droop response (Figure 13), and voltage control (Figure 14).

For inertial response control, we used the approach allowing a 10%–15% short-term increase of turbine power. More aggressive inertial response algorithms are possible. However, such a conservative approach takes into account loading and structural limitations and has been implemented in commercial WPPs.

Inertial response by wind turbines does not require curtailment since it extracts available kinetic energy stored in rotating blades, gearbox, and generator. For any other active power service that requires up-regulation, some level of curtailment is needed. Both Type 4 and Type 3 turbine models have the capability to curtail the wind turbines to a certain level below available wind power, so they can provide fast frequency response and primary frequency response as well as participate in automatic generation control. A control diagram for primary frequency control or frequency droop response is shown in Figure 13. This control has a programmable droop setting (typically 5%) and dead bands. Similarly, voltage droop control is shown in Figure 14.

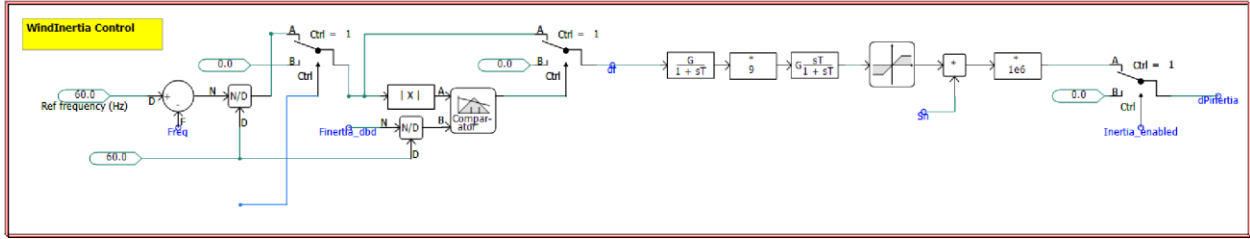


Figure 12. Inertia control implemented in PSCAD

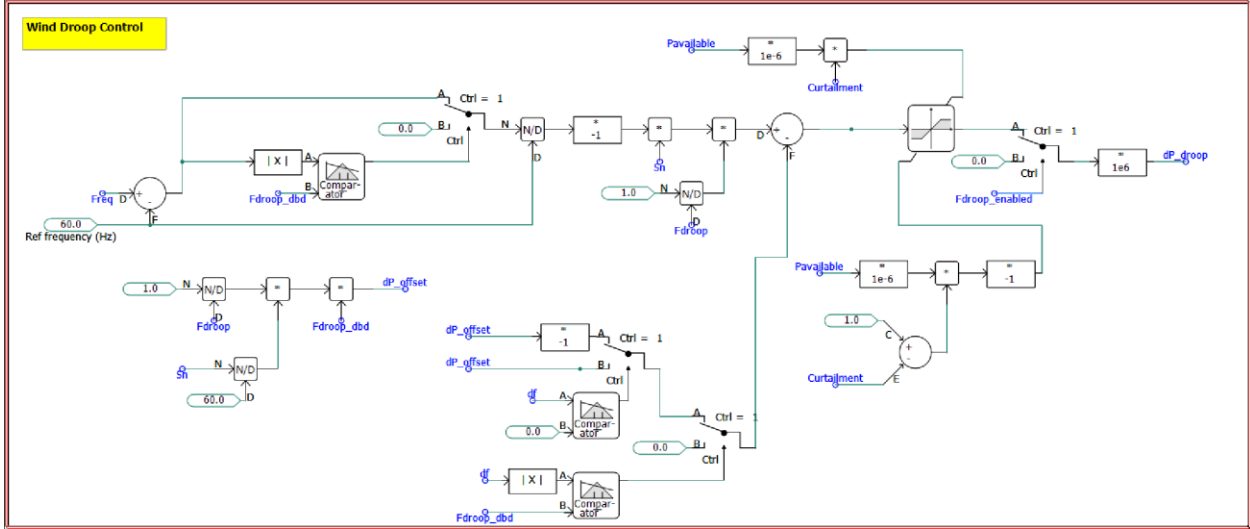


Figure 13. Frequency droop control implemented in PSCAD

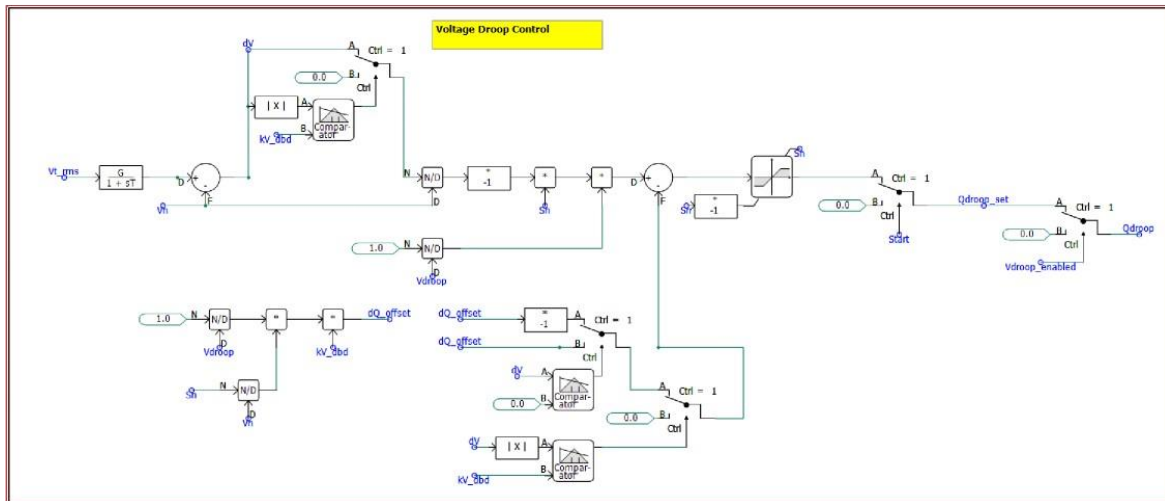


Figure 14. Voltage control implemented in PSCAD

In addition to the Type 4 wind turbine model, the NREL team also developed a model of a Type 3 wind turbine as well since it was required by the project statement of work. It is important to note that the use of Type 3 wind turbines in offshore WPPs is not planned in the future anywhere in the world, including U.S. offshore development. We conducted such simulations to satisfy the requirement of the NORWDC/NYSERDA contract. Simulation results for Type 3 and Type 4 offshore WPPs were conducted with results shown later in this report.

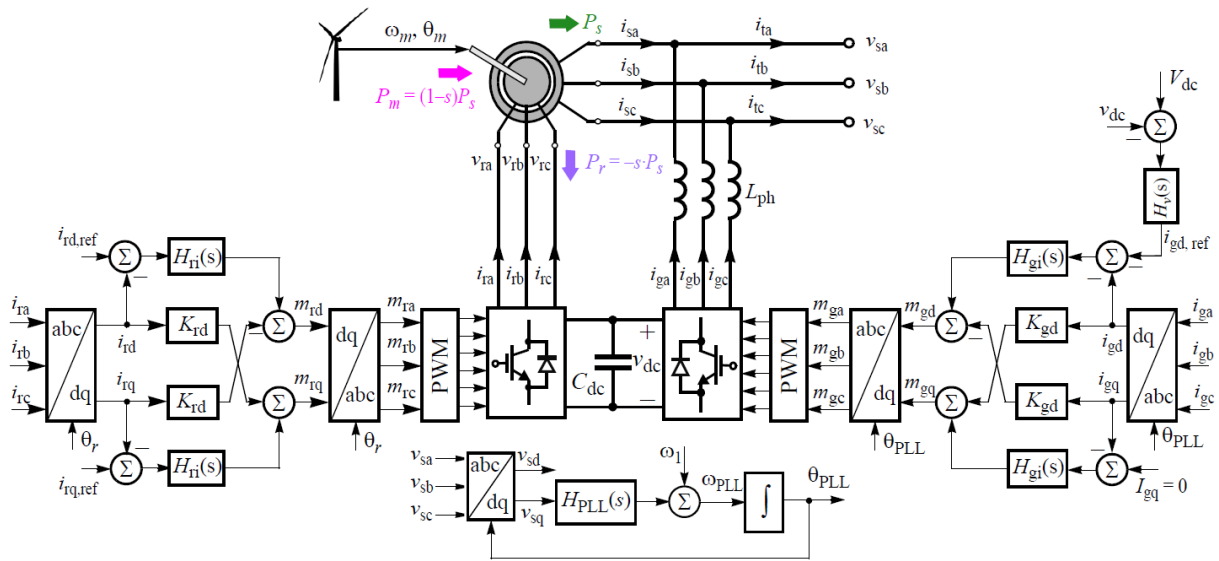


Figure 15. Diagram of Type 3 wind turbine generator

Figure 15 describes the Type 3 turbine control diagram, The letters “s” and “r” indicate variables that are related to the stator and rotor windings of the doubly fed induction generator, respectively, and the letter “g” indicates variables that correlate to the grid-side converter. The current references of the rotor-side converter, rotor reference currents $i_{rd,ref}$ and $i_{rq,ref}$, are obtained from the outer-loop control depending on turbine active or reactive power controls that are enabled.

The full WPP models implemented in PSCAD for HVAC- and HVDC-interconnected offshore WPPs are shown in Figure 16 and Figure 18, respectively. Both models use a 66-kV collector system with 10- to 15-MW Type 4 wind turbines. The HVAC-interconnected plant is modeled with a 30-mile, 230-kV submarine export cable with shunt compensation. Models of a STATCOM, battery system (either GFM or GFL), or synchronous condensers can be added to the onshore substation. A model of battery energy storage of desired power and energy rating can be added to the onshore substation as well.

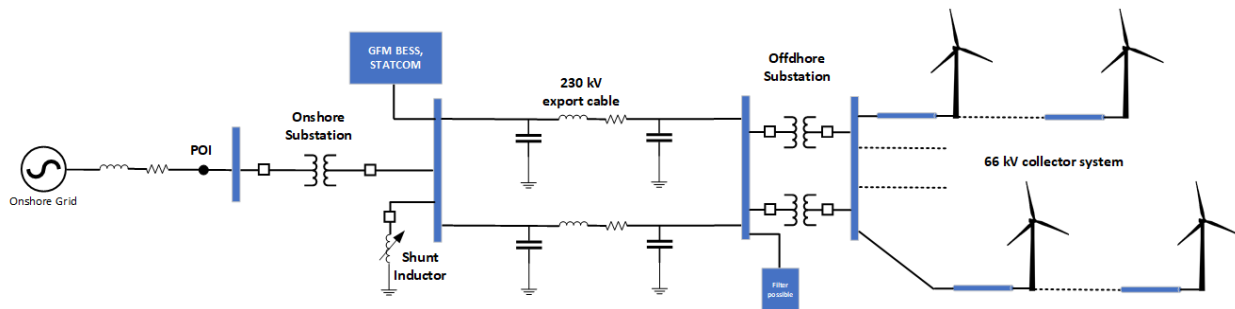


Figure 16. HVAC-interconnected offshore WPP

Figure 17 is a diagram of the HVAC-interconnected offshore WPP realized in PSCAD. The model can be easily configured to include a number of individual 100–600 MW plants connected to the same onshore POI. Dynamic and transient performance of individual plants as well as interactions between plants connected to the same POI can be modeled this way. Cable impedances and lengths as well as the SCR at the POI can be programmed, so performance of the plant is tested under strong and weak grid conditions.

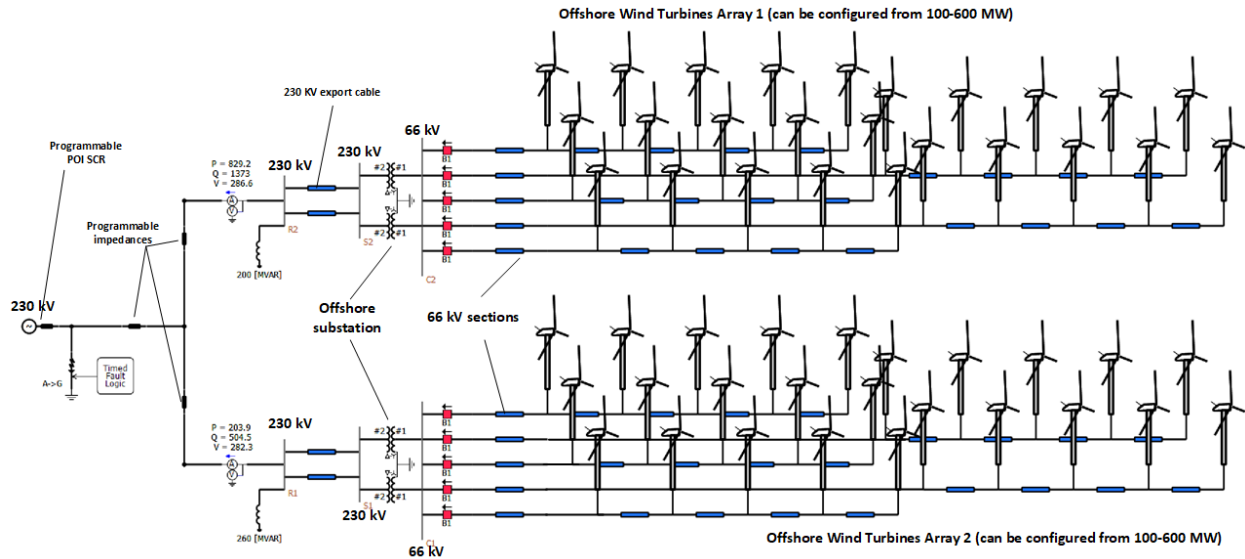


Figure 17. Detailed PSCAD model of HVAC-interconnected offshore WPPs with Type 4 wind turbines

The HVDC-interconnected plant uses a 320-kV DC export system with HVDC MMC terminals in both sending and receiving ends, as shown in Figure 18.

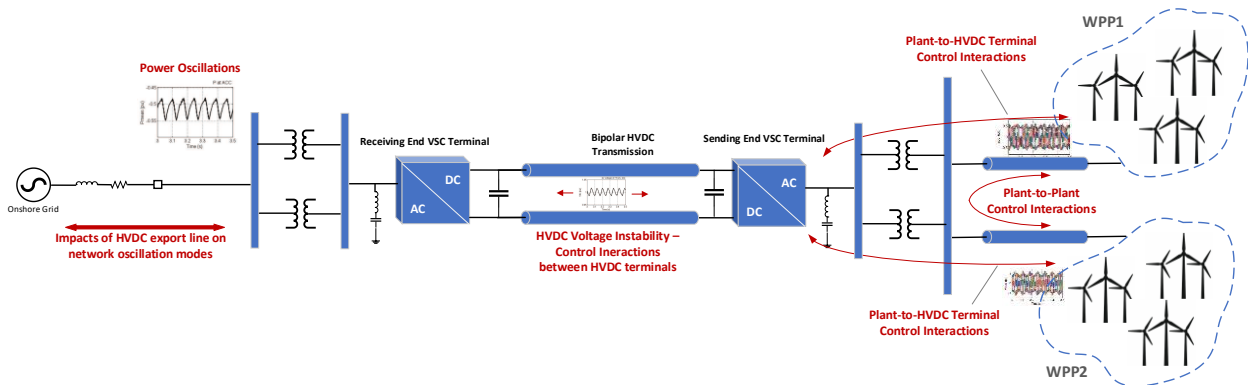


Figure 18. HVDC-interconnected offshore WPP

The EPRI team developed an average MMC-HVDC system model in PSCAD [13]. To emulate the switching of the MMC submodules, the EPRI team used voltage sources with nearest level control [17] assuming equal voltages across each submodule’s capacitors. Wind turbine models can be combined to represent full WPP models and then coupled with models of HVAC or HVDC transmission. The model of symmetric-monopole 320-kV HVDC transmission system developed by the EPRI team is shown in Figure 19. MMC-HVDC terminals are connected to the model of onshore WPP at one end and to the grid on the other. In this case, a model of the synchronous condenser at the grid POI is also shown.

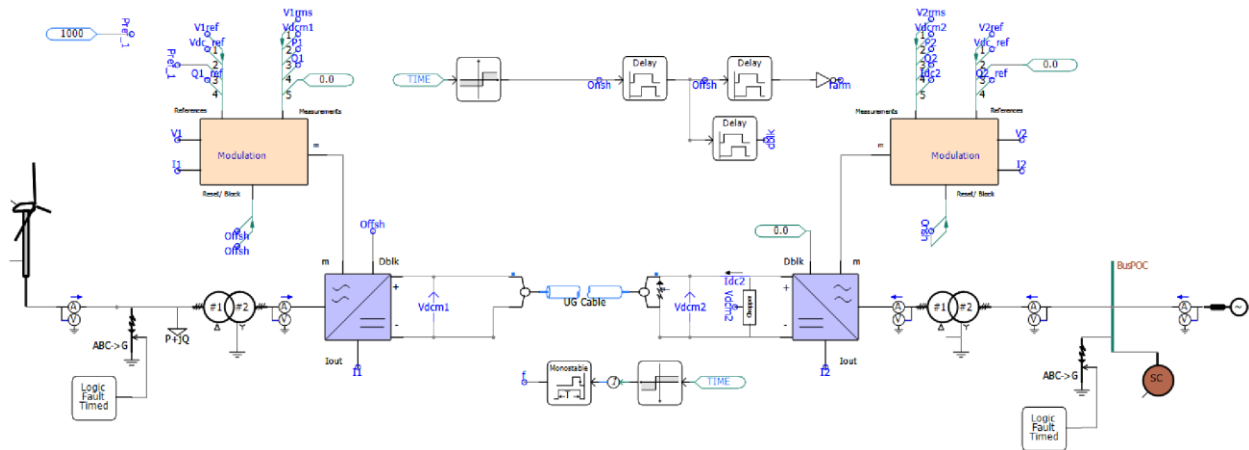


Figure 19. Point-to-point HVDC transmission model (symmetric-monopole 320-kV DC, 1000 MW)

Models of both onshore and offshore HVDC terminals can operate in either GFL or GFM modes. Simplified control diagrams of for these modes are shown in Figure 20 and Figure 21. In GFM mode, the HVDC inverter models also have a “soft” start mode enabled allowing for black start of offshore assets without excessive inrush currents during energization of offshore plant transformers and cables.

Grid Following Modes

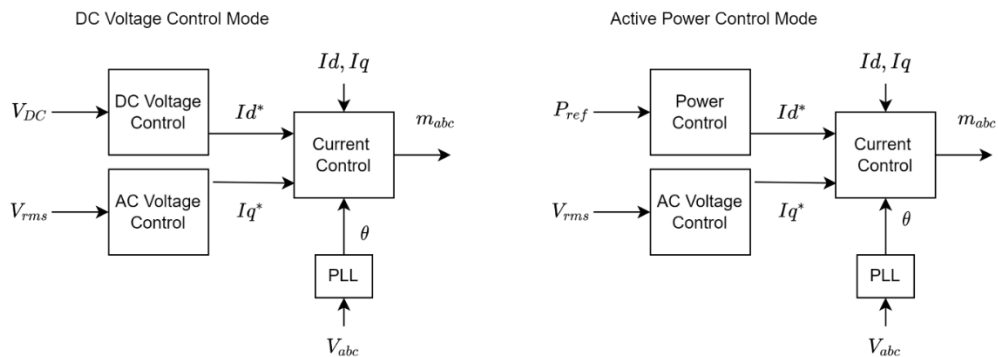


Figure 20. HVDC MMC control diagram in GFL mode

Droop Based Grid Forming Modes

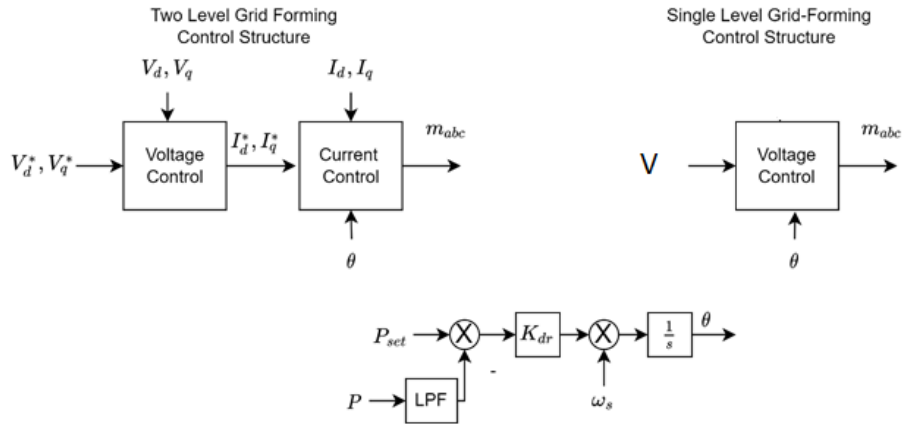


Figure 21. HVDC MMC controls in GFM mode [14]

The model of the HVDC MMC transmission system allows for emulating the following control modes:

- GFL mode [15]:
 - DC control
 - Active power control
 - Voltage control with choice for intermediate reactive power controller
- GFM mode:
 - Droop control
 - Voltage/current control mode
 - Voltage control mode
- Current limitation
 - P or Q current priority
 - Voltage-dependent active power current limitation

Results of example case studies for HVDC line initial energization and voltage fault ride-through are shown in Figure 22 and Figure 23, respectively, for a test system shown in Figure 24 (cable model used for this test from [16]). In the first case, a 1000-MVA offshore WPP (Type 4 wind turbines) is interconnected with the onshore grid via a 1200-MVA MMC-HVDC export system. Energization of onshore terminals happens at $t=0.25$ s is followed by energizing of an offshore GFM terminal at $t=2.25$ s. Offshore AC voltage is formed with enforced ramp to avoid inrush currents in offshore substation transformers and collector system.

In the second case, a three-phase bolted fault to ground applied for 0.15 s on the HV side of onshore transformer. Active power current recovery is tuned to 5 per unit/s. DC side voltage is managed by a chopper circuit. The terminal voltage recovers within 0.25 s after the fault (0.1 s after clearance).

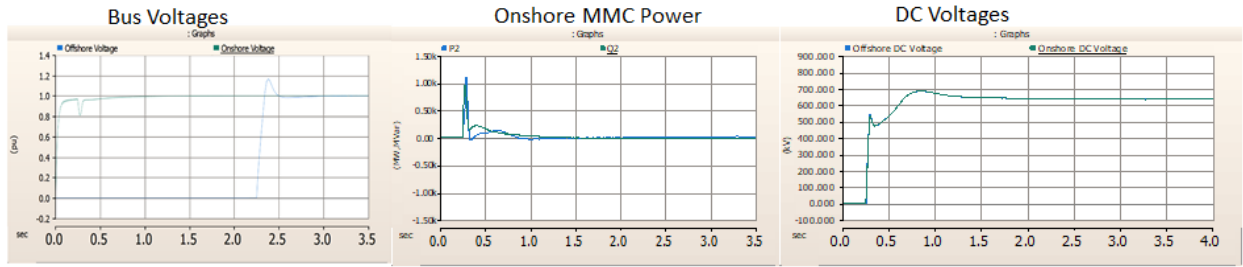


Figure 22. HVDC energization

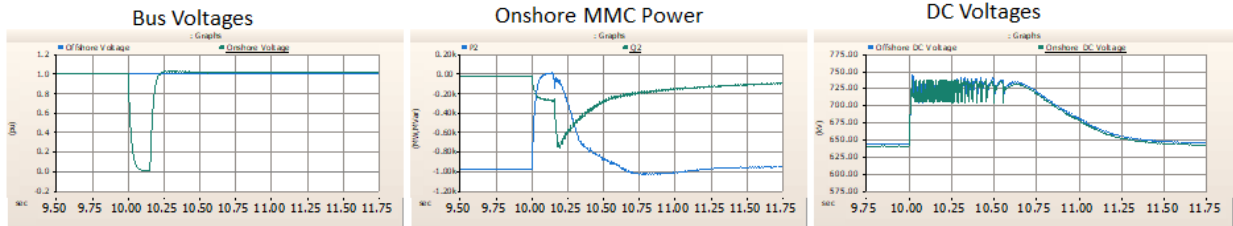


Figure 23. HVDC fault ride-through

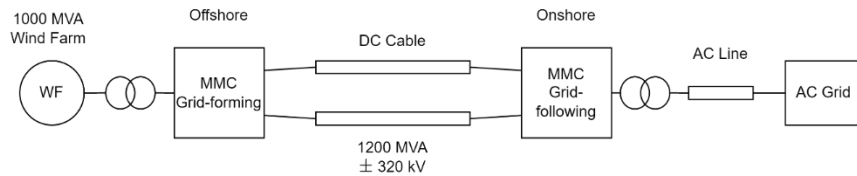


Figure 24. HVDC system diagram for a test system

3.6 Simulation Results for Type 3 and Type 4 Wind Power Plants

In this section, we show results of simulations when Type 3 and 4 offshore WPPs are interconnected with the onshore grid via HVAC and HVDC transmission. For the HVAC case, we use the example of the Indian River POI in PJM footprint, as shown in Figure 25. In this case, we added 250 MW of Type 3 wind power to the modeled POI that already had two Type 4 offshore WPPs with a combined capacity of ~1 GW. All plants are using a 66-kV offshore collector system. This voltage is stepped up to 230 kV by an offshore substation transformer. In the onshore substation, the 230 kV voltage is stepped down to 138 kV for interconnection with the PJM system.

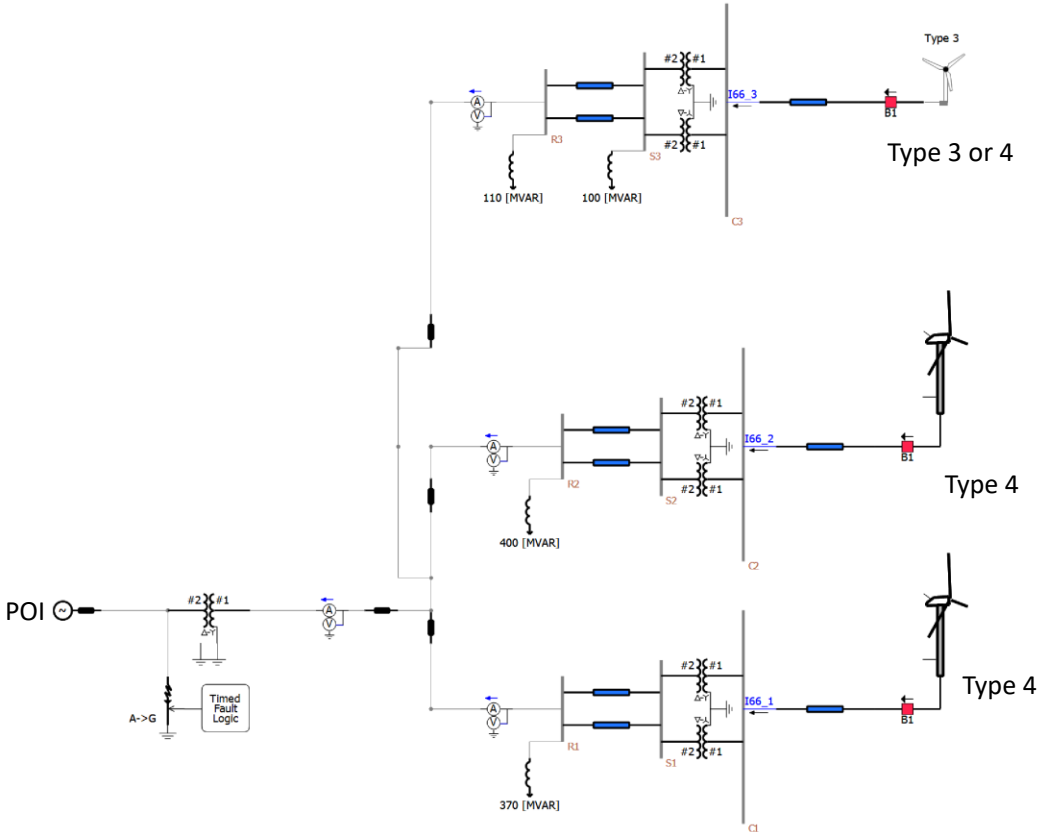


Figure 25. Model of the Indian River POI with Type 3 and Type 4 HVAC-interconnected offshore WPPs

Results of simulations for the system shown in Figure 25 are listed below:

- Figure 26: All three plants experience a three-phase 100-ms voltage fault at the POI. Successful ride-through is demonstrated by all three plants (graph a). Active and reactive power during the fault is shown in graphs c and d. Currents at the 230-kV landing point are shown for all plants (figures e, f, and g). Total currents in the 66-kV collector systems in each plant are shown in figures i, j, and k.
- Figure 27: All three plants experience a single-phase 200-ms voltage fault at the POI. Successful ride-through is demonstrated by all three plants.
- Figure 28: All plants experience a step change in the POI SCR (from 5 to 2) caused by a line trip in the 138-kV network. Successful ride-through is demonstrated by all three plants.
- Figure 29: All plants experience a 30 deg phase jump in POI voltage. Successful ride-through is demonstrated by all three plants. A significant DC component is observed in the current produced by the Type 3 plant (expected behavior by doubly fed induction generator-based wind power generation).

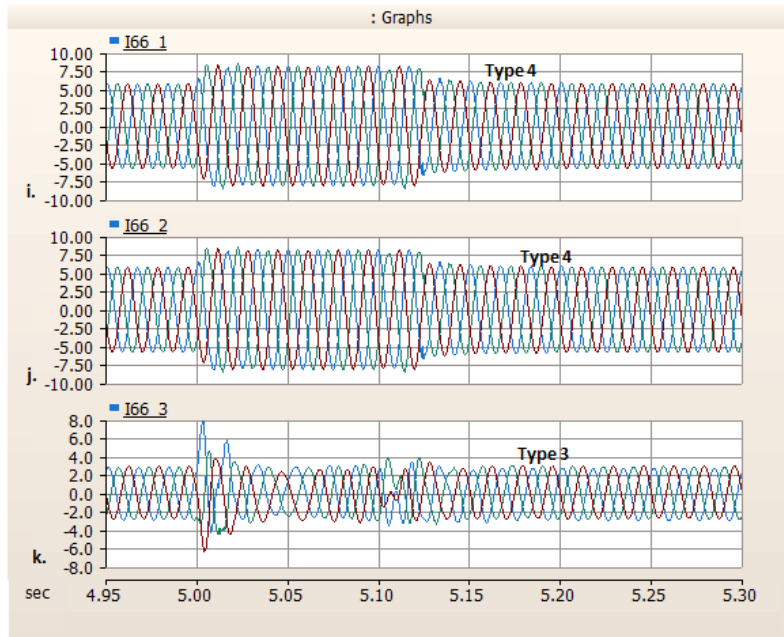
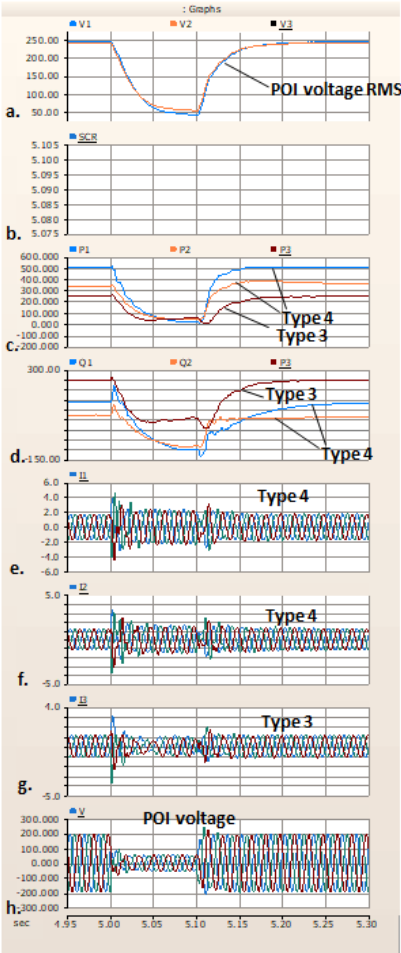


Figure 26. Three-phase low-voltage ride-through performance at the PJM Indian River POI (two Type 4 and single Type 3 WPPs, HVAC interconnection)

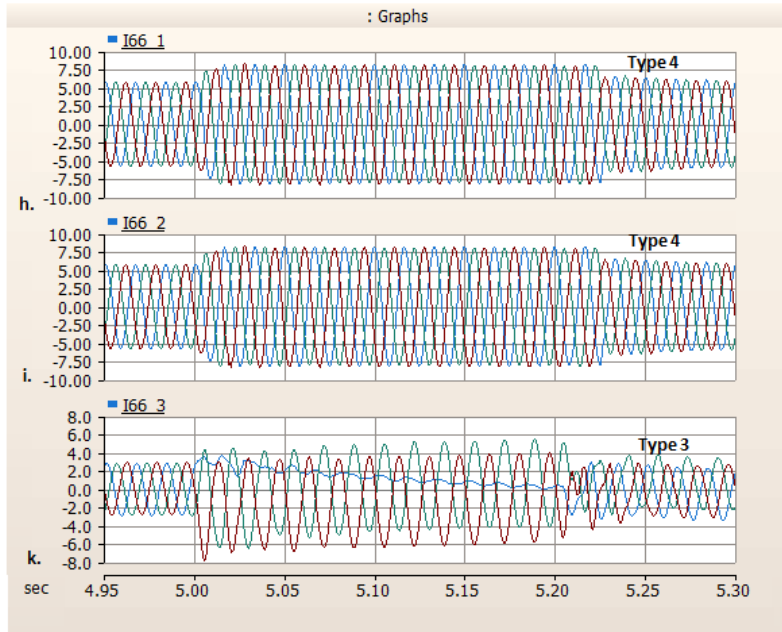
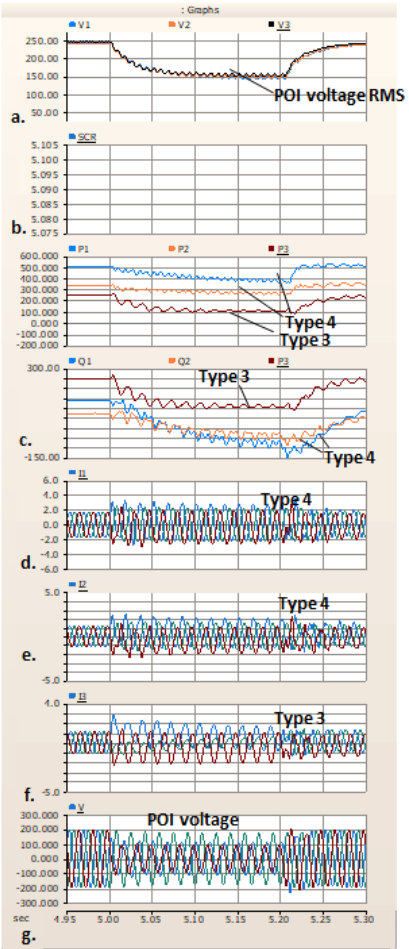


Figure 27. Single-phase low-voltage ride-through at the PJM Indian River POI (two Type 4 and single Type 3 WPPs, HVAC interconnection)

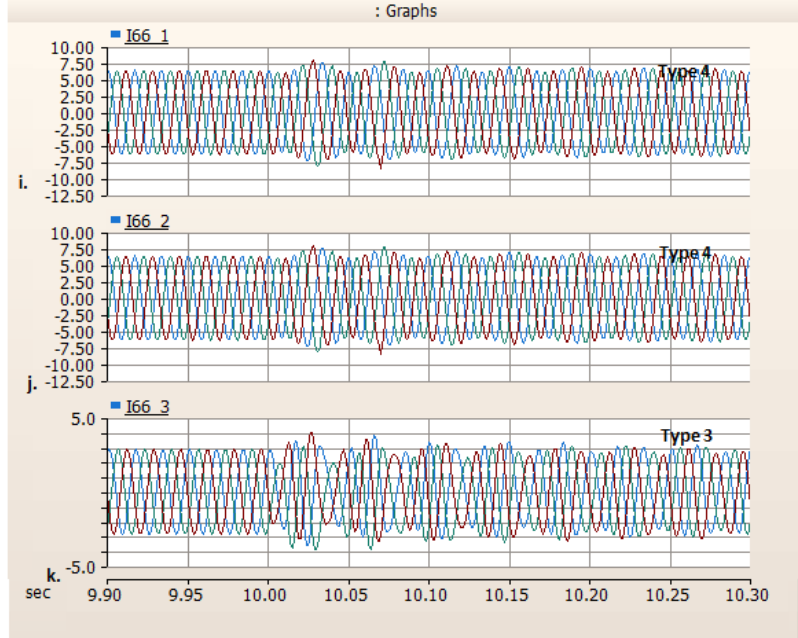
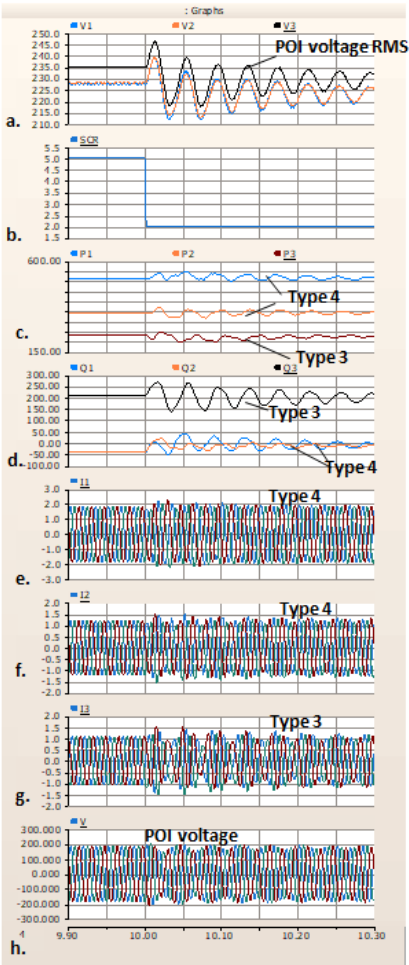


Figure 28. Response of PJM Indian River POI to SCR step change (two Type 4 and single Type 3 WPPs, HVAC interconnection)

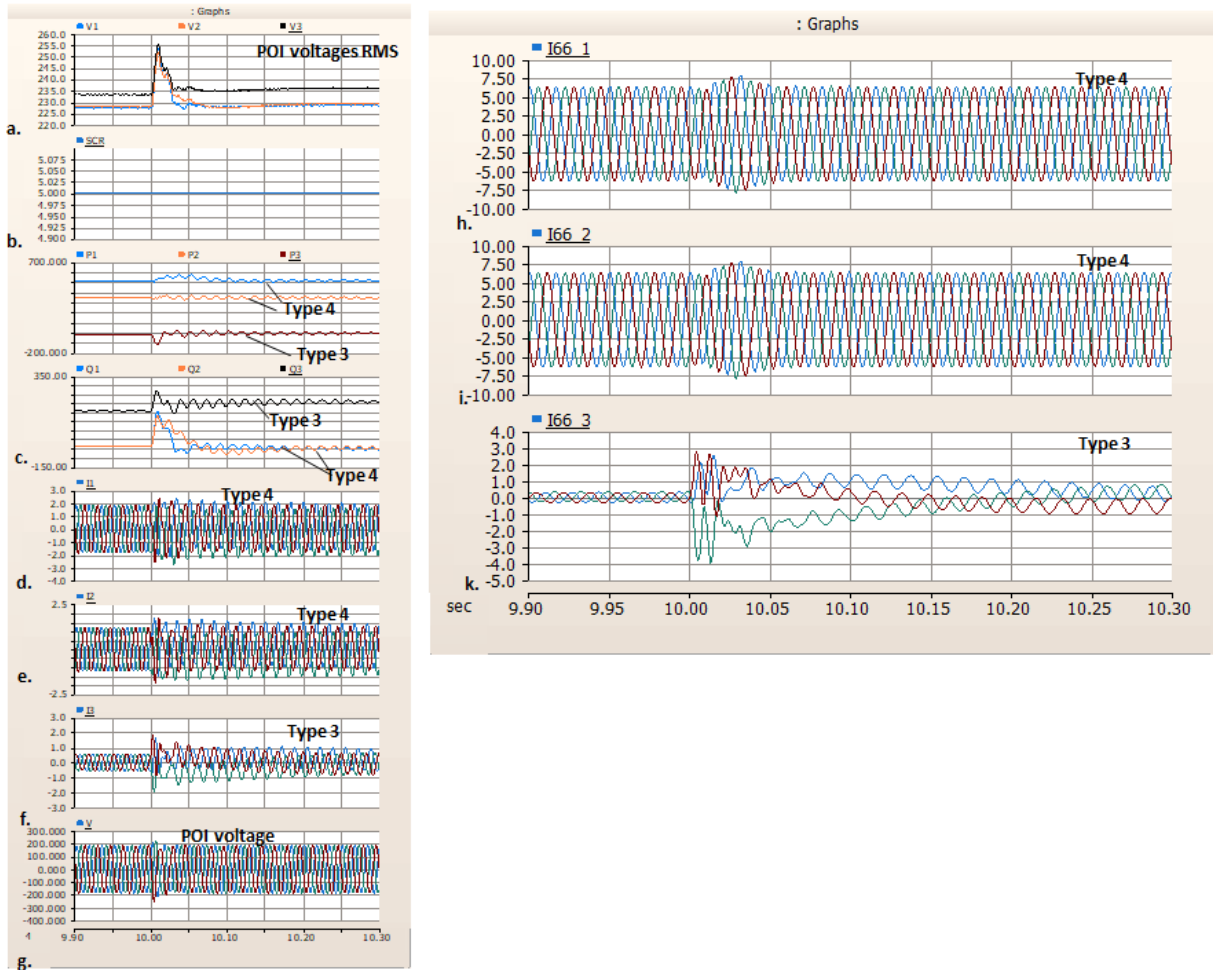


Figure 29. Response of PJM Indian River POI to POI voltage phase angle 30deg jump (two Type 4 and single Type 3 WPPs, HVAC interconnection)

Operation of Type 3 and Type 4 WPPs has been demonstrated with HVDC interconnection as well (diagram is shown in Figure 30). Both plants are connected to the same 320-kV DC HVDC terminal. It was observed from simulations that connecting plants with two different turbine topologies to the same HVDC terminal may cause instabilities, like the simulated case after the Type 3 plant starts generating (Figure 31). It is possible to tune up the controls of the HVDC converter to mitigate such instabilities. However, we did not spend much time doing that since this scenario of Type 3 and 4 wind plants connected to the same HVDC terminal is not realistic.

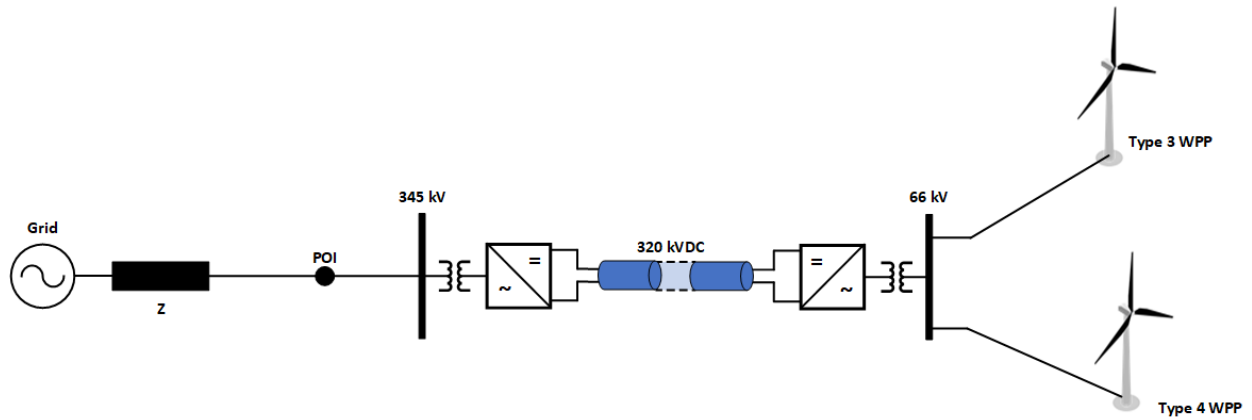


Figure 30. Type 4 and Type 3 offshore WPPs connected to the same offshore HVDC terminal

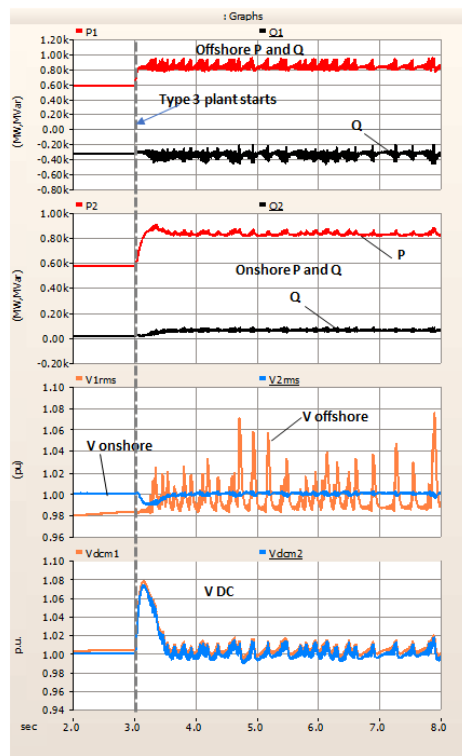


Figure 31. Instability observed during simultaneous operation of Type 3 and Type 4 WPPs connected to the same offshore HVDC terminal

4 Examples of Stability Impacts of Onshore Wind Generation in NYISO, PJM, and ISO-NE

The NREL-developed PSCAD model of a large HVAC-interconnected offshore WPP was configured and used in simulations to evaluate stability impacts on sample POIs located in the NYISO, PJM, and ISO-NE systems. The selection of POIs was based on SCR screening for all planned projects for the 2030 system (summer and winter peak load cases) using results of the analysis conducted under NREL’s Atlantic Offshore Wind Transmission Study [9]. Of 24 POIs considered in the study for the 2030 system only 9 can be classified as strong ($SCR > 5$), 3 as moderate ($3 < SCR < 5$), and 17 as weak ($SCR < 3$). Similar screening was conducted for 2030 planning cases with 30 GW of offshore wind under conditions selected from the nodal production cost modeling for three typical days representing summer peak, winter peak, and spring off-peak seasons. In this case, of 24 POIs, only 5 can be classified as strong, 5 as moderate, and 14 as weak. These results from [9] were used for selecting the weakest POIs for conducting simulations using the co-simulation platform developed in this project. The map of SCR levels generated under Atlantic Offshore Wind Transmission Study study are shown Figure 32 [9].

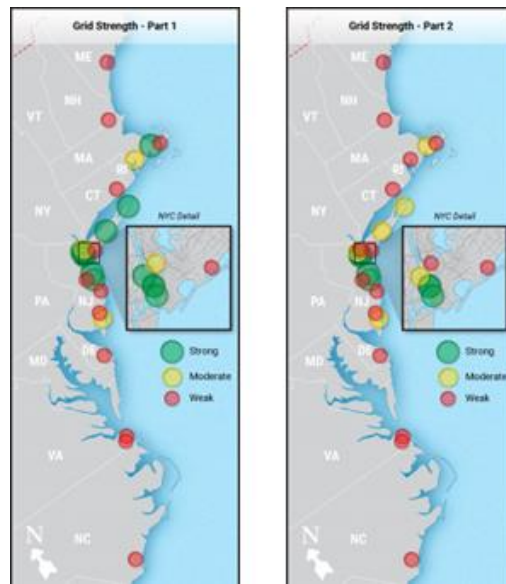


Figure 32. Atlantic Offshore Wind Transmission Study 2030 SCR screening results for two dispatch conditions

4.1 Simulations for NYISO POIs

The Barrett 138-kV substation, located in the Long Island Power Authority territory, was selected to test the model of a 1000-MW Type 4 offshore WPP (Empire Offshore Wind LLC) connected with the Barrett POI via a 30-mile 230-kV export cable with shunt compensation in both ends. The Barrett substation is located in the southeast tip of Long Island, as shown in the right map in Figure 33. The POI was modeled with different SCR values to emulate different grid strengths identified in PSS/E simulations.

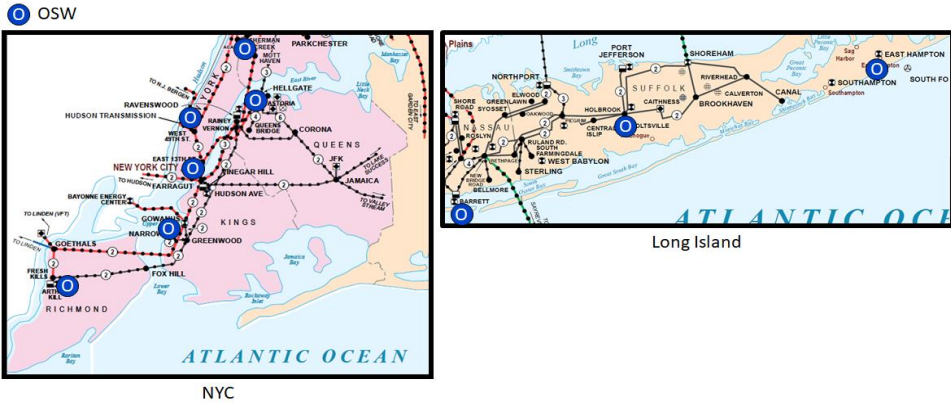


Figure 33. Map of NYISO POIs

Simulations were conducted using the PSCAD model to demonstrate the impact of the POI SCR on stability of interconnection. In case of a weaker interconnection ($SCR < 3$), the plant may exhibit unstable behavior depending on the impedance characteristics of the POI and the offshore plant itself (combined impedance of export cables with compensation, offshore transformers, collector system, and turbines). Figure 34 shows the results of steady-state plant operation when the POI SCR has a small change (plant is operating with 5% voltage droop setting). The plant becomes unstable during an extremely small change in SCR (at around $SCR = 2.44$). This result is specific to the turbine models, cable/transformer parameters, and level of compensation used in the model. Nevertheless, it demonstrates the impact of small changes in SCR on interconnection stability. In the case of onshore transmission trips and other faults in the onshore network, the POI SCR may drop dramatically causing significant stability impact. In such a case, the plant controller needs to curtail its power to maintain stability. Simulations need to be conducted for each offshore project using accurate parameters of all components and accurate turbine models to evaluate stability issues and mitigation measures.

Ability of the modeled plant to provide low-voltage ride-through was also tested for different POI strengths for three-phase and single-phase voltage faults happening in the 138-kV network, as shown in Figure 35 and Figure 36, respectively. The plant is able to ride through both types of faults under weaker and stronger POI conditions.

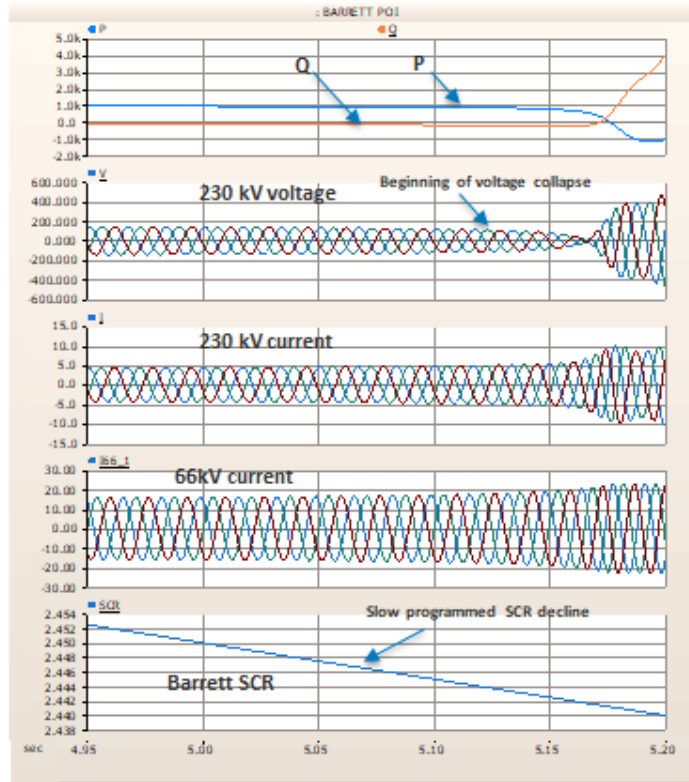


Figure 34. Impact of the POI SCR on Barrett stability

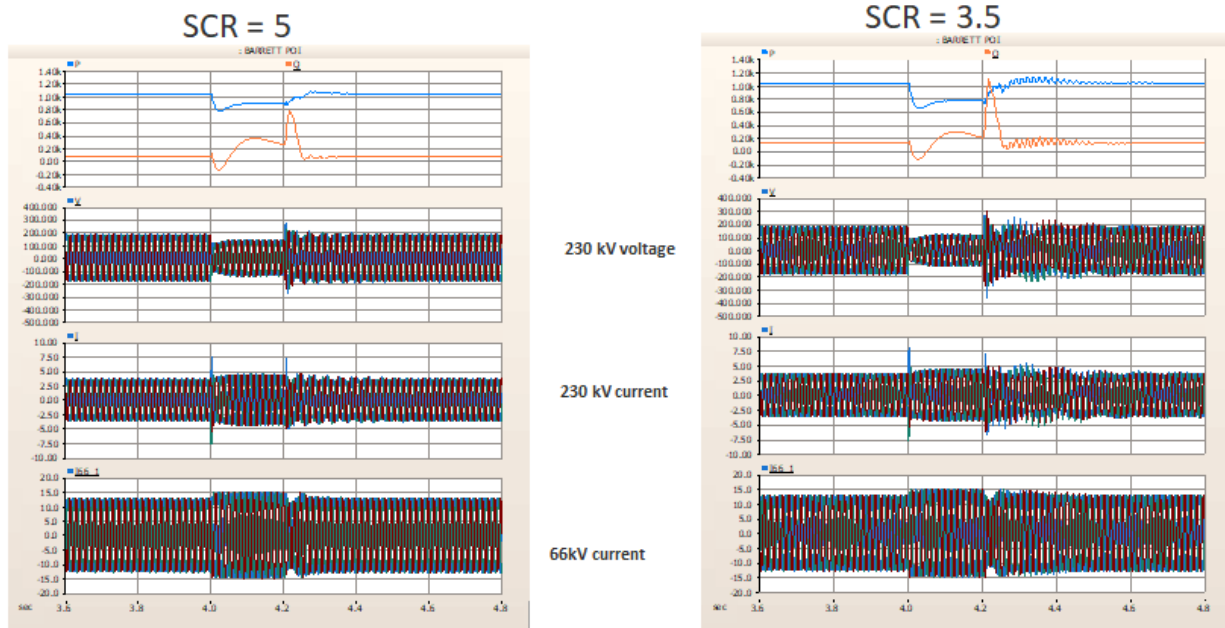


Figure 35. Balanced voltage fault ride-through for two different POI SCRs

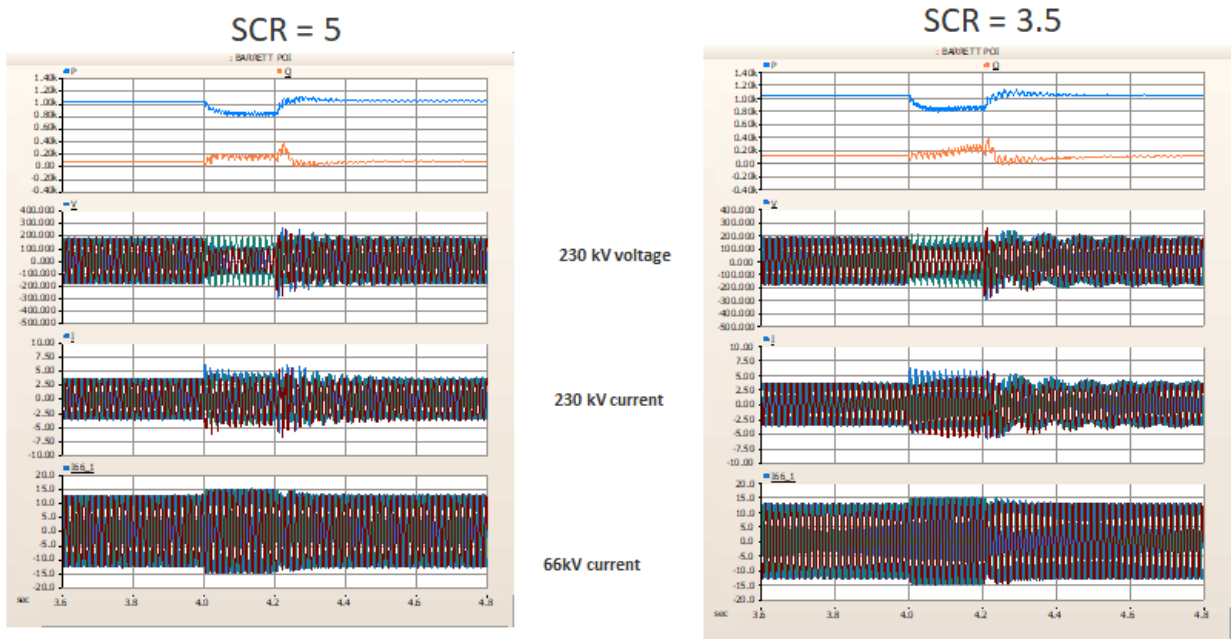


Figure 36. Unbalanced voltage fault ride-through for two different POI SCRs

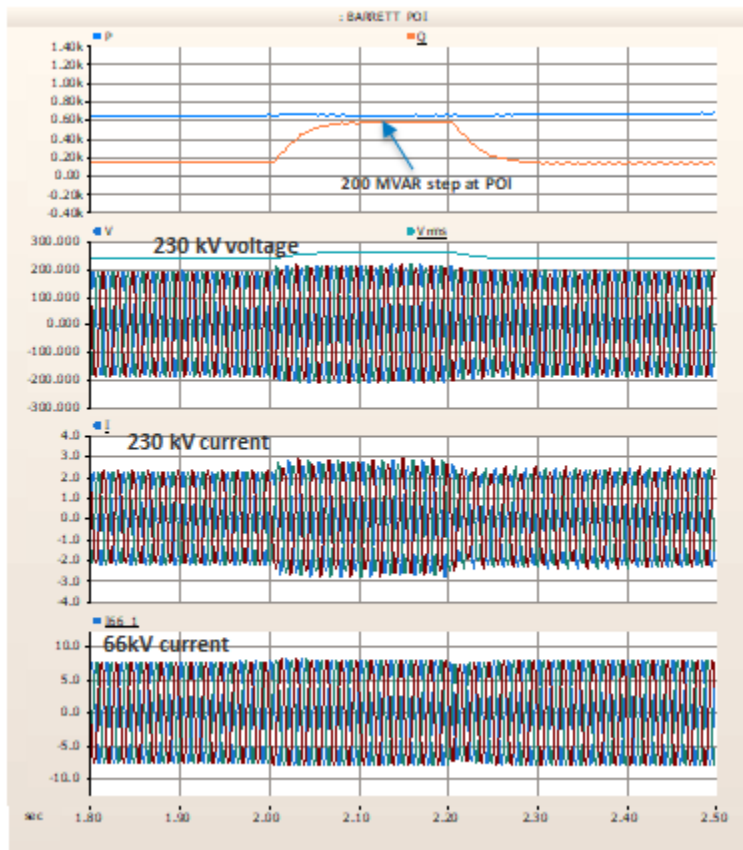


Figure 37. Increase in plant reactive power at the POI

During fault conditions shown in Figure 35 and Figure 36, the WPP was programmed to produce fault current (within the current limits of the turbine converters). This can be observed in the lower graphs in both figures that show combined well-controlled plant current at 66-kV terminals of the offshore substation. However, the fault current injected into the POI has more transient behavior due to the large impedance between the WPP and the POI.

It is important to consider the ability of offshore WPPs to provide short-circuit current during faults at levels that are adequate for protection systems. In some cases, the use of synchronous condensers at the POI may be justified to provide adequate level of fault currents. Additional benefits of synchronous condensers include their ability to increase grid strength and provide voltage controls and real rotating inertia to the system.

Offshore WPPs can provide volt/VAR support at POIs. Such capability is important for maintaining voltage stability in onshore networks when other conventional generators are not online. This is important for the New York City –Eastern Long Island area where voltage stability constraints exist and spinning reserves inside New York City load pockets are dispatched to provide voltage support. Wind can replace such spinning reserves and provide volt/VAR in those areas to respect existing voltage stability constraints.

The co-simulation platform was demonstrated for the NYISO system for different transient and dynamic cases. One example of a co-simulation configuration is shown in

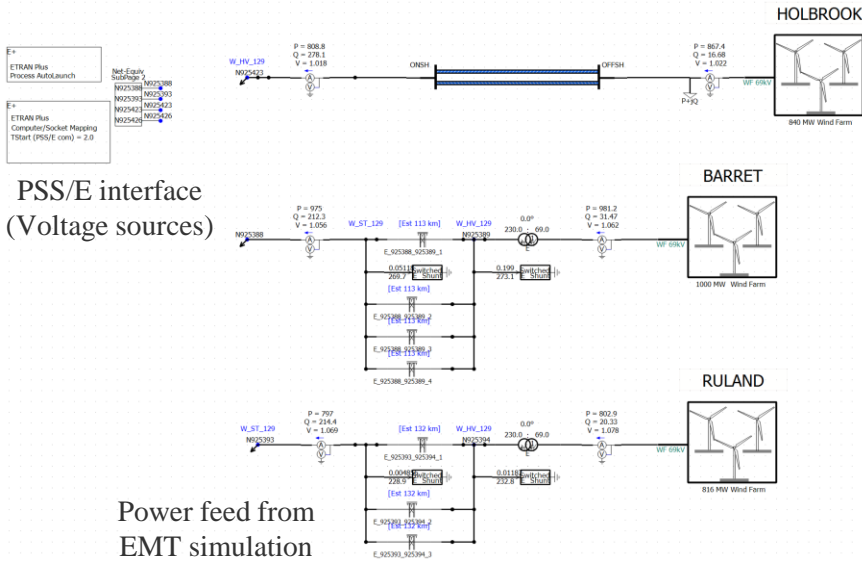


Figure 38 with three offshore projects (Holbrook 840 MW, Barret 1000 MW, and Ruland 816 MW) modeled in PSCAD and then interfaced with the PSS/E model of the NYISO system with three different POIs (three POIs in total). First, the response of the system to a 150-ms, zero-voltage fault in the Long Island grid is shown in Figure 39, demonstrating successful ride-through for all three offshore WPPs. Results for another co-simulation case are shown in Figure 40 for a trip of a 1,283-MW generator in the NYISO grid causing a small frequency deviation with fast recovery. However, in the case of a large generator trip in Long Island (Figure 41), the frequency response of the system is more dynamic, resulting in a deeper frequency deviation with some oscillatory behavior. The last example (Figure 42) shows the impact on stability when the POI SCR is degrading from a very strong level to weaker levels. In this case, the onshore POIs become unstable when the SCR reaches levels of 5 or lower.

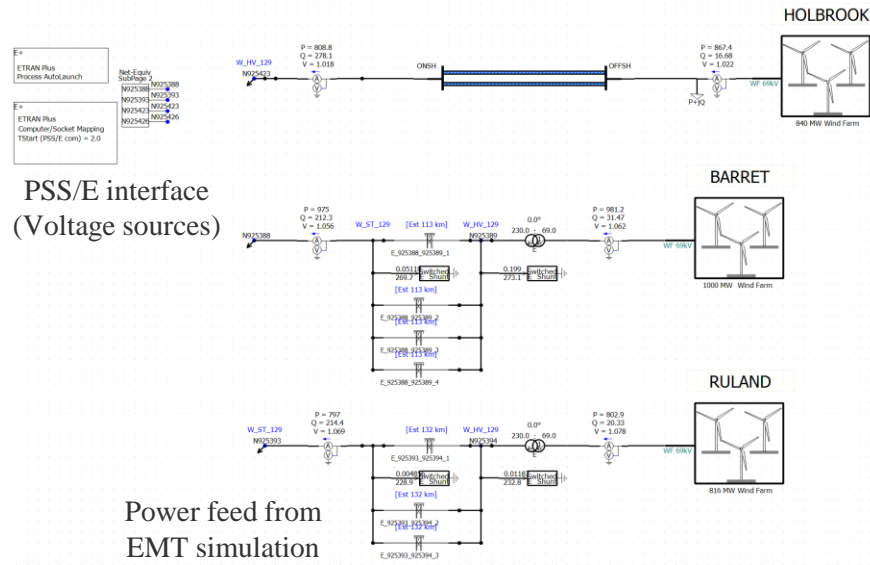


Figure 38. Example of an NYISO co-simulation configuration: EMT models of three offshore WPPs interfaced with the PSS/E model of the interconnection through three different POIs.

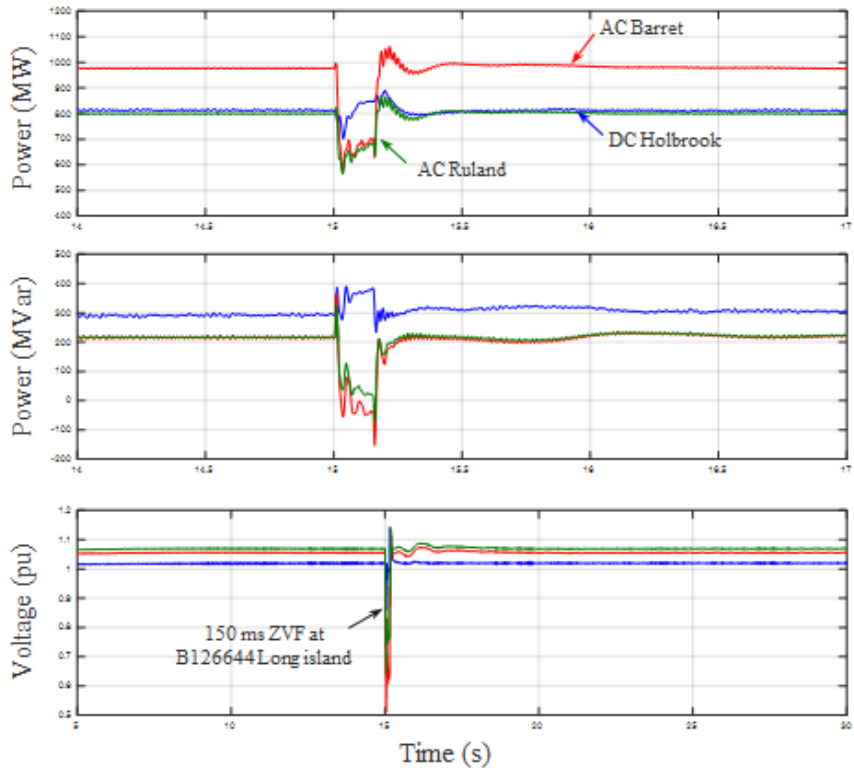


Figure 39. NYISO co-simulation results: zero-voltage fault ride-through

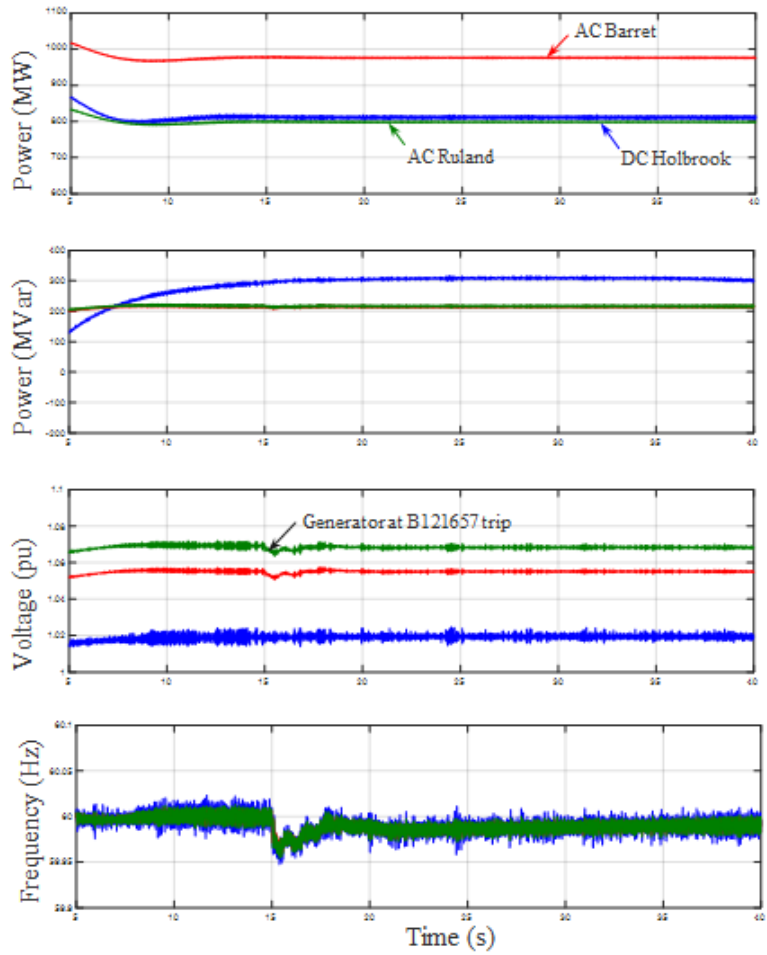


Figure 40. NYISO co-simulation results: response to a 1,283-MW generation trip in NYISO

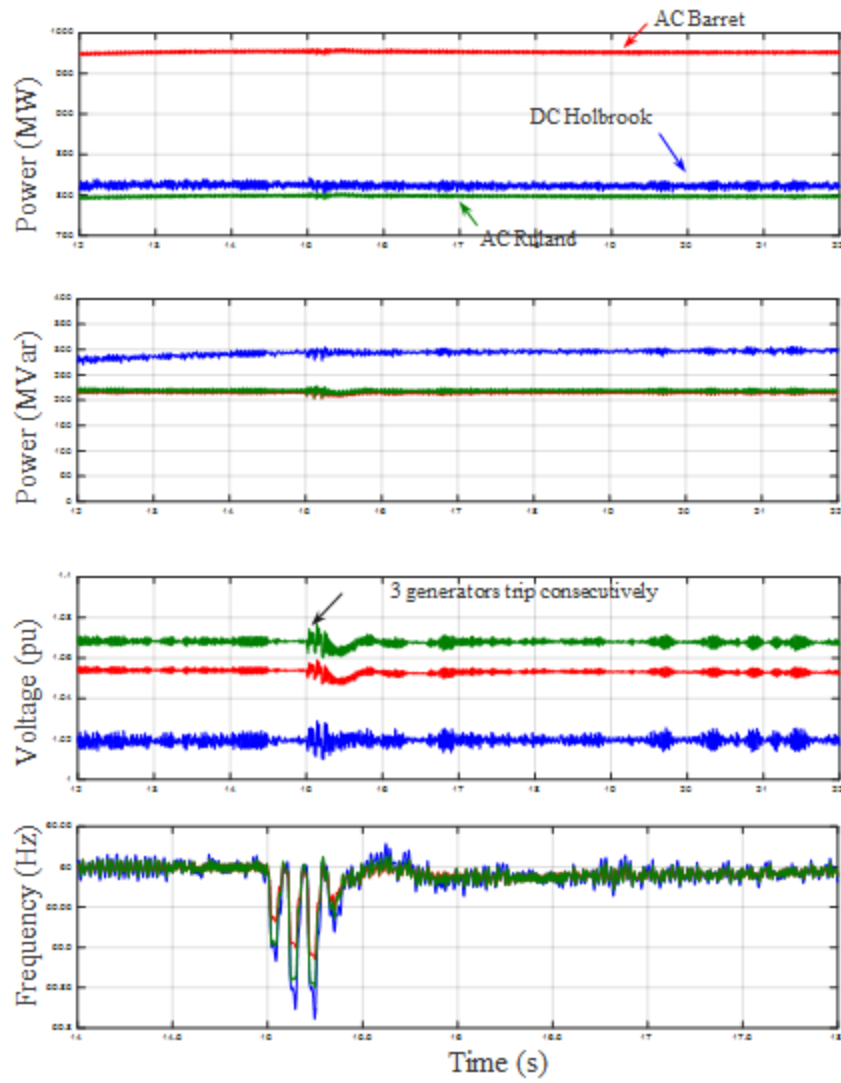


Figure 41. NYISO co-simulation results: response to a generation trip in Long Island

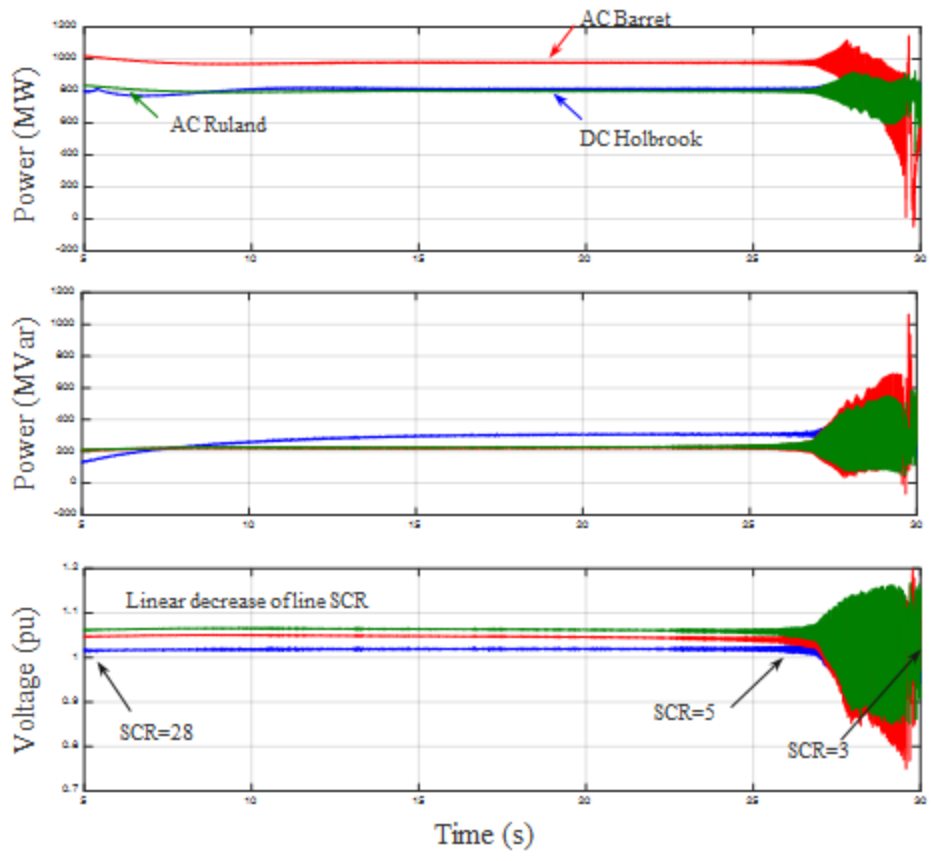


Figure 42. NYISO co-simulation results: response to simulated SCR degradation

4.2 Example of Impedance Analysis Using the Co-Simulation Platform Interfaced With GIST

An example application of the co-simulation platform combined with GIST is described here for an 800-MW offshore WPP interconnected with the Gowanus substation in Brooklyn via 230-kV HVAC transmission. The PSCAD portion of the model is shown in Figure 43 with GIST inserted between the 66-kV terminals of the wind plant and rest of the system. The PSS/E portion of the interconnection model is interfaced with PSCAD node N925381 shown in Figure 43.



Figure 43. GIST used between PSCAD model of an offshore WPP and PSS/E model of the grid

GIST conducts frequency scanning of both the WPP and the power system, producing positive and negative sequence admittance characteristics for the WPP (Figure 44) and power system (Figure 45). GIST allows for separating the dynamics of an offshore WPP from the grid. Such characteristics, combined with Nyquist stability criteria, can be used to identify frequencies of possible oscillations between offshore WPPs and the power system.

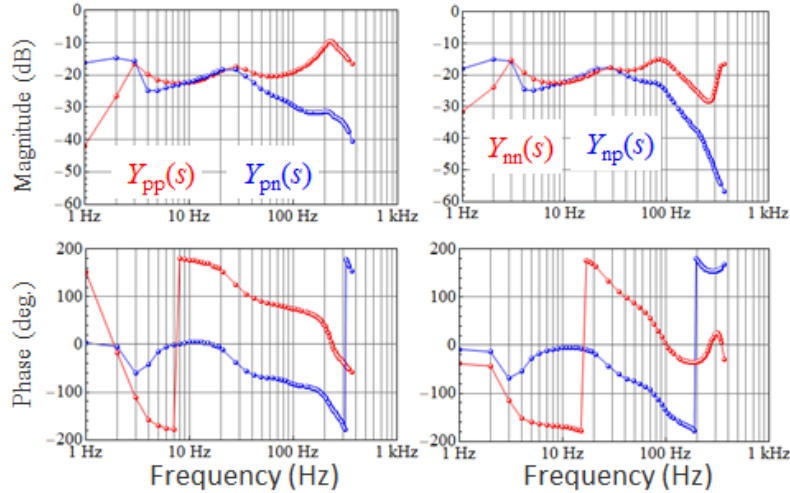


Figure 44. Wind power plant admittance

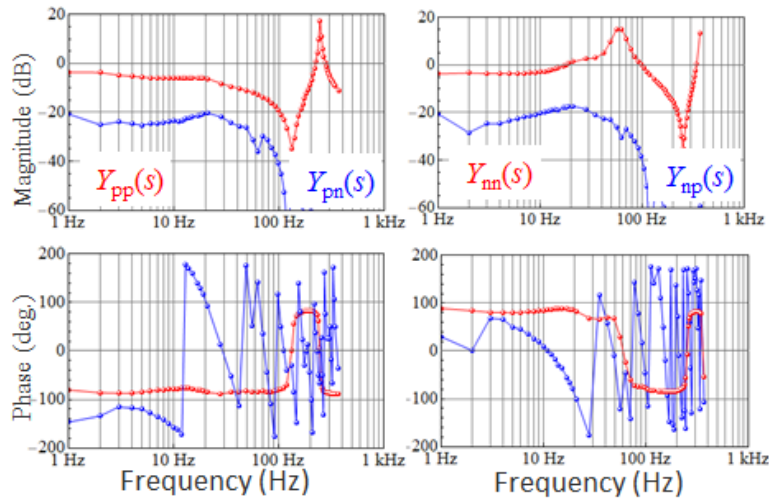


Figure 45. Power system admittance

One example of identifying possible instabilities is illustrated in Figure 46 when comparing sequence impedance characteristics of an offshore WPP and the grid. Potential resonance between the plant and grid exists at around 158 Hz, but the phase margin of 25° makes it stable for a given set of system parameters. A relatively small increase in inductance between the plant and grid can cause instability. As shown in Figure 46, an increase of impedance magnitude from 10 dB to 19 dB at 100 Hz will cause instability. Such an increase corresponds to a 7.5 mH increment in inductance (can be caused by longer lines or high-impedance transformers). Additional 7.5 mH inductance at the terminal of the offshore WPP is a 0.48 per unit increase for base of 66 kV and 816 MW. In the same manner, stability margins for any offshore WPP and any POI can be evaluated using a combination of PSS/E-PSCAD co-simulation integrated with GIST.

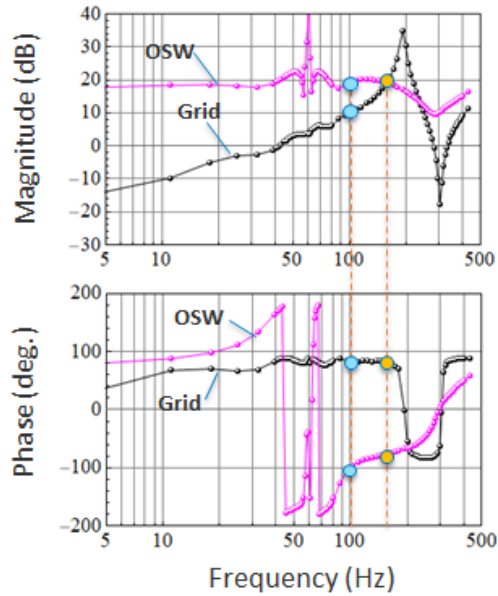


Figure 46. Sequence impedance analysis

4.3 Simulations for PJM POIs

The Indian River 230-kV substation in Maryland was selected to model the interconnection of three offshore WPPs with 800 MW of total capacity. The one-line diagram of the substation with 230-kV and 138-kV buses is shown in

Figure 47. Offshore WPPs are connected to the substation via 230-kV export cables with shunt compensation at both ends. The EPRI team conducted PSS/E simulations identifying the POI SCR under different contingency conditions (Table 6). Depending on the fault scenario, the SCR of the Indian River POI can vary from 4.24 to 2.35. The lowest SCRs appear when more than one onshore transmission lines are tripped. Lower SCRs can cause serious stability issues and should be avoided.

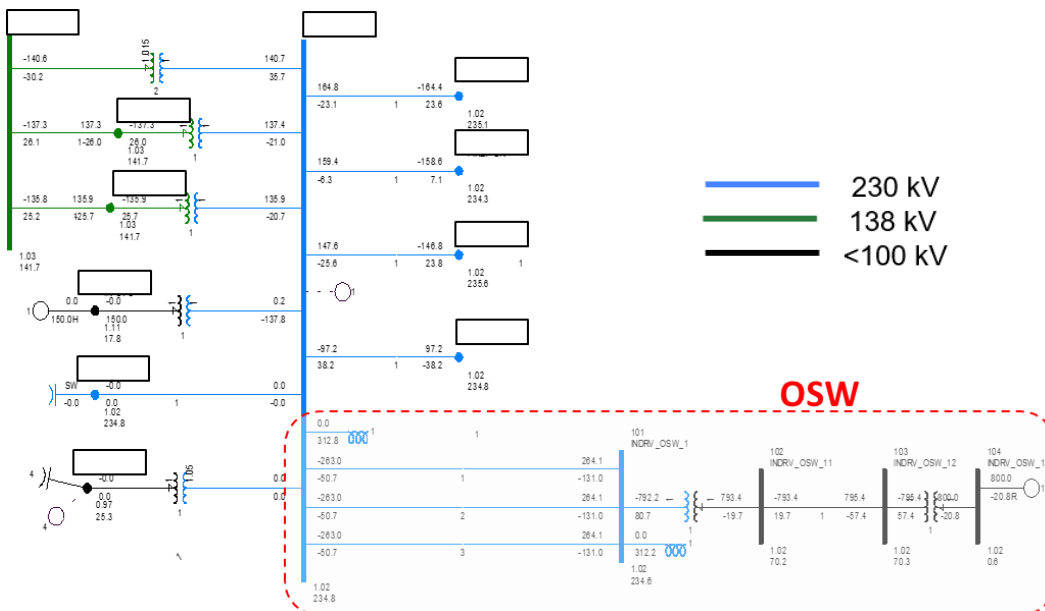


Figure 47. Indian River substation

Table 6. Spring light load case: short-circuit results

Location	Base case as is All line in service			IndianRiver-XX 230 kV line out			IndianRiver-XX 230 kV line out + IndianRiver-XX2 230kV line out			IndianRiver-XX 230 kV line + IndianRiver-XX2 230kV line out + IndianRiver 230/138 kV trf out		
	SCMVA	SCR	X:R	SCMVA	SCR	X:R	SCMVA	SCR	X:R	SCMVA	SCR	X:R
POI (232006)	3388.87	4.24	0.008836+j0.031250	2385.64	2.98	0.020188+j0.049536	1943.82	2.43	0.017478+j0.053823	1880.03	2.35	0.017442+j0.055850
Station highside (101)	2987.3	3.73	0.009371+j0.035610	2183.84	2.73	0.021502+j0.055314	1806.03	2.26	0.018013+j0.058183	1750.6	2.19	0.017978+j0.060209
Station lowside (102)	2366.2	2.96	0.009569+j0.045493	1872.77	2.34	0.021929+j0.065936	1561.2	1.95	0.018211+j0.068065	1519.14	1.90	0.018175+j0.070091

The model of offshore projects connected to the Indian River POI was tested for various voltage fault ride-through scenarios under different levels of SCR. Figure 48 shows the simulation results when the plant was exposed to three-phase and single-phase voltage faults at the POI (voltage droop control was disabled in all plants, and no additional onshore line trips were simulated). The plant demonstrated both stable ride-through and post-fault recovery at SCR=3 with a substation transformer with Y_g-Y_g configuration. At lower SCRs, the modeled plant was not able to provide stable ride-through under the same conditions and tripped off.

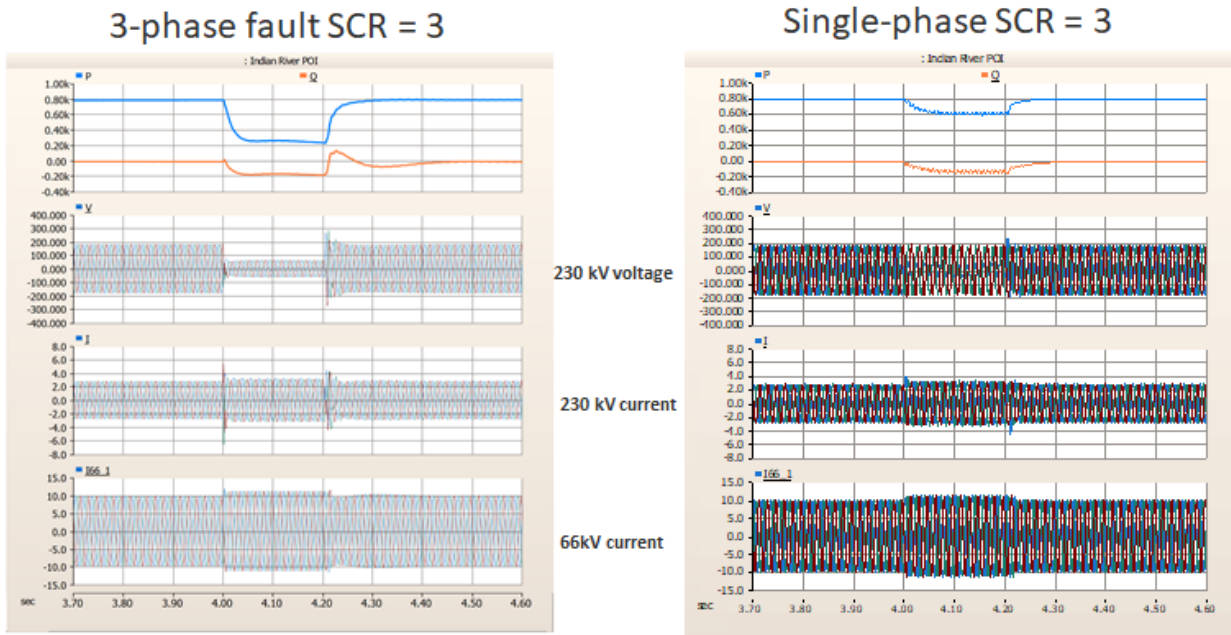


Figure 48. Indian River three-phase and single-phase faults at two different SCRs (no voltage droop)

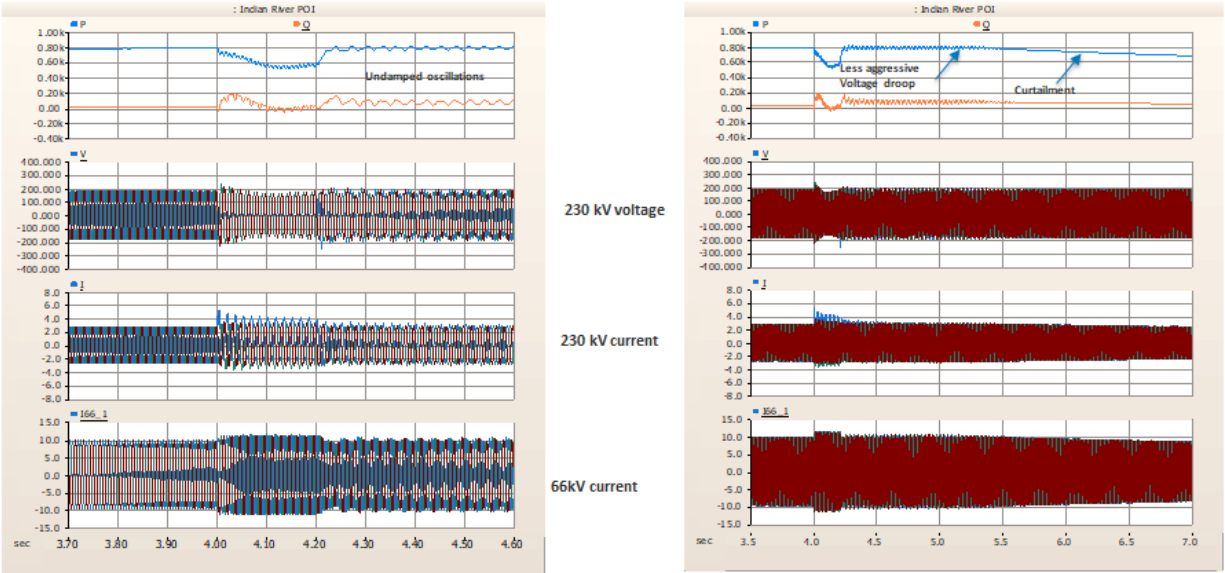


Figure 49. Indian River single-phase faults (SCR = 3). Left: undamped oscillation, plants have 5% voltage droop enabled. Right: stable recovery (with less aggressive droop and plant curtailment)

Enabled plant voltage droop may cause some oscillatory behavior triggered by a voltage fault at the POI. Figure 49 (left) shows the case when offshore plants were exposed to the same voltage fault at SCR=3 but with 5% voltage droop enabled. In addition, the voltage fault causes the trip of additional lines in the onshore grid, resulting in further reduction of the SCR to 2.5. In this case, offshore plants go into undamped oscillation modes that will eventually grow with time causing tripping of all plants. One mitigation strategy can be disabling (or reducing) the voltage droop setting along with rapid plant curtailment to maintain stable system operation. Figure 49 (right) shows that wind plants continue stable operation after the voltage fault with reduced voltage droop and initiation of the curtailment process.

One observation from multiple simulations is that the onshore substation transformer configuration can have an impact on stability under some simulation scenarios. For example, if a Y_g-Y_g substation transformer is substituted with $\Delta-Y_g$ configuration, the ride-through characteristic shown in **Figure 50** changes dramatically. Figure 50 shows results of the same voltage fault ride-through simulation with a $\Delta-Y_g$ transformer. In this case, offshore plants demonstrate stable ride-through and recovery.

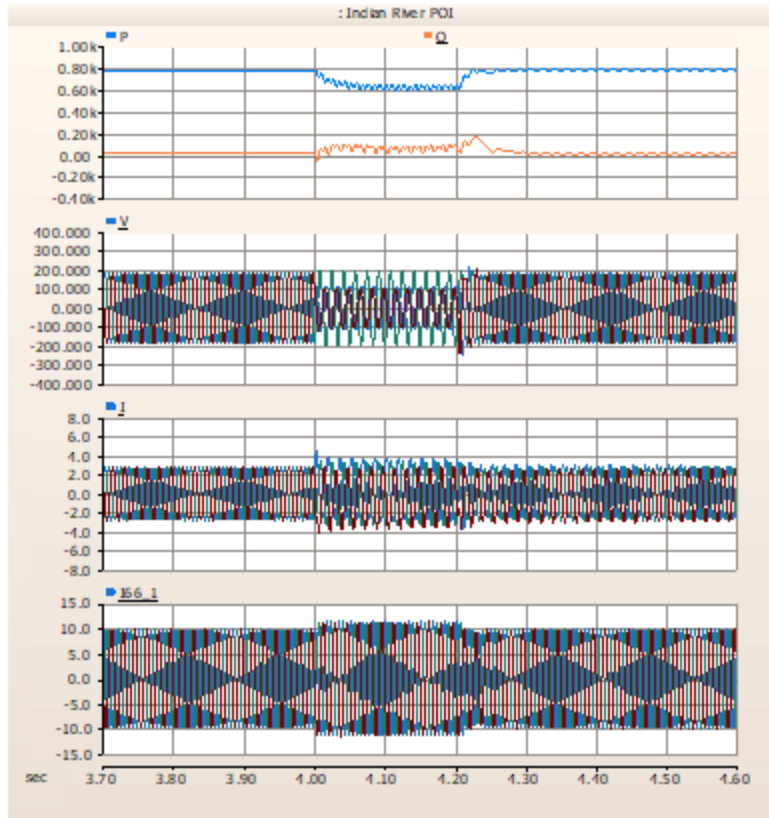


Figure 50. Indian River single-phase faults (SCR = 3) with a Δ - Y_g substation transformer

The NREL-developed generic model of offshore WPPs with an offshore substation, export cables, and compensation can be used to evaluate stability impacts on large shares of offshore wind power on onshore grid. NREL's PSS/E-PSCAD co-simulation tool is used for this purpose. Stability related issues identified during PSCAD simulations in this report will be verified by using the NREL impedance-scanning tool during co-simulation studies.

Example results of PJM system PSCAD-PSS/E co-simulations for two POIs and two offshore WPPs have demonstrated the use of the co-simulation platform to identify possible frequency response and stability issues. The system diagram is shown in Figure 51 with two offshore WPPs interconnected with an onshore substation in PSCAD and then interfaced with a PSS/E model of the entire system. The response of the system to a 100-MW generation trip in PJM is shown in Figure 52, revealing no stability concerns at this contingency. However, tripping 3000 MW of generation in the PJM system causes significant frequency decline (Figure 53) that may result in underfrequency load shedding. Figure 54 shows a severe transient case the results in an offshore WPP becoming unstable and tripping off. This is a result of tripping one of the lines connecting to the Indian River substation causing SCR reduction to a very low level (SCR=1.9).

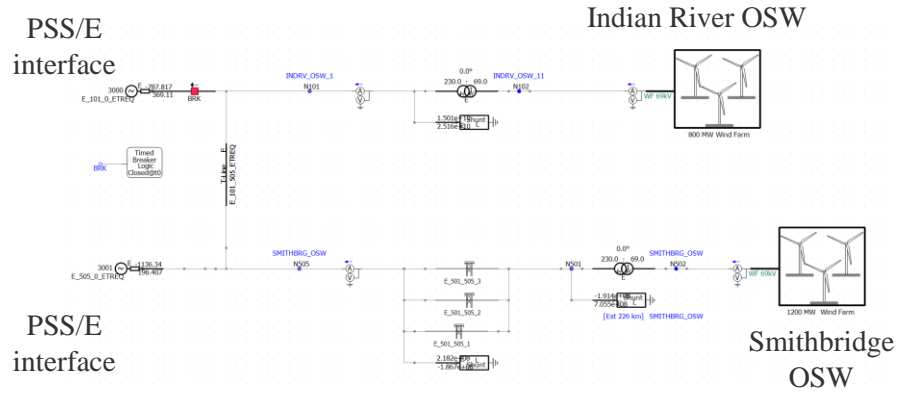


Figure 51. Co-simulation example for PJM POIs

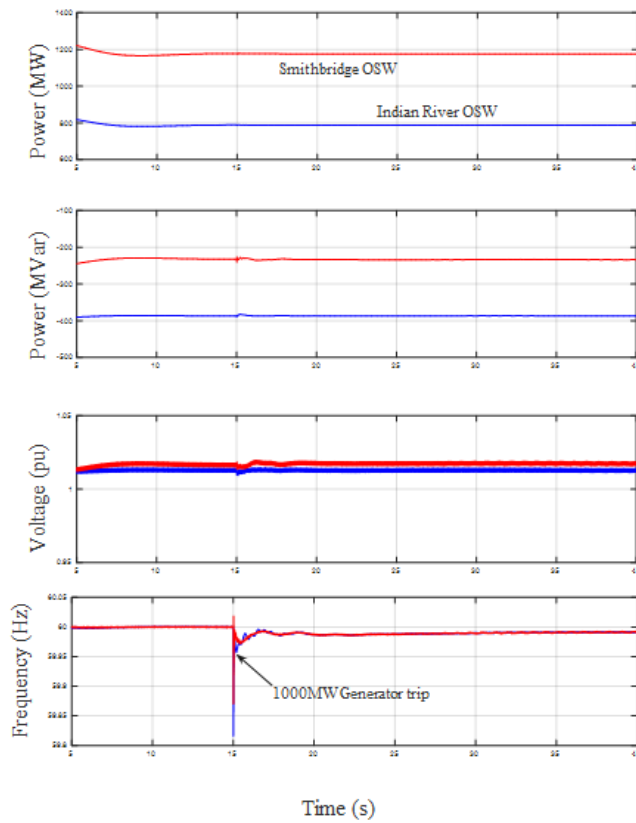


Figure 52. Response to 1000-MW generation trip in PJM

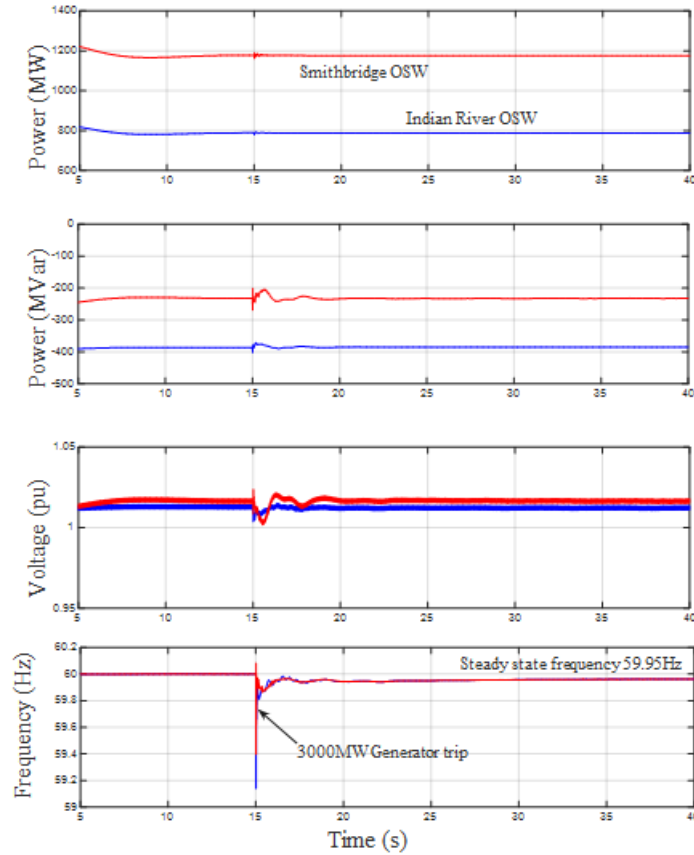


Figure 53. Response to 3000-MW generation trip in PJM

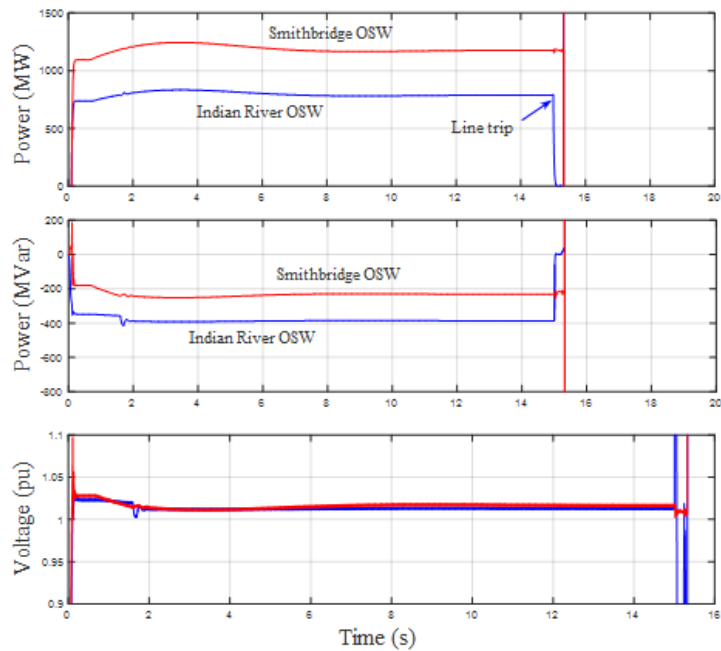


Figure 54. Response to a trip of one line connecting with the Indian River substation

4.4 Simulations for ISO-NE POIs

Several POIs in the ISO-NE system have been considered as candidate POIs for model demonstration. The list of potential POIs is shown in Table 7. Some of these POIs have low SCRs even under normal conditions. The SCRs will go further down under N-1 or N-2 contingency conditions. Low SCR values for all POIs under N-1 and N-2 conditions are shown in Table 8 for the 2031 multiregional modeling working group summer base case and redispatch case produced by NREL’s Atlantic offshore wind study (low SCR values are highlighted in red). Normally, SCR values below 5 are considered very weak and require special attention during studies.

Table 7. ISO-NE POIs

Bus name	Voltage (kV)	POI limit (MW)
YARMOUTH	345	2200
W BARNSTABLE	345	838
BOURNE345	345	1200
WARD HILL	345	1200
BRAYTN POINT	345	2330
MONTVILLE	345	1200

Table 8. Grid strengths for the 2031 multiregional modeling working group summer case (results from NREL-PNNL Atlantic offshore wind study)

POI	Base Case			Offshore Wind Redispatch		
	SCR(N-0)	SCR(N-1)	SCR(N-2)	SCR(N-0)	SCR(N-1)	SCR(N-2)
Yarmouth	3.1	2.2	1.9	3.1	2.2	1.9
West Barnstable	11.0	9.4	2.4	12.1	10.2	2.4
Bourne	9.3	7.4	5.6	10.6	7.8	5.8
Ward Hill	10.9	6.2	2.1	11.0	6.2	2.1
Brayton Point	5.1	5.0	4.2	5.2	5.1	4.3
Montville	10.8	5.8	1.4	10.9	5.8	1.4

System strength quantifies the ability of a power system to maintain stable voltage waveforms at different nodes. It usually comes from synchronous generators in conventional energy resources. Low system strength can cause many dynamic stability problems, including oscillations and control interactions, degradation of generator fault ride-through performance, failure or mal-operation of protection systems, and more severe under/over voltages during grid events.

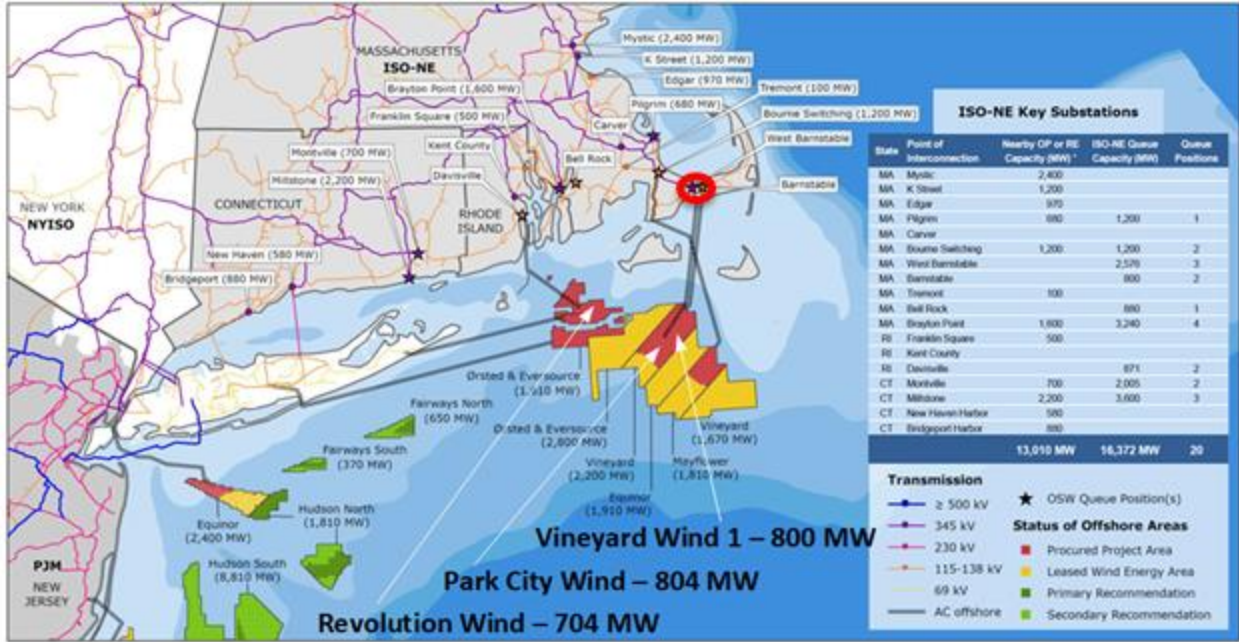


Figure 55. 800 MW Vineyard Wind 1 project interconnected with W Barnstable bus.

The NREL-developed model was tested for the Vineyard Wind 1 offshore project interconnected with the W Barnstable bus (Figure 55) for different SCR values shown in Table 8.

Figure 56 shows the results of the simulation for the Vineyard Wind 1 plant operating at around the 780-MW level when the POI SCR was changing from an initial level of SCR=11 to SCR=9.4 at $t=10$ s, and then to SCR=2.4 at $t=20$ s. Step change of the SCR from 11 to 9 does not have visible transient impact on power and voltage at the 345-kV bus, since the grid strength is still relatively high. However, the transition from SCR=9.4 to the weaker 2.4 level causes significant transient overvoltage, as shown in Figure 56. It also causes the POI voltage to go down to about the 330-kV level, since voltage droop control in the Vineyard plant was disabled in this simulation case. A zoomed-in view of the same event is shown in Figure 57, revealing details of transient behavior at the POI during the SCR step change. After enabling the voltage droop control in the Vineyard plant, voltage in the 345-kV bus stabilizes at a higher level (340 kV) for the same SCR switching event (Figure 58). Figure 59 shows the dependence of POI voltage at the 345-kV bus on SCR. The plant can operate in a stable manner at SCRs below 2. Adding a 100-MVA synchronous condenser at the 230-kV bus increases the range of stable operation for even lower SCRs all the way down to SCR=1.

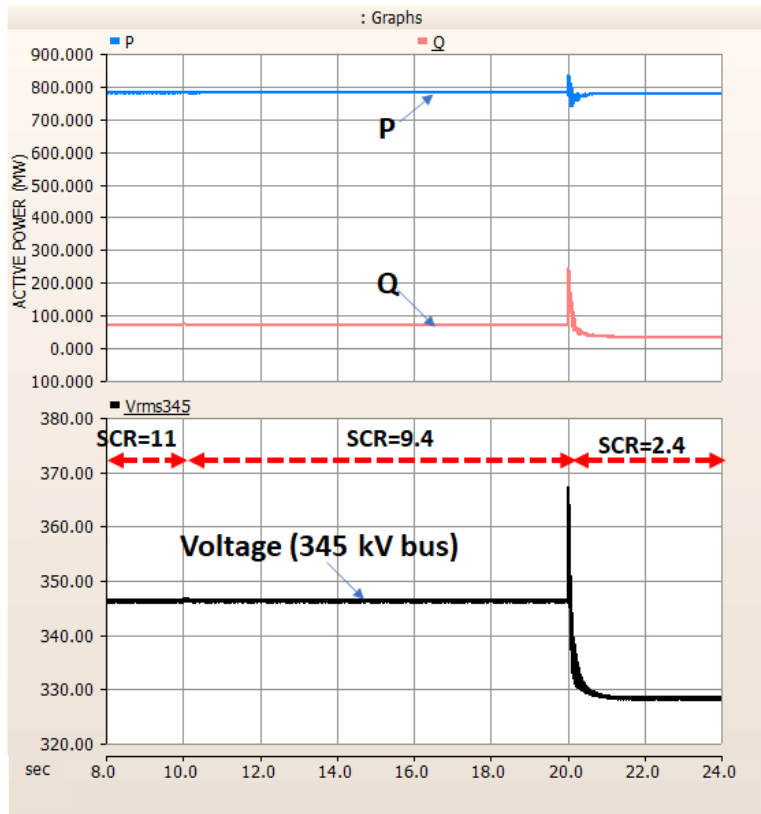


Figure 56. Step changes in W Barnstable SCR

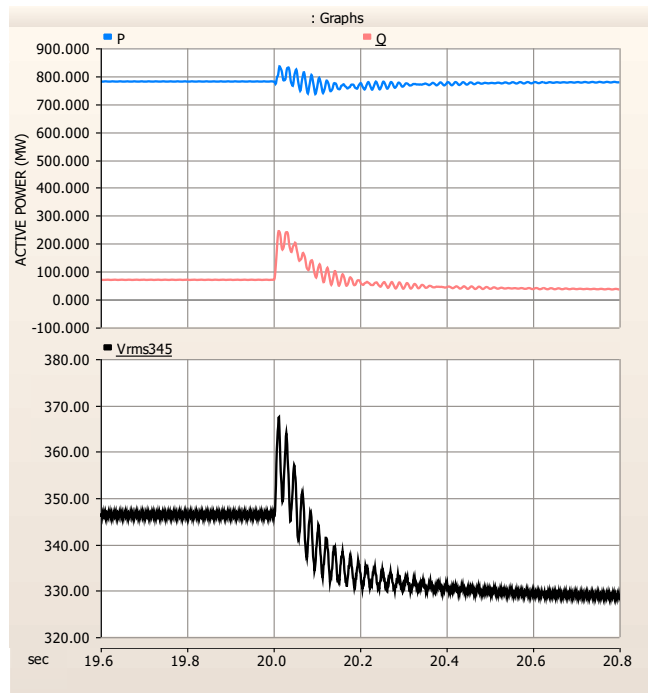


Figure 57. Zoomed-in view of Barnstable SCR switching from 9.4 to 2.4 level (no voltage droop)

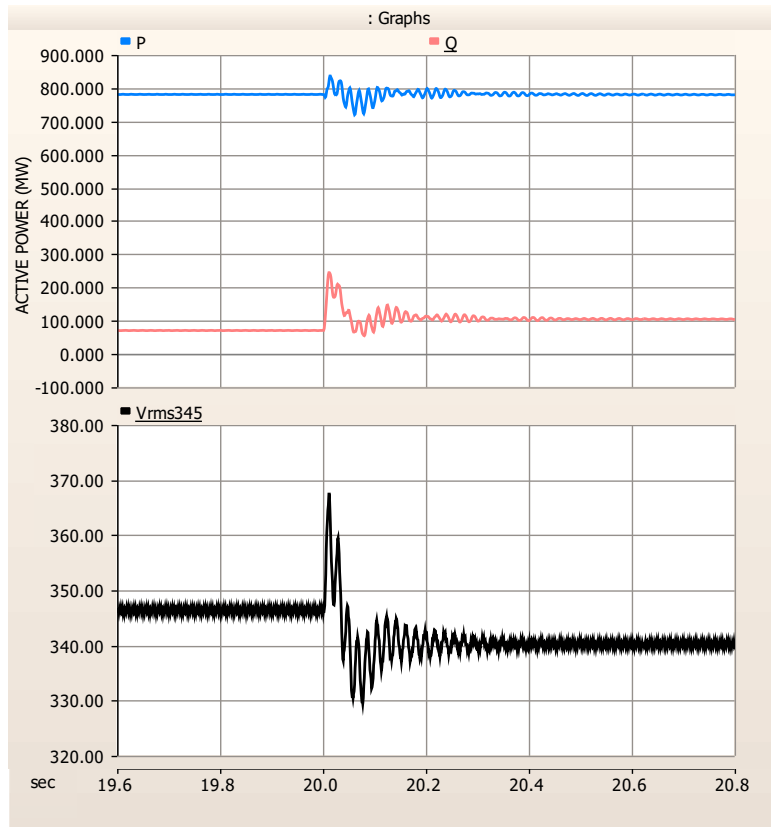


Figure 58. Zoomed-in view of Barnstable SCR switching from 9.4 to 2.4 level (voltage droop enabled)

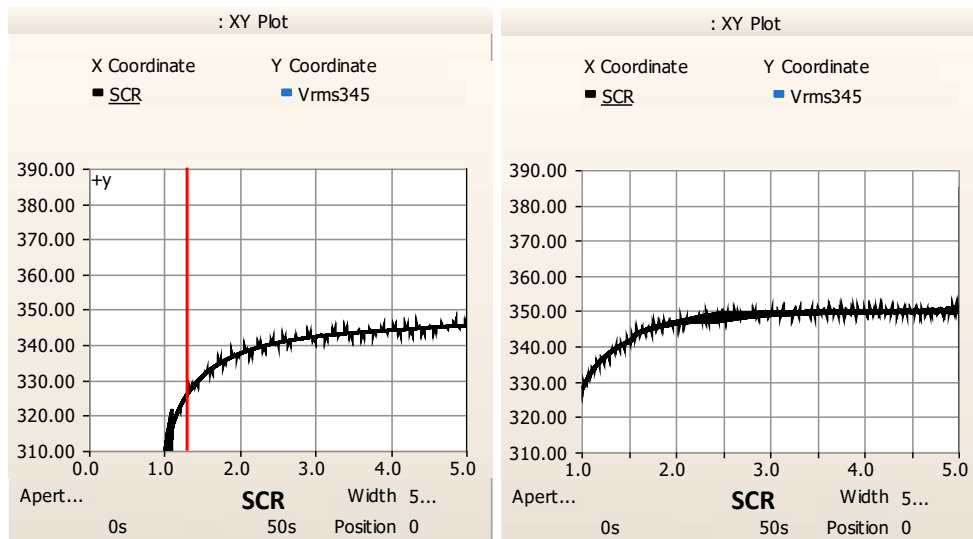


Figure 59. 345-kV bus voltage as a function of SCR (left – no synchronous condenser, right – with 100-MVA synchronous condenser)

Examples of PSCAD-PSS/E co-simulation scenarios are shown below for an ISO-NE region depicted in **Figure 60**. The PSCAD model shown in **Figure 61** consists of a group of 200-MW wind turbine arrays as part of a larger 800-MW WPP. The plant is connected to the Barnstable substation, which is reinforced with two 267-MVA synchronous condensers for enhanced voltage stability. The system becomes unstable and crushes eventually when both synchronous condensers supporting the Barnstable substation trip off, and the offshore WPP is the only source to control the voltage, as shown in **Figure 62**. Such instability can be mitigated by adjusting the WPP voltage control gains using GIST. An additional case when a single synchronous condenser trips off in the substation is shown in **Figure 63**. In this case the sustained undamped oscillations appear on the system that can be damped by disabling voltage control in the offshore WPP.

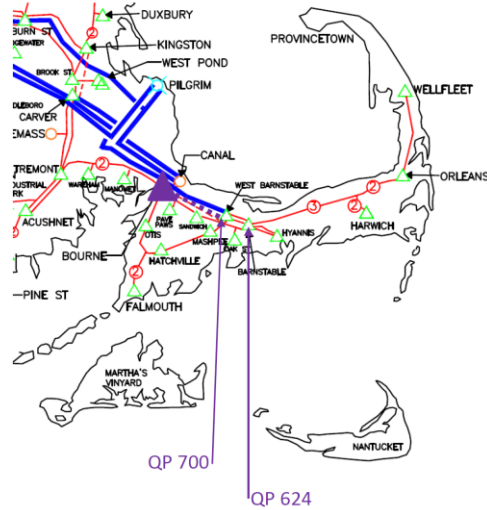


Figure 60. EMT co-simulation region

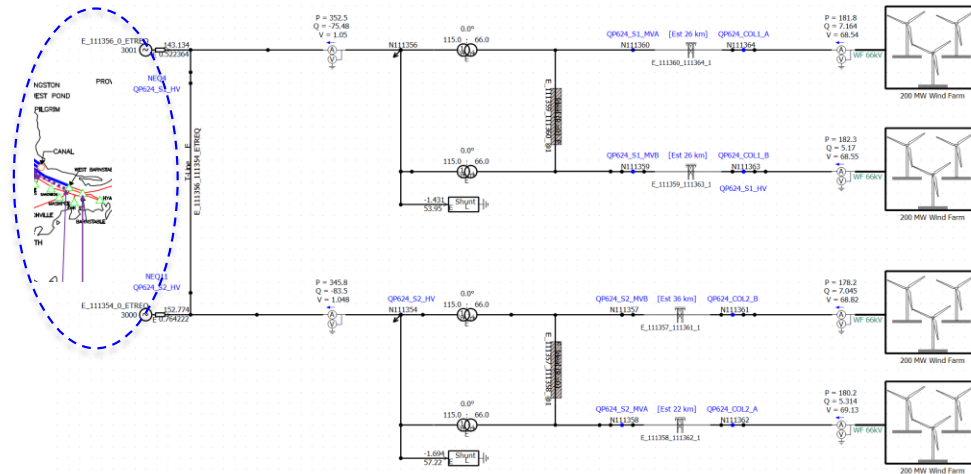


Figure 61. PSCAD EMT interfaced with PSS/E model of ISO-NE system

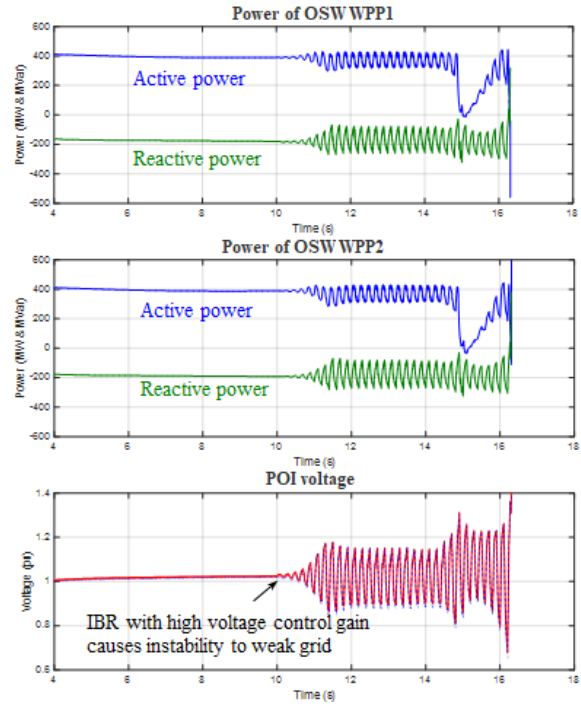


Figure 62. Instability caused by tripping of two synchronous condensers (offshore WPP operates with voltage control)

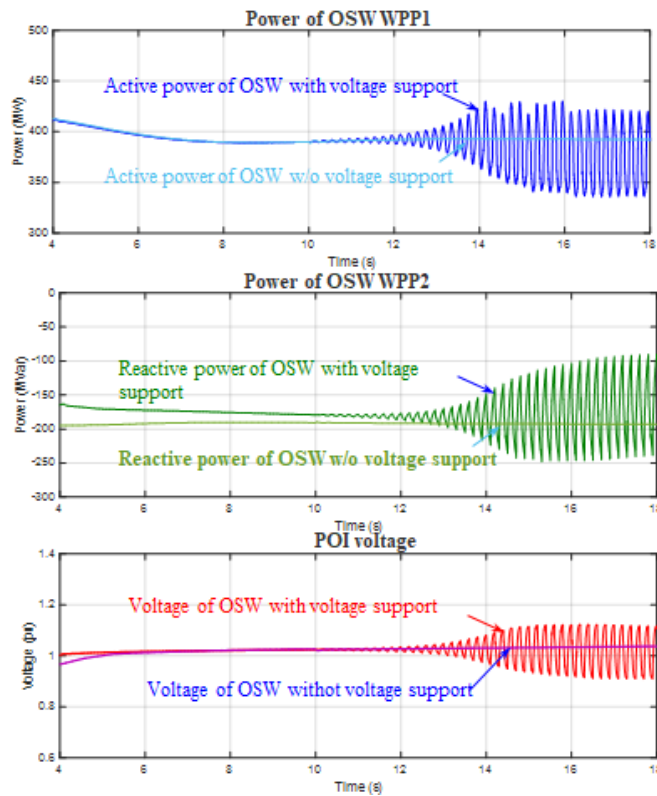


Figure 63. Response of an offshore WPP with and without voltage control to the loss of one synchronous condenser

5 Simulation Results

5.1 Interactions Between HVAC- and HVDC-Interconnected Offshore Wind Power Plants

Two offshore wind projects connected to the NYISO grid through HVAC and HVDC links are shown in Figure 64. After an SCR step change in the Farragut POI (from 5 to 2.5), both plants develop undamped active and reactive power oscillations (Figure 65) that is hard to damp using plant controls since the POI becomes too “weak.” One solution to maintain the POI strength is adding a 100-MVA synchronous condenser in the Farragut POI. Figure 66 shows the results of simulations with a synchronous condenser added to the model. The same large reduction in SCR does not result in undamped oscillations because of the damping effect introduced by a synchronous condenser.

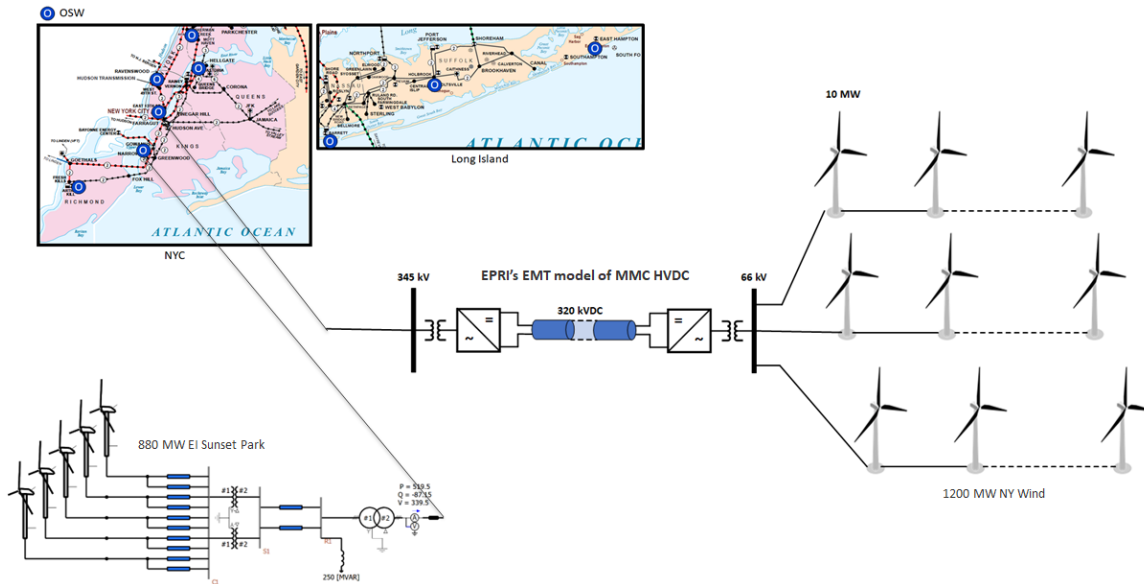


Figure 64. HVDC and HVAC wind plants interconnected with the onshore grid

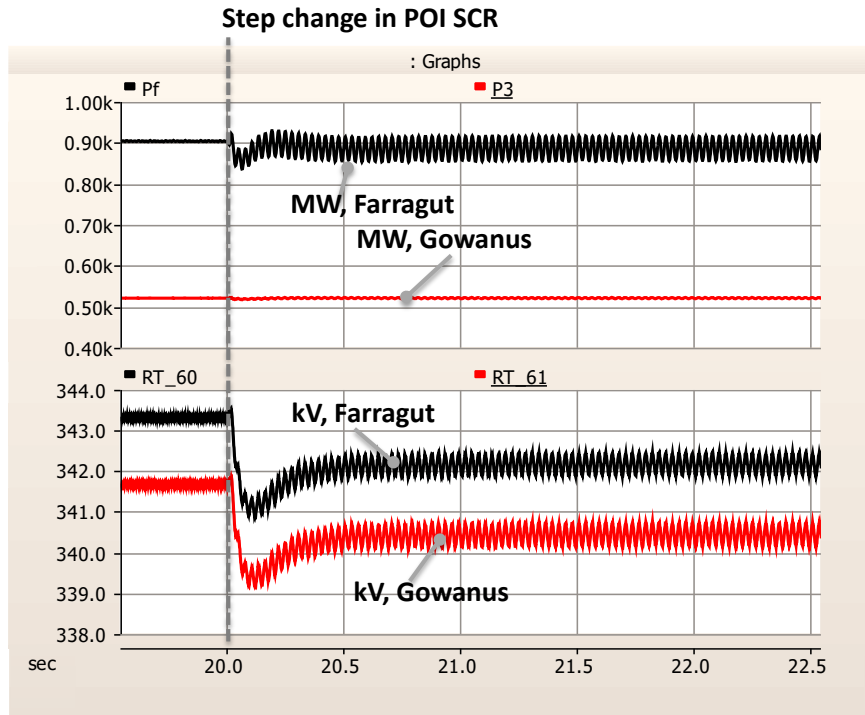


Figure 65. Undamped oscillations in the Farragut and Gowanus POIs after SCR reduction

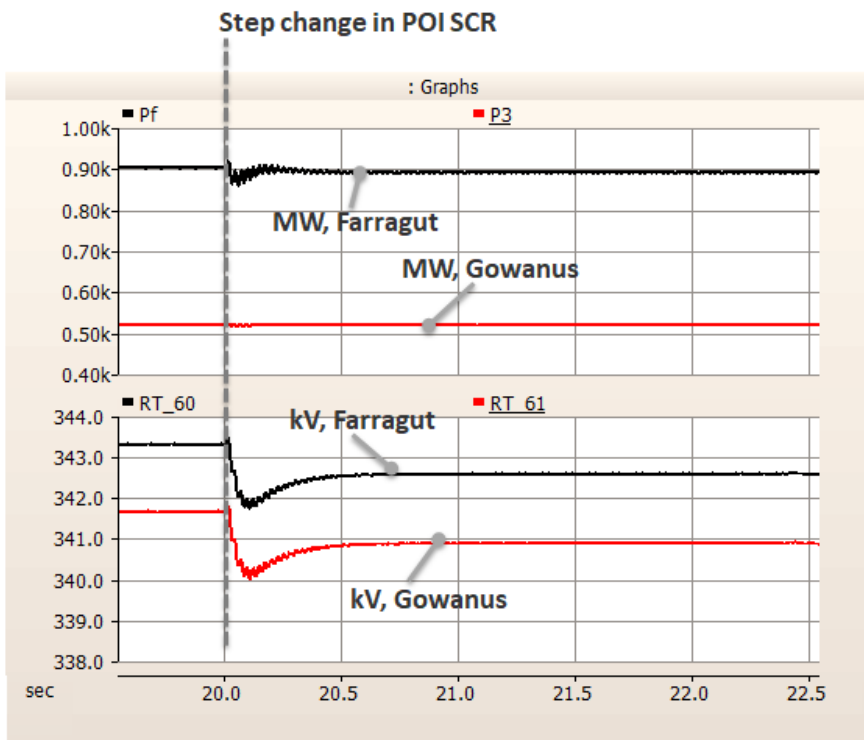


Figure 66. Stable performance provided by a 100-MVA synchronous condenser

5.2 Sensitivity of an HVDC-Interconnected Wind Power Plant to the POI SCR

Voltage source converters of MMC-HVDC transmission systems are expected to have an enhancing impact on grid stability in weaker grids. However, controls of the HVDC converter need to be properly tuned to provide maximum benefit to the system. In particular, fast inner-loop, current-controller parameters need to be selected properly. Results of simulations shown in Figure 67 demonstrate zero-voltage ride-through performance of an HVDC-interconnected WPP (Farragut POI). It can be seen that the large voltage transient in the onshore grid does not have impact on the offshore WPP because of the HVDC link and DC chopper action at the sending end. However, on the onshore side, the transient is quite visible resulting in significant overcurrent and an active power spike after the voltage is restored. The control parameters of the HVDC converter were modified to provide more aggressive current limiting control. As a result, for the same voltage event, visible improvement in converter current and active power response can be observed (Figure 68).

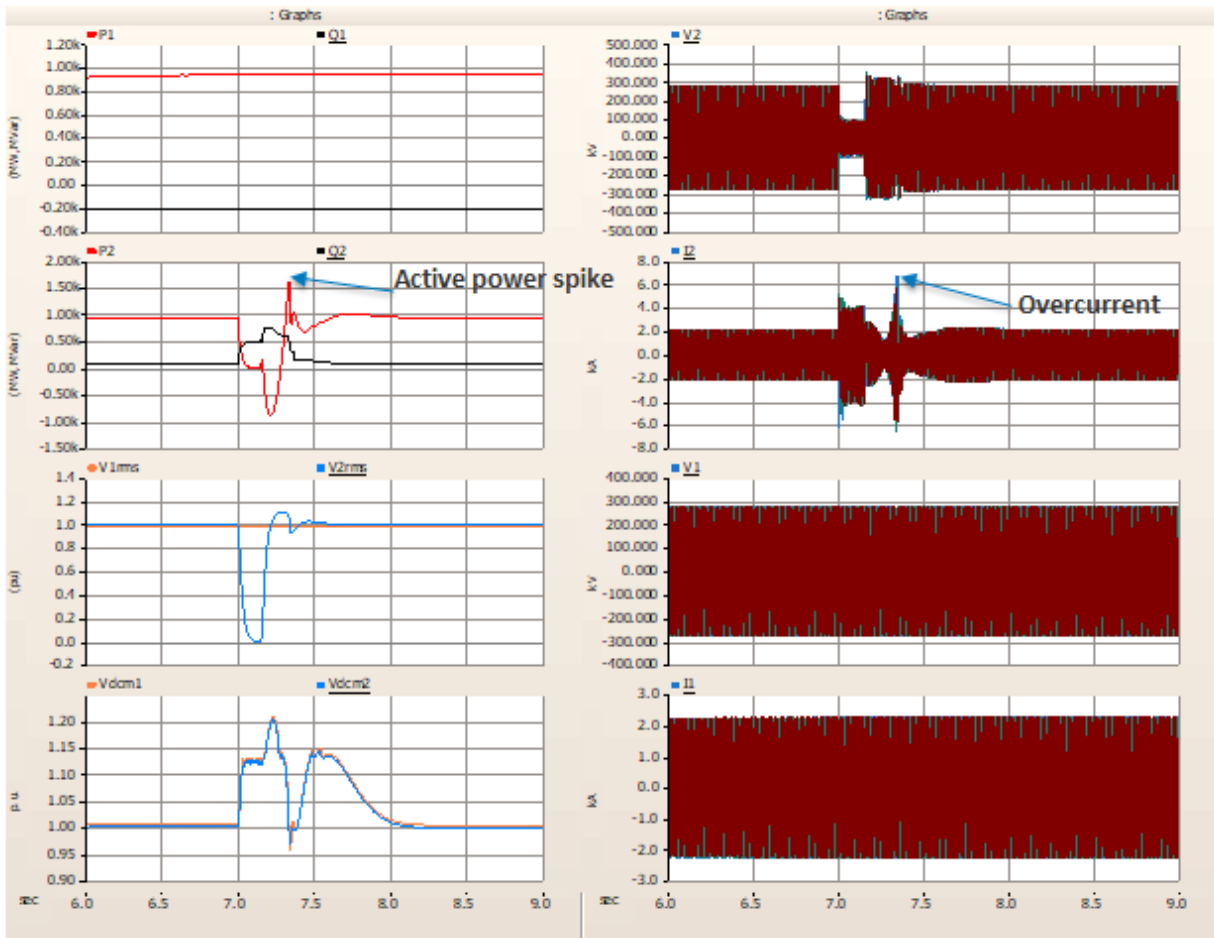


Figure 67. Zero-voltage ride-through of an HVDC-interconnected plant

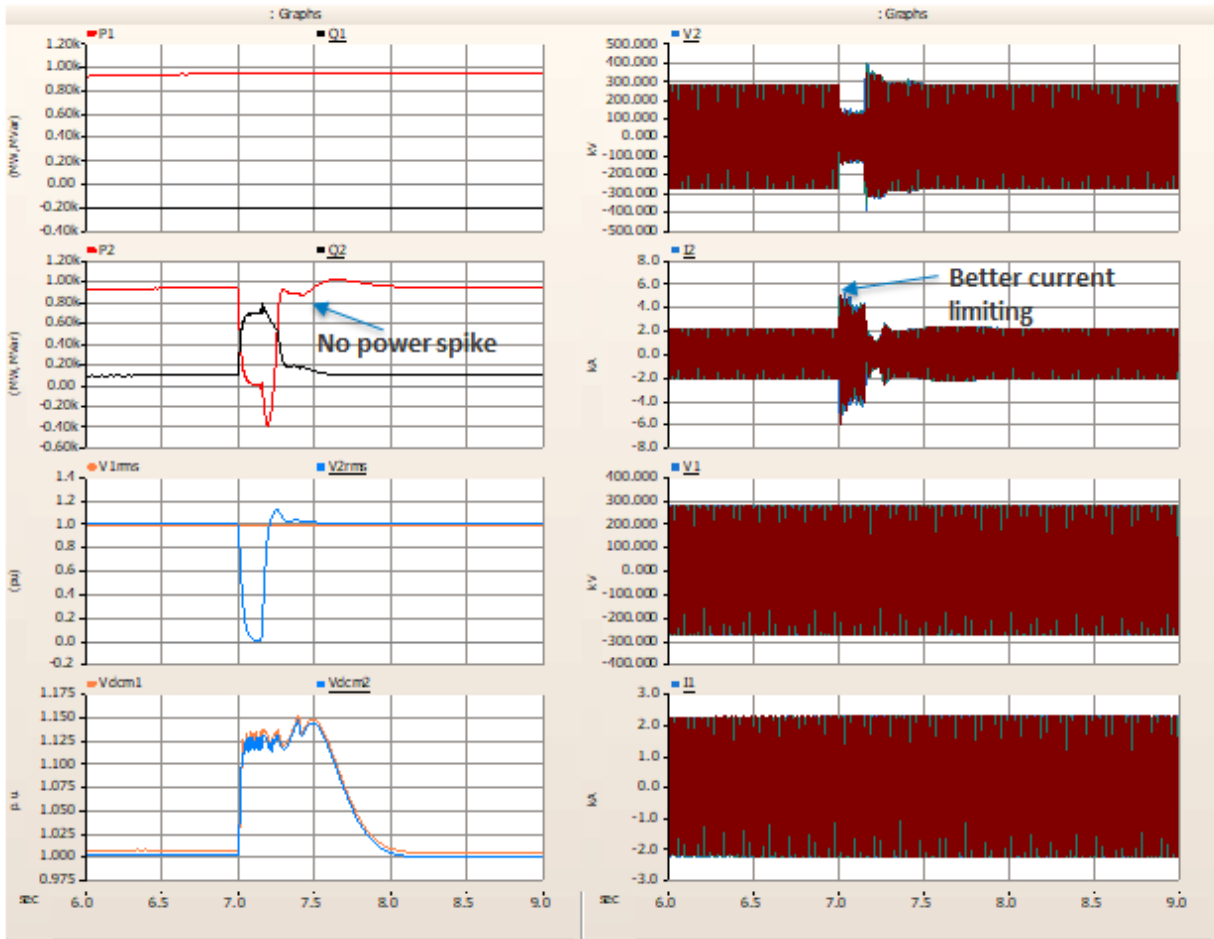


Figure 68. Zero-voltage ride-through of an HVDC-interconnected plant

In addition, we conducted an SCR scan of the HVDC system to demonstrate the impact of HVDC converter controls on its ability to operate stably with weaker grids. Two cases in Figure 69 and Figure 70 show the ability of the HVDC system to operate at a lower POI SCR. By tuning the parameters of the current controller, the SCR stability threshold is reduced from ~ 2.25 in Figure 69 to ~ 2.1 in Figure 70.

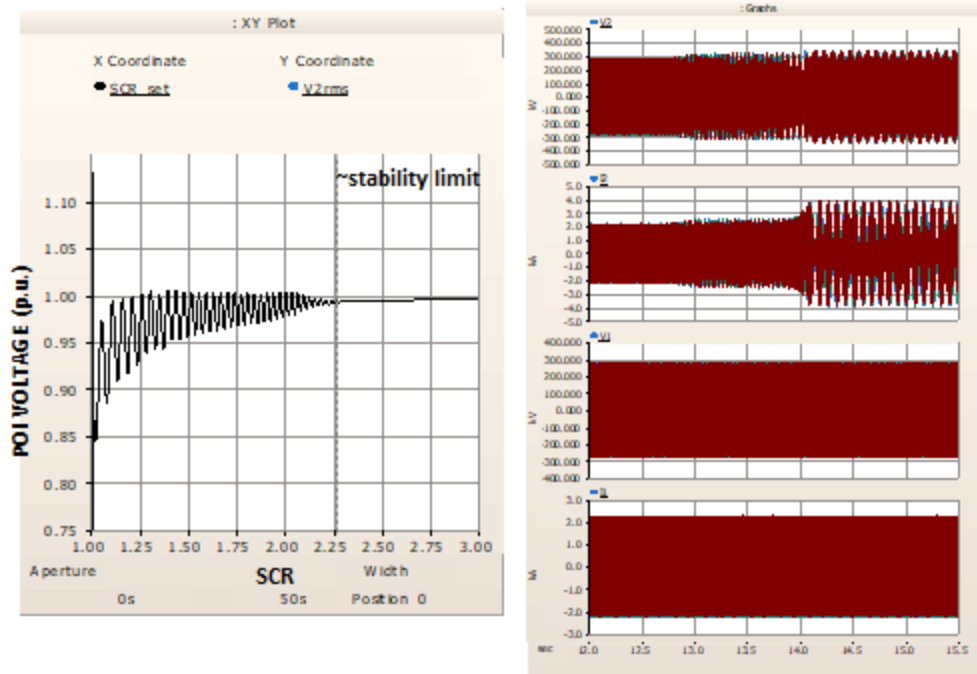


Figure 69. SCR scan of an HVDC-interconnected plant (less aggressive current control gain)

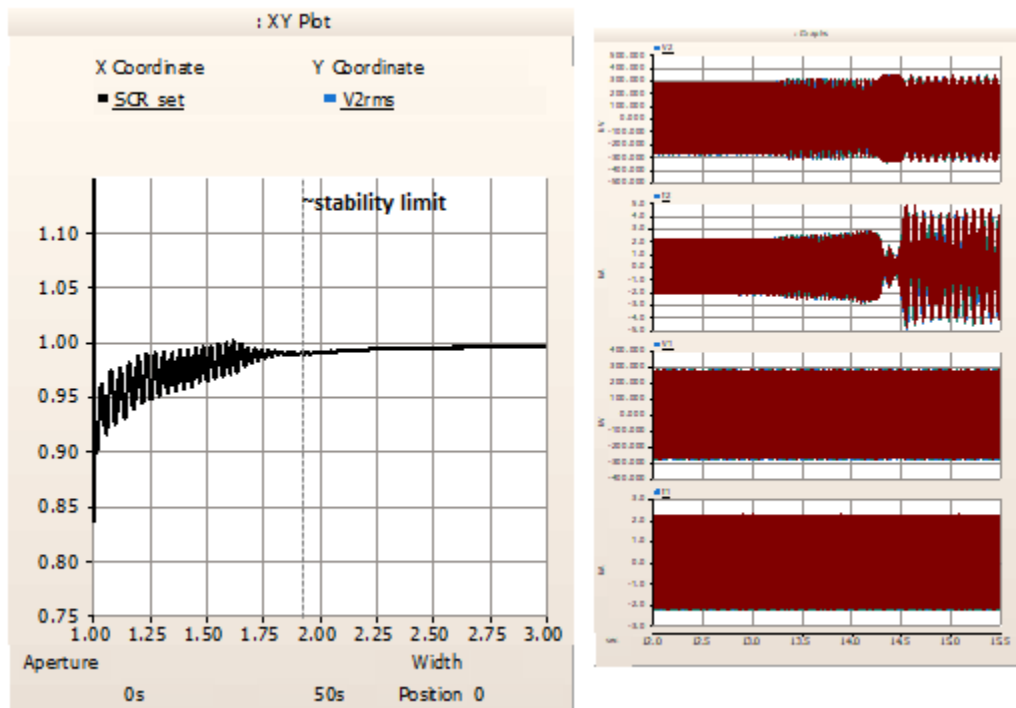


Figure 70. SCR scan of an HVDC-interconnected plant (more aggressive current control gain)

5.3 Sensitivity of an HVAC-Interconnected Wind Power Plant to POI SCR

The ability of HVAC-interconnected offshore WPPs to operate at a lower POI SCR was simulated using the ISO-NE 345-kV Barnstable POI with 800 MW of interconnected wind power via 230-kV AC transmission (conceptual diagram is shown in Figure 71). A mitigating solution in the form of a synchronous condenser to improve system stability for low SCR cases was explored for this system. Simulation results in Figure 72 show single-phase voltage fault ride-through for an 800-MW plant with and without a 100-MVA synchronous condenser installed at the POI. It can be observed from both cases that the synchronous condenser helps to improve transient performance of the plant. Comparison of a steady-state SCR scan for both cases is shown Figure 73, demonstrating that the synchronous condenser allows stable operation of the plant at very low SCRs.

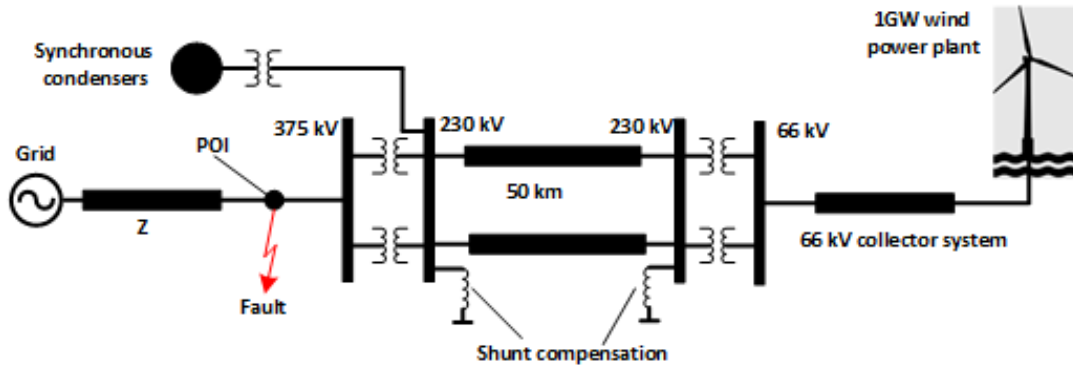


Figure 71. Low-voltage ride-through of an HVAC-interconnected Type 4 plant with a synchronous condenser

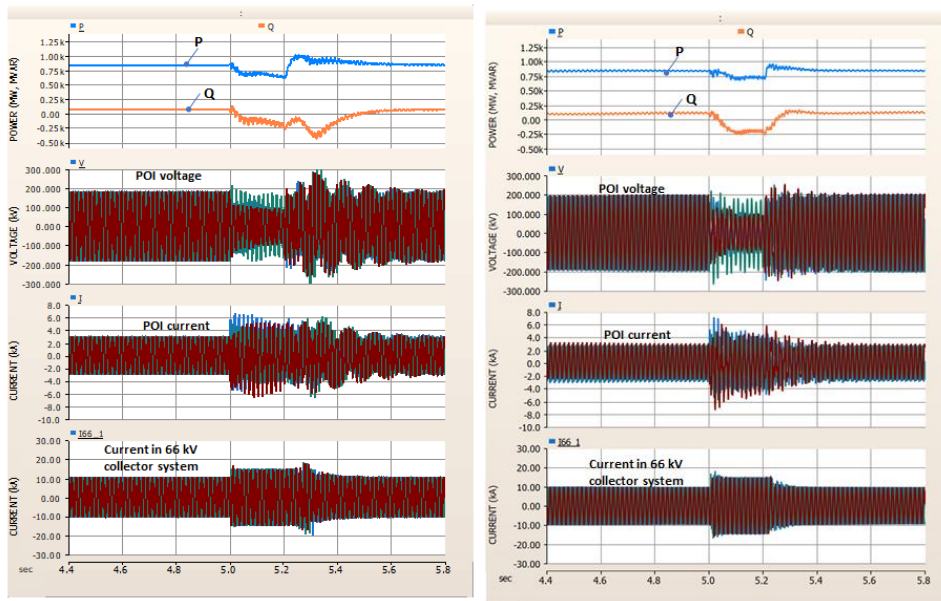


Figure 72. HVAC-interconnected plant ride-through 200-ms L-to-G fault, SCR=3 (no synchronous condenser – left, with synchronous condenser – right)

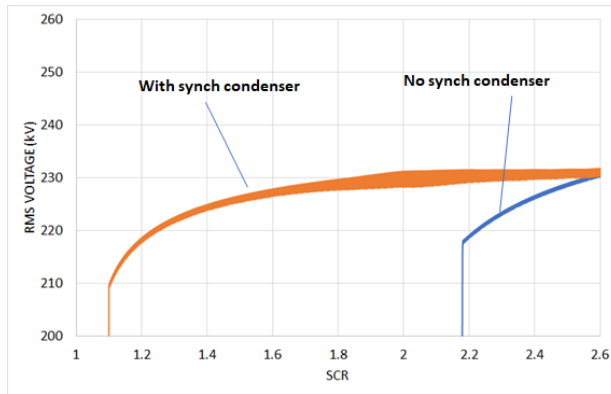


Figure 73. SCR scan of HVAC-interconnected plant for different configurations

5.4 Active Power Controls by HVDC-Interconnected Offshore Wind Power Plants

HVAC-interconnected onshore WPPs already have controls available to provide all types of reliability services to the grid, including many forms of active and reactive power control for frequency response, frequency regulation, and voltage support. Some subsets of these controls are used by utilities and system operators depending on locations and markets. HVAC-interconnected offshore wind plants can also provide similar types of services. However, for HVDC-interconnected plants, services related to plant response to frequency and voltage conditions at the POI cannot be provided in a traditional way since the DC link introduces full isolation between offshore plant collector system and the onshore grid.

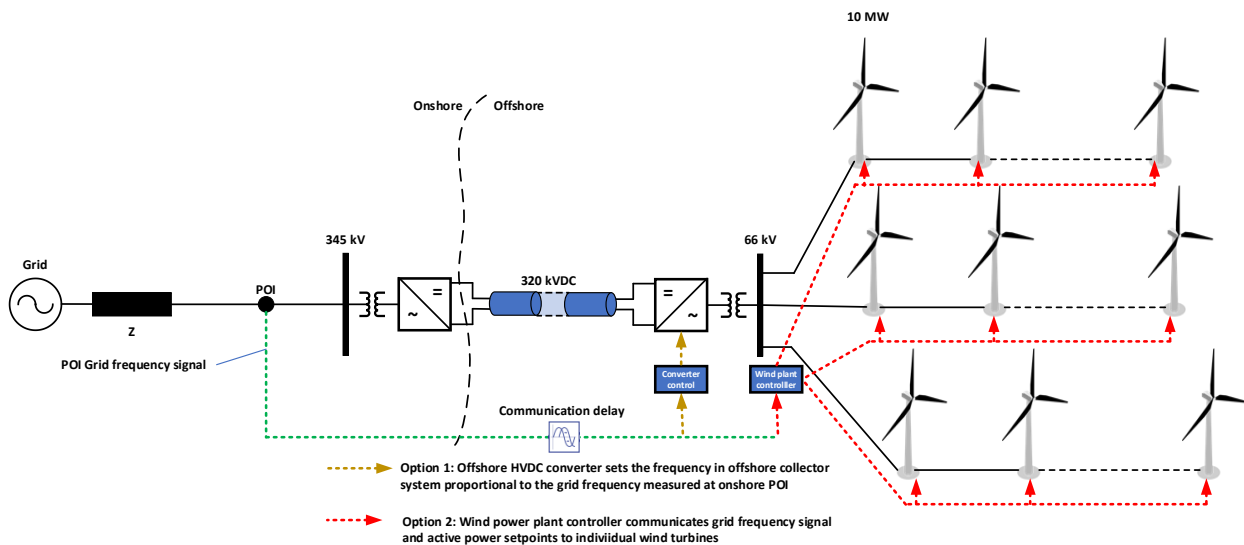


Figure 74. Provision of frequency responsive services by an HVDC-interconnected offshore plant

We simulated controls allowing HVDC-interconnected offshore plants to provide two frequency responsive services: inertial response and primary frequency response (frequency droop response). In normal operation, the frequency of the offshore HVDC converter is not changing, so controllers of the offshore WPP are unaware of a frequency event that may be happening in the onshore grid. To overcome this limitation, we developed and simulated two types of controls (Figure 74):

- Option 1: Grid frequency is measured at the onshore POI and communicated to the offshore HVDC converter controller in real time. If a grid frequency event is detected (based on frequency deviation from scheduled frequency and rate of change of frequency), the offshore terminal controller will command the offshore AC frequency to change proportionally to the onshore grid frequency. In this way, the WPP will be exposed to a real frequency event that is the same as the frequency at the POI (with some delay caused by communications).
- Option 2: There is no real physical change of frequency in the offshore collector system. Instead, the measured POI frequency signal is communicated to the offshore WPP controller, which interprets it as a real frequency change and sends set points to individual WPPs. Normally, the inertial response is turbine-level control, so individual turbine controllers will respond to the rate of change of frequency. Primary frequency control is plant-level control, so active power set points proportional to frequency are sent to individual wind turbines.

For both Option 1 and Option 2, proper thresholds and bandwidth need to be set for both frequency and rate of change of frequency to avoid unnecessary nuisance responses from offshore WPPs.

Results of simulations for both options are shown in Figure 75 and Figure 76. In both cases, a 100 ms communication delay was used. As can be seen from the figures, the HVDC-interconnected offshore WPP provides both inertial and primary frequency response. Active power in both cases is the power at the onshore POI.

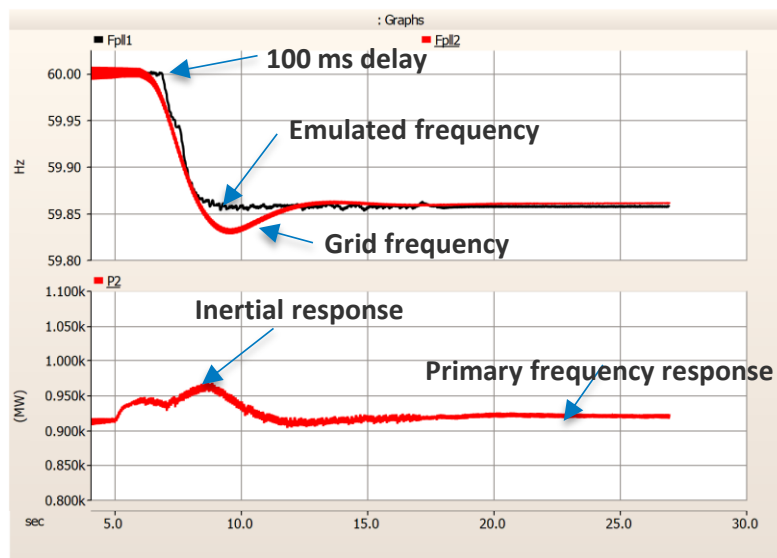


Figure 75. Plant frequency response with Option 1 controls

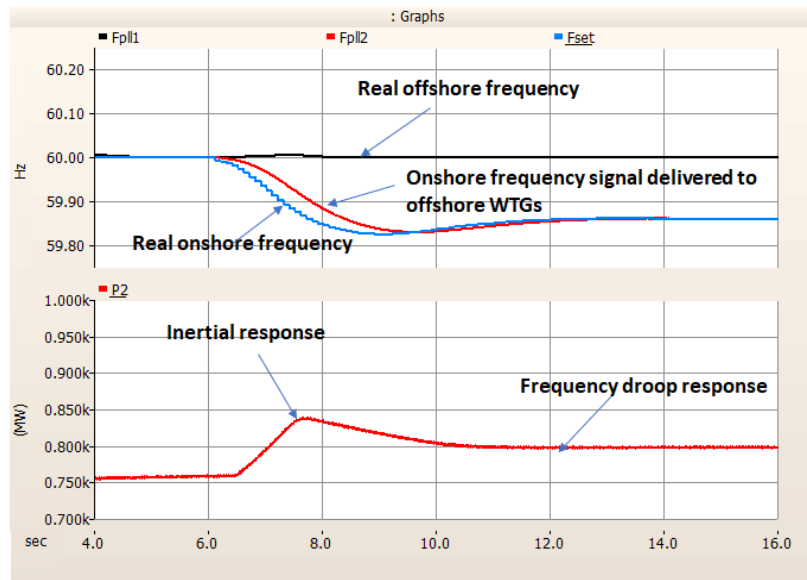


Figure 76. Plant frequency response with Option 2 controls

5.5 Active Power Controls by HVAC-Interconnected Offshore Wind Power Plants

Figure 77 shows the results of simulations for an HVAC-interconnected offshore WPP providing various types of frequency response to the same frequency event. In this case we simulated the following controls:

- Inertial response: turbine-level control that uses kinetic energy stored in wind turbine rotors to provide response proportional to the rate of change of frequency. This service does not require turbine curtailment.
- Primary frequency response: plant-level control that uses the available headroom in the plant with curtailment to provide response proportional to grid frequency. Plant active power trace for 5% frequency droop is shown in Figure 77.
- Inertial and primary frequency response: results of the simulation with both inertial and 5% frequency droop control enabled. At the beginning of the frequency event, the response of the plant is dominated by inertial response because of the high rate of change for frequency. Then, the droop response takes over, as can be seen in Figure 77.
- Fast frequency response: in this case, the fast frequency response is represented by aggressive droop control (1%), so it produces fast and higher power response. However, system-wide

simulations need to verify that such fast changes in plant production do not cause any stability risks.

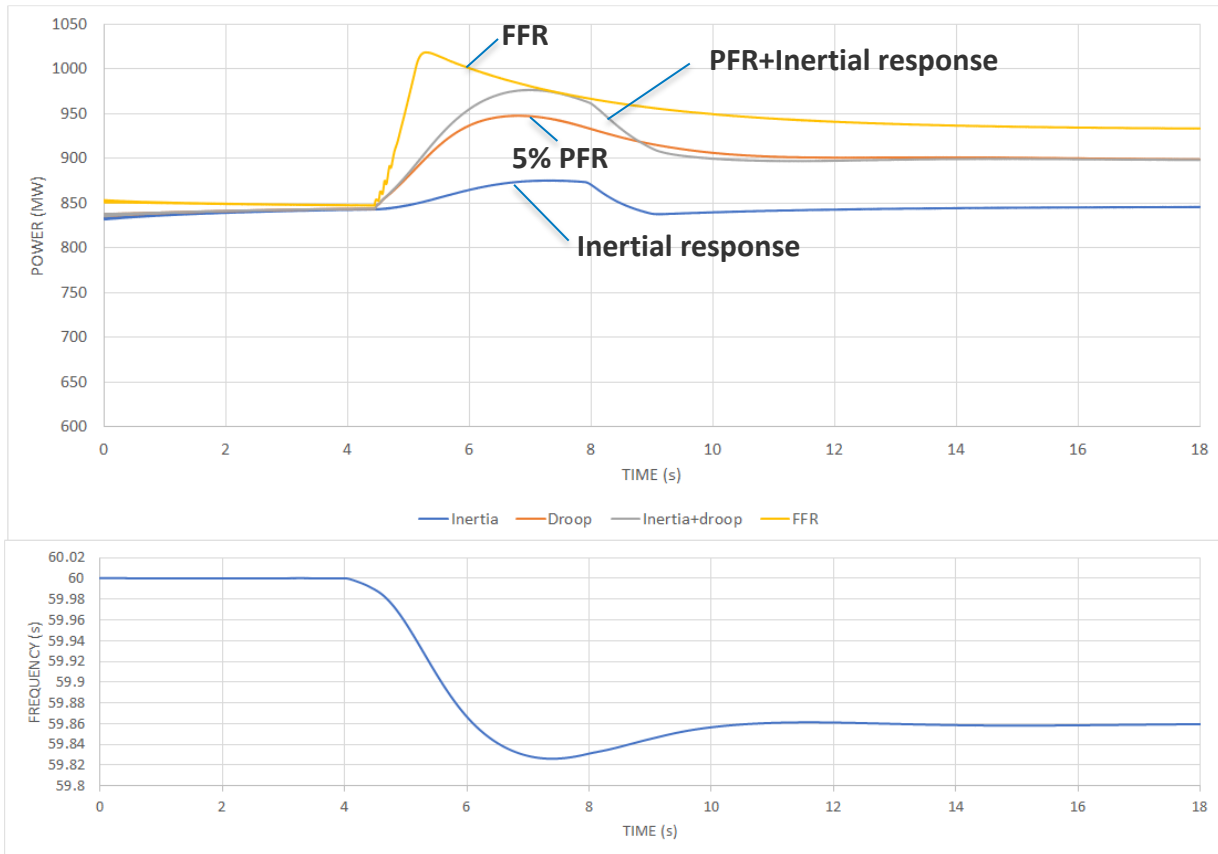


Figure 77. Frequency responsive controls of an HVAC-interconnected WPP

5.6 Offshore Wind Power Participation in Automatic Generation Control

Simulation results for a 1 GW offshore plant providing automatic generation control response is shown in Figure 78. The plant is operating in curtailed mode, so it has headroom to respond to up-regulation signals. For any type of up-regulation service, it is important that the plant controller can accurately evaluate its available power. Any under- or over-estimation of available power for the next automatic generation control

time step will result in either inability to provide the awarded service or in excessive curtailment causing financial loss to the plant operator. In

Figure 78, the simulation was performed for the offshore wind plant with a 12 m/s average wind speed. A communication delay of 100 ms was used to simulate network delay causing latency when sending signals from system operator automatic generation control to the wind plant controller.

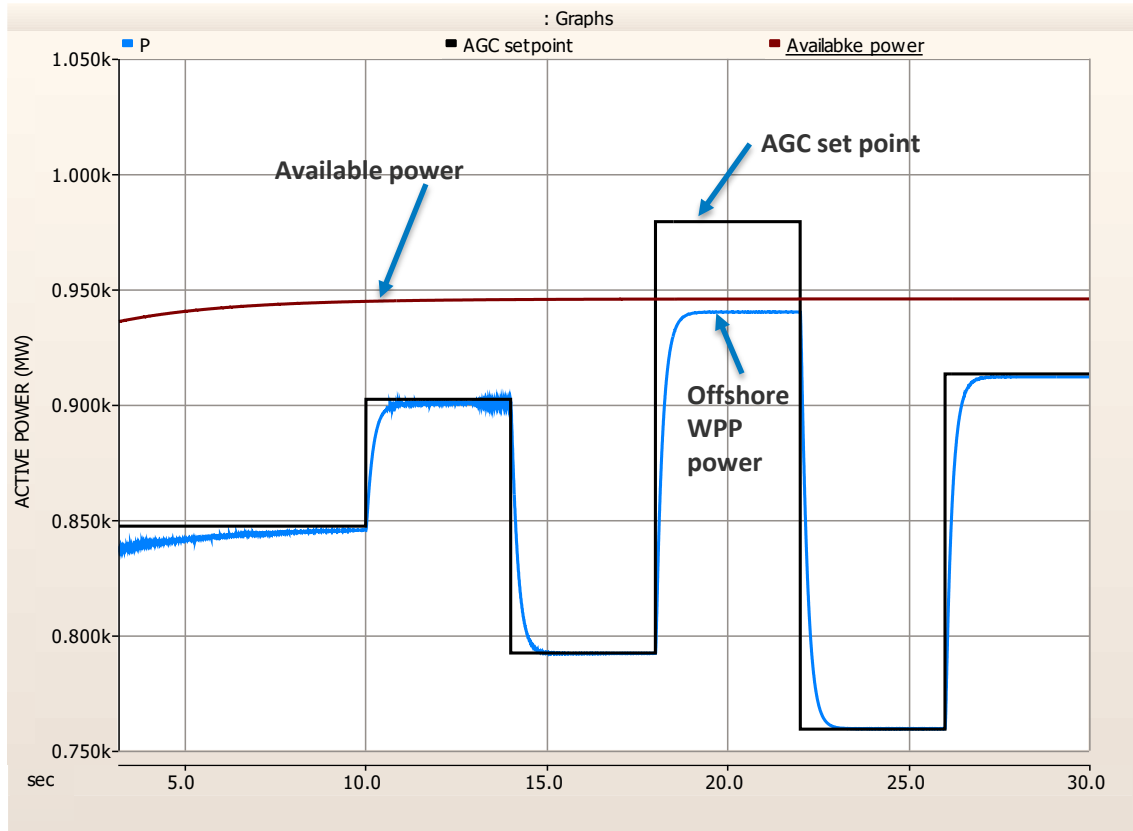


Figure 78. Offshore plant following automatic generation control set points

5.7 GFM Offshore Wind Power Plant

GFM operation by IBRs is considered a stabilizing service in low-inertia weaker power systems. Degrading grid strength is considered a main stability “deteriorator” in the evolving grid, along with decreasing inertia and short-circuit ratio. Droop-controlled GFM converters, as first-order nonlinear systems, can improve stability better than phase-locked loop-based GFL converters, which act as second-order nonlinear systems. GFM converters can become unstable in strong grids, however, and their limited overcurrent capability establishes another constraint to the transient stability of IBR-based grids. Even though the latter problem can be addressed either by oversizing the GFM converters or by large-scale deployments of synchronous condensers to maintain the system strength, both solutions are costly. Further, another challenge with GFM IBRs is how to determine the optimal control structure and how to control them for the best grid stability.

NREL developed a PSCAD model of GFM controls for offshore wind turbine generators. Wind turbine generators are operating in GFM mode. The system has an onshore battery energy storage system that can also operate in GFM mode. A synchronous condenser is present as well, mainly for provision of fault current in the islanded system in case of voltage faults. There is about 50 MW of onshore load. The system

diagram is shown in Figure 79. Figure 80 shows a simulated case when an offshore WPP becomes isolated from the grid when the POI circuit breaker trips open (breaker B_{grid}) at $t=2s$. Transition to islanded operation happens automatically. The GFM wind turbines change their power automatically to match the load. After the initial transient, both voltage and frequency in the island settle to steady-state levels. This is an example of resiliency services that offshore wind can provide to the onshore grid when operating in GFM mode.

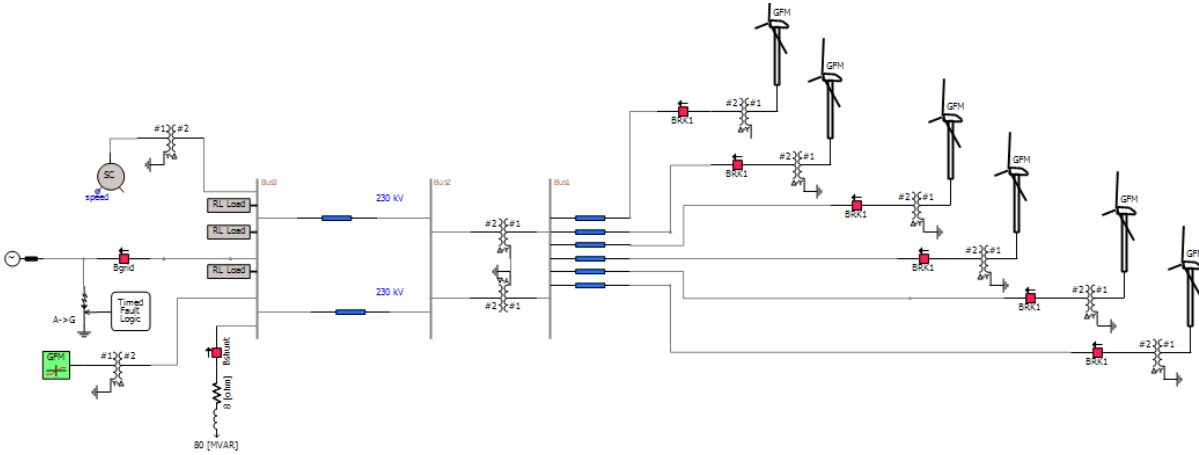


Figure 79. Offshore WPP with GFM Type 4 wind turbine

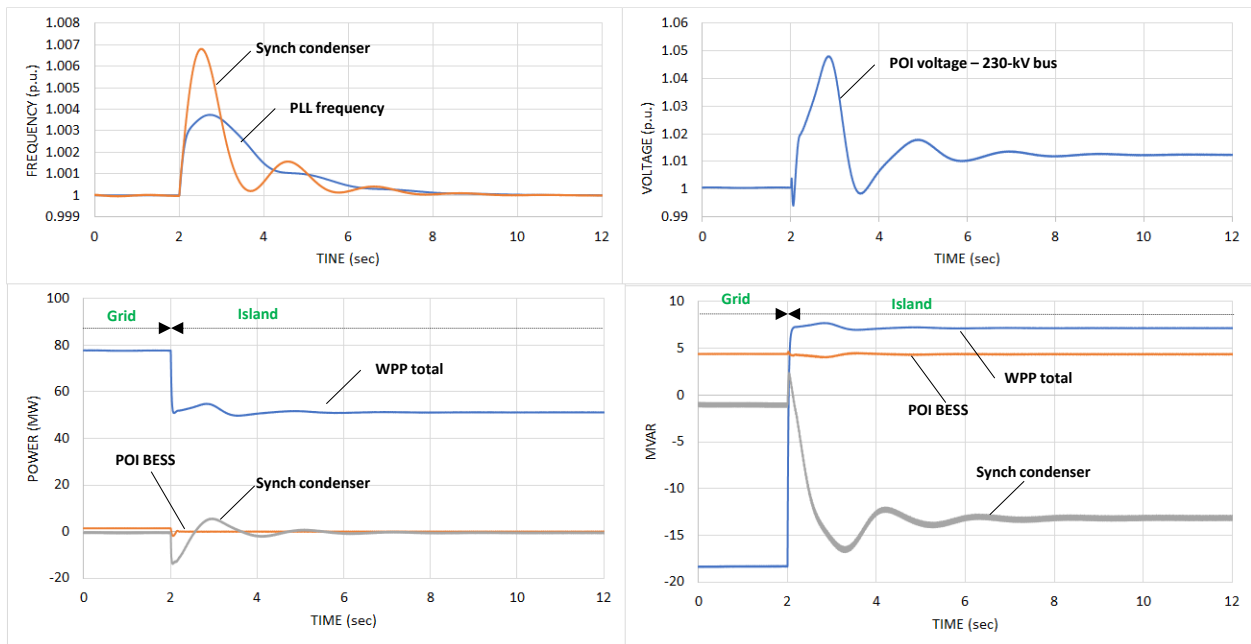


Figure 80. Transition to islanded operation

6 GFL and GFM Operation

6.1 Models of Offshore Wind Turbine Generators in GFL and GFM Modes

In this section, we discuss models of Type 4 wind turbine generators operating in GFL and GFM modes. GFL operation is a conventional mode that all existing commercial onshore and offshore WPPs are operating in. In GFL mode, the wind turbine inverter adjusts its injected power with respect to the grid voltage at its terminals. More precisely, the GFL converter controls the values of active and reactive power by controlling the amplitude and phase of the injected current. A three-phase, phase-locked loop controller is required to estimate the fundamental frequency phasor of the grid voltage, so it can generate the instantaneous current phasor that is used for independent control of active and reactive power. Therefore, in GFL mode, the wind turbine operation depends on availability of grid voltage. It won't be able to operate if the connection with the grid is lost. However, by using higher-level active and reactive power regulators, GFL wind power can provide frequency and voltage responsive services to the grid to support reliability.

On the other hand, in GFM mode, the turbine inverter adjusts the magnitude and phase angle of its voltage, so knowledge of the fundamental frequency phasor of the grid voltage is not necessary (no phase-locked loop is needed). The GFM inverter can operate in an isolated system where no other voltage sources are present and can provide power to the loads. From an electrical standpoint, the GFM inverter behaves like a voltage source behind an impedance, or a synchronous generator without inertia. The increasing need for power grids to maintain system strength because of IBRs is a main concern for grids in transition.

GFM technology for IBRs is gaining traction in the energy industry as the grid continues to evolve with increasing shares of IBRs and retiring conventional generators. GFM controls by IBRs can replace some services that synchronous generators have been providing. Mainstream wind power based on Type 3 and Type 4 electric topologies, as an IBR technology, is fully capable of providing GFM services. Testing and demonstrations have been conducted for both topologies. Although it is not yet commercially available (like GFM battery storage), GFM wind can make a quick market entry when required. There are still several aspects related to controls and design improvements of GFM wind power that the industry can address when there is a market in place to incentivize the provision of such services. The stabilizing impacts of GFM controls for IBRs have been demonstrated in many studies. Despite many stabilizing characteristics of GFM IBRs as an enabler for the future carbon-free renewable grid, GFM technology alone is not a sufficient measure to resolve all integration challenges described in this paper, with degrading grid strength and the resulting reduction in the fault current levels being the primary challenge. The substantial deployment of other enabling technologies, such as synchronous condensers, might be necessary to keep the grid strength within acceptable limits.

NREL team developed full models of Type 4 wind turbine generators for both GFL and GFM modes of operation. Model diagrams for GFL and GFM operation are shown in Figure 81 and Figure 82, respectively. Both models include all electrical components of the system (generator, power converter, transformer), controls, and mechanical components (wind rotor, pitch, and yaw systems).

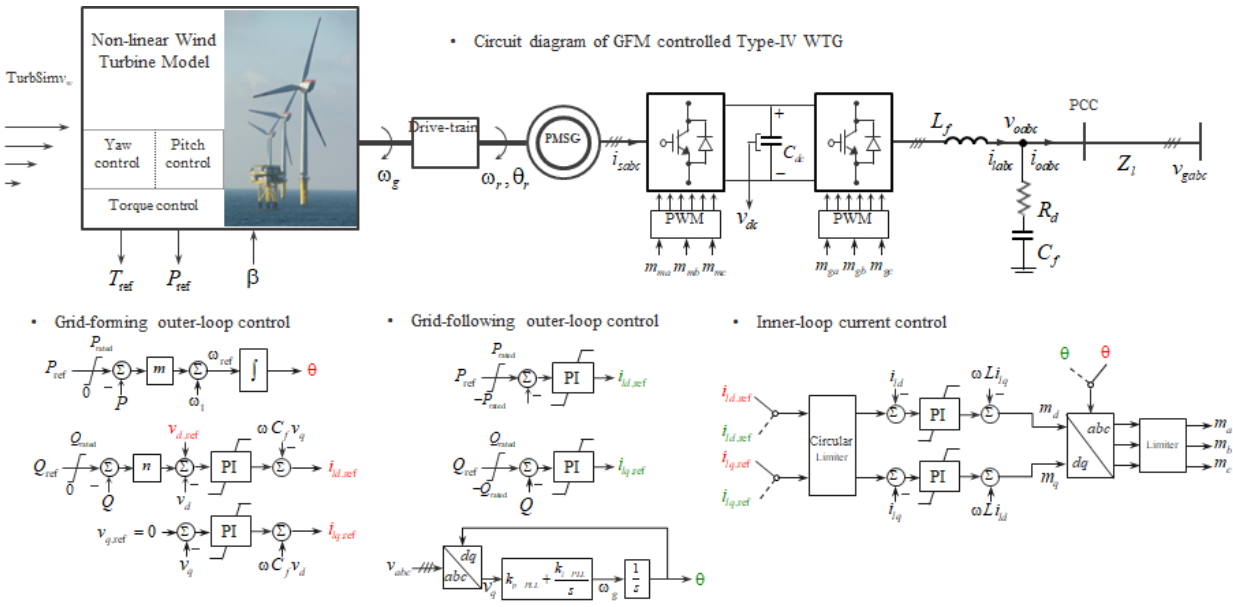


Figure 81. Model of an offshore wind turbine generator operating in GFL mode

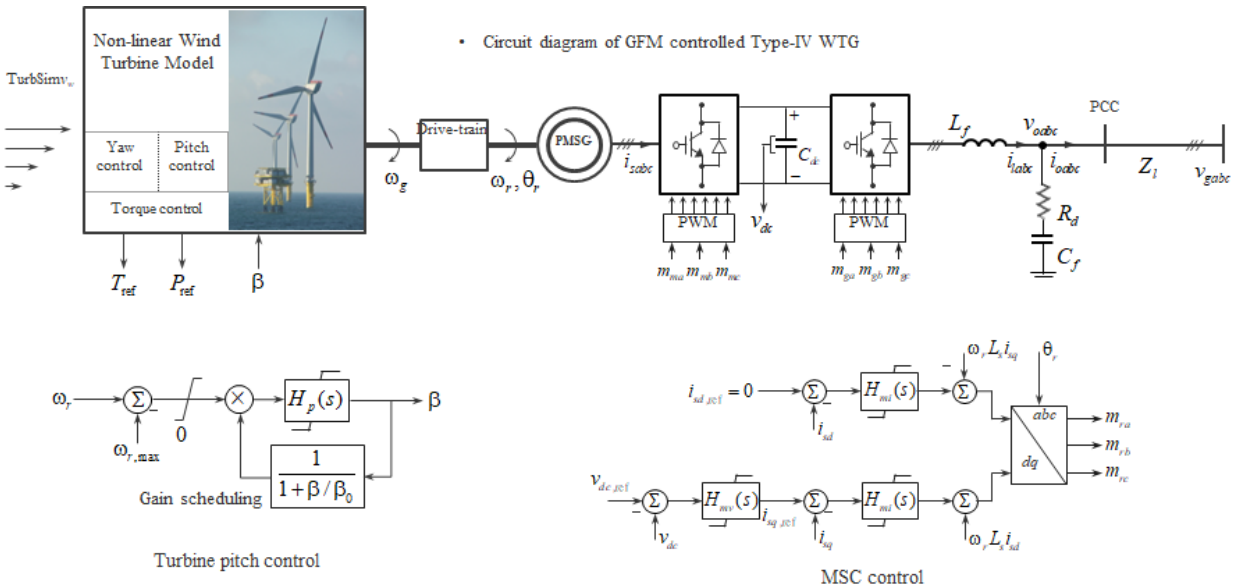


Figure 82. Model of an offshore wind turbine generator operating in GFM mode

Both turbine models are connected to the WPP controller model that provides set points to individual wind turbines. Controls for the GFL model include:

- Active power set point control/controlled curtailment (plant-level control)
- Inertial response (turbine-level control)
- Primary frequency response or frequency droop control (plant-level control)
- Voltage/reactive power/power factor control (turbine-level control)

The GFM operation is realized through the P-f and Q-V droop control method. With this control, the turbine operates like a voltage source behind an impedance.

Both models were developed in PSCAD in generic form. They do not represent any existing commercial wind turbines but are practical enough to understand the stability impacts of offshore wind power on the onshore grid. Both models are in public domain and can be shared with NOWRDC stakeholders.

6.2 GFL and GFM Operation of Offshore Wind Power Plants

In this report, we discuss GFL and GFM operation of offshore WPPs that are interconnected with an onshore grid via an HVAC export line. The operation of HVDC-interconnected plants was explained in previous deliverable documents. In HVDC operation, both onshore and offshore HVDC terminals can operate in GFM mode, so GFM operation of wind turbines in HVDC-interconnected WPPs is not needed.

A model of an offshore WPP connected to an onshore substation was used to demonstrate differences between GFL and GFM operation. The model, shown in Figure 83, represents the Vineyard offshore project interconnected with the West Barnstable substation in the ISO-NE system. The project is connected to a 345-kV transmission system (represented by a voltage source behind impedance) through a 230-kV submarine export line. A 66-kV collector system is used to connect individual wind turbines to the offshore substation. In this system, we used models of wind turbines operating in GFL or GFM modes.

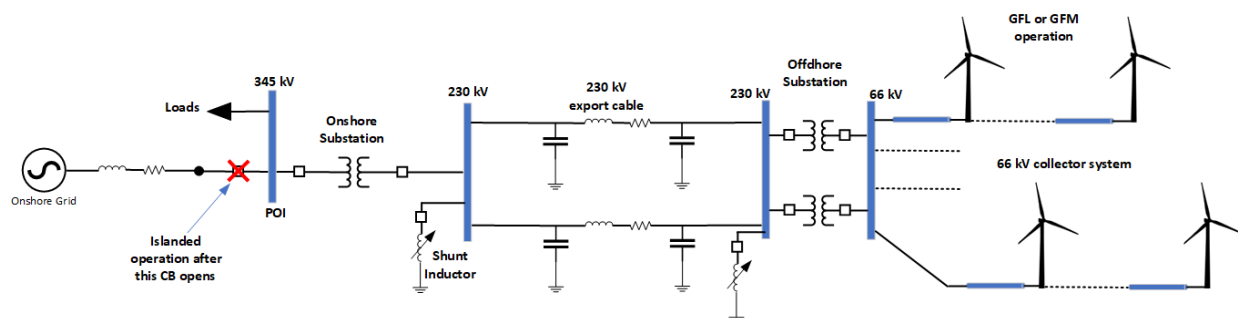


Figure 83. Model of an offshore WPP connected to the onshore grid

A GFL resource is expected to absorb or inject active and/or reactive power to resist changes in the positive-sequence voltage phase angle and is expected to do so without exceeding equipment limits. Similarly, a GFM wind turbine is expected to absorb or inject reactive/active power to reduce changes in the positive-sequence voltage magnitude. Further, following grid events, a GFM turbine is expected to contribute to positive damping of any oscillations that may arise. Synchronous machines perform a similar damping service. Using the model shown in Figure 83, we show some examples of simulations to demonstrate differences between GFL and GFM operation of an HVAC-interconnected offshore plant.

The grid voltage vector can experience phase angle jumps during grid faults, which can give rise to significant transient synchronization errors that might threaten the stability of GFM power converters. Phase angle jumps manifest as a shift in zero-crossing of the instantaneous voltage. Phase angle jumps during three-phase faults are due to the difference in X/R ratio between the source and the feeder and the transformation of sags to lower voltage levels. For a GFL inverter, the response to a phase jump is a controlled response. Examples of simulated responses for GFL and GFM WPP to a 30° phase jump in grid voltage are shown in Figure 83 and Figure 84, respectively (WPP active/reactive power and voltage at a 345-kV POI).

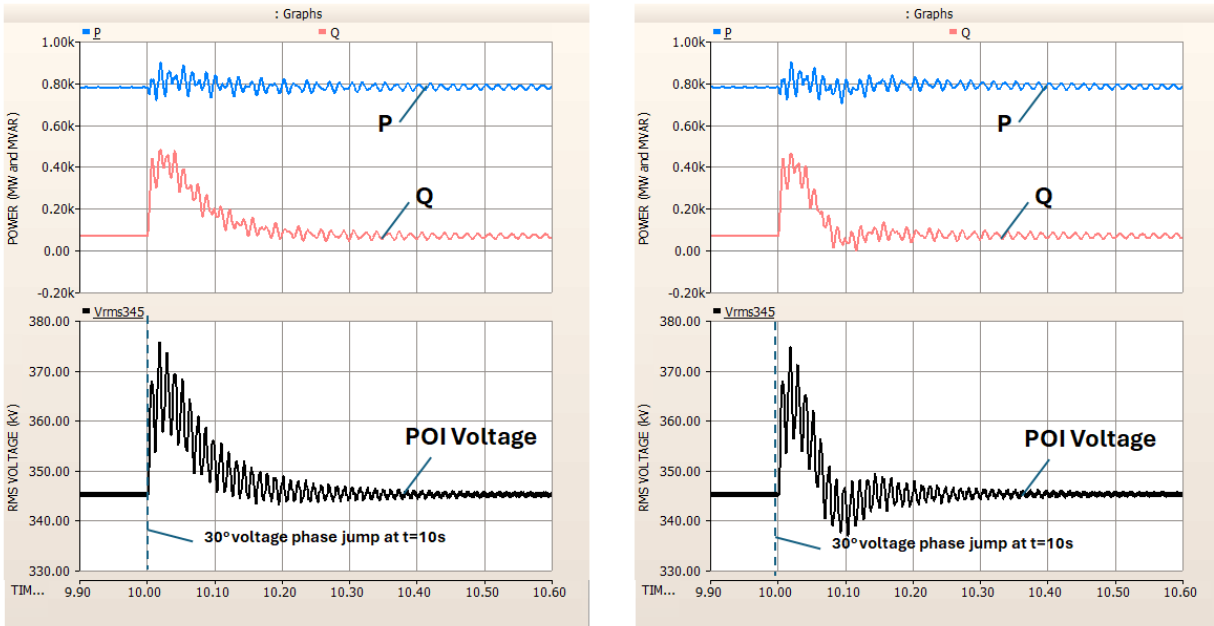


Figure 84. Simulated response of a GFL WPP to a 30° phase jump in a 345-kV grid (right – no voltage droop control, left – 5% voltage droop control enabled). Plant response is shown for 345-kV bus.

The WPP operating in GFL mode exhibits a current source behavior during grid voltage phase jump transients. This can be observed in Figure 84 for two cases: (1) wind turbines do not have any voltage response control and (2) wind turbines have 5% voltage droop control enabled. In both cases, an overvoltage occurs at a 345-kV POI because plant reactive power increases immediately after the phase jump.

On the other hand, in GFM mode, the same plant exhibits a response of a voltage source behind an impedance while within its current capability limits (Figure 85). The plant follows its main control objective in the sub-cycle time frame to control its voltage waveform. This contrasts with a GFL inverter, which controls its output current as the main objective. The magnitude and phase angles of the internal voltage source remain nearly constant within the transient time frame following a disturbance. This is essential for providing the GFM inverter with capabilities like instantaneous active and reactive power response when disturbances occur. In GFM mode, the inverters of wind turbines are inherently resisting fast changes in the voltage and phase angle and hence can improve power system stability. In addition, on longer timescales (multiple power frequency cycles), the reference voltage phasor of a GFM inverter could vary to support the secure operation of the power system.

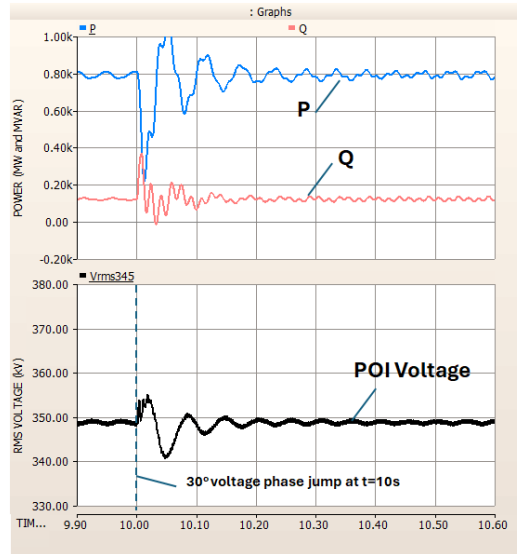


Figure 85. Simulated response of GFM WPP to a 30° phase jump

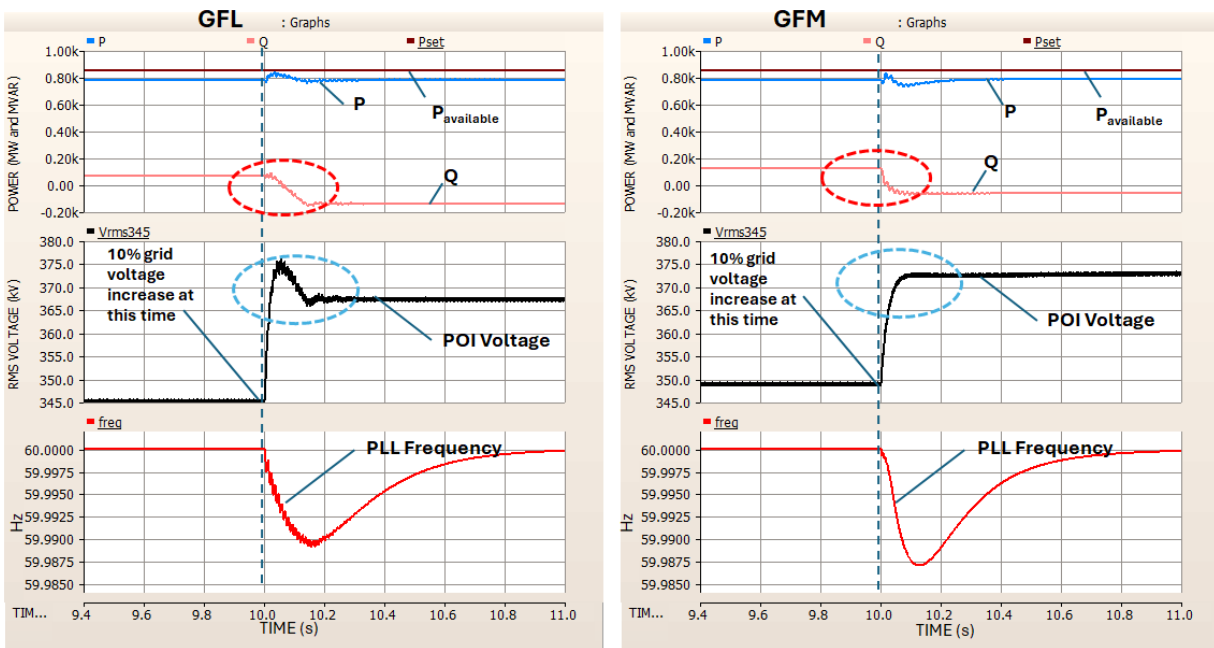


Figure 86. Simulated response of an offshore WPP to a 10% step increase in voltage in a 345-kV grid (left – GFL operation, right – GFM operation)

The simulated response of a WPP to a 10% step increase in grid voltage is shown in Figure 86. In GFL mode, the response of the plant is inherently slower than in GFM mode. Comparison of reactive power response (red circles) and voltage response (blue circles) indicates a faster response in GFM mode, as expected.

6.3 GFL and GFM Operation at Lower SCRs

As mentioned above, reduced grid strength is one of main stability challenges in the evolving grid. Grid strength is characterized by the SCR at the POI. A lower SCR means weaker interconnection. Grid weakness is manifested by the fact that changes in plant power production will cause voltage changes due to relatively larger impedance in the system. There are several factors that can contribute to this:

- Very long transmission or distribution lines without compensation
- Low local generation-load ratios
- Low inertia in the system
- Large amounts of inductive load without compensation.

As a result, voltage instabilities and interactions between various system components may appear to jeopardize reliability. GFM resources are expected to provide more stabilizing impact for the grid because of their ability to operate stably in weaker grids compared to GFL resources. Simulation results for the plant in Figure 81 operating in GFL and GFM mode is shown in Figure 87 for steady-state operation at different SCR values. It can be observed that an HVAC-interconnected WPP operating in GFM mode has better voltage stability at very low SCRs (min SCR=1.2 in GFM operation compared to SCR≈2 in GFL operation). It is important to note that these steady-state results do not indicate SCR limits for transient stability (such as the ability of offshore WPPs to provide robust voltage fault ride-through performance in weak grids).

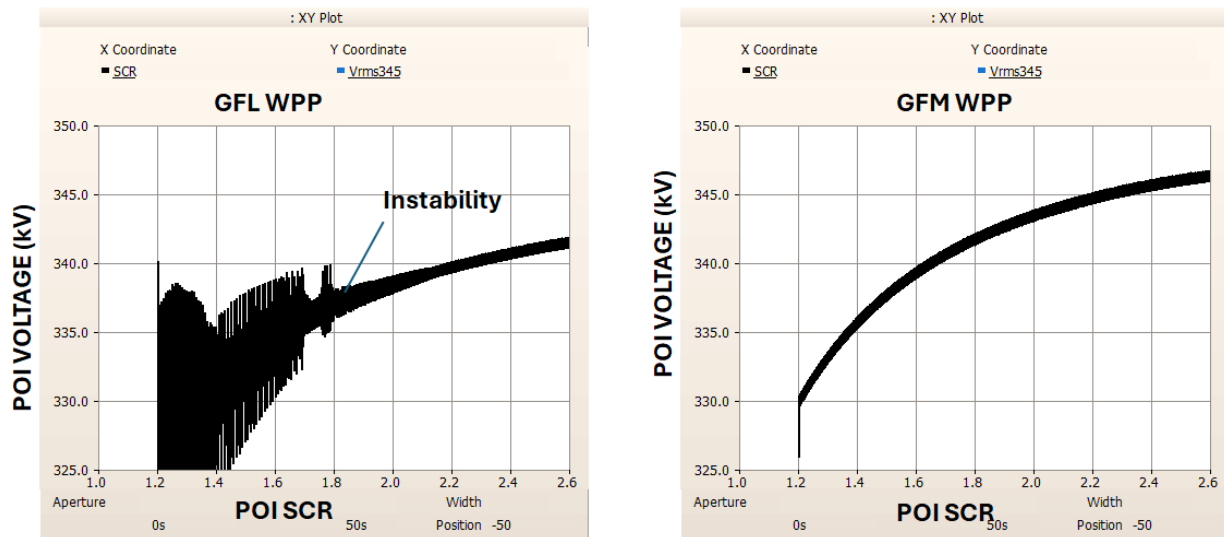


Figure 87. 345-kV POI voltage dependence on SCR (GFL – left, GFM – right)

6.4 GFM Operation in Islanded Mode

One essential advantage of GFM operation by IBRs is their ability to operate loads in the absence of a power grid. We demonstrated such a mode of operation with simulations for an offshore WPP using the model of the Vineyard project shown in Figure 81. After the circuit breaker trip off on the 345-kV bus (indicated as a red X in Figure 81), the whole offshore wind plant with local loads connected to the same bus becomes an islanded grid fully isolated from ISO-NE power system. The advantage of GFM operation by offshore wind is that it can continue its operation after the main grid is lost. It can also provide automatic

load tracking. This is demonstrated by simulation results shown Figure 88 (left). Before the fault, the offshore wind plant was operating at 800 MW. Immediately after the fault, the wind plant automatically reduces its power in accordance with its P-f droop setting to meet the 600-MW local load. The offshore WPP is the only source that sets voltage and frequency in this isolated system ensuring stable operation.

On the other hand, in GFL mode, the system will be disconnected shortly after the circuit breaker tripping because of voltage and frequency collapse, as shown in Figure 88 (right). In GFL mode, the wind plant is not capable of operating in a stable way because it depends on grid voltage and frequency to generate power.

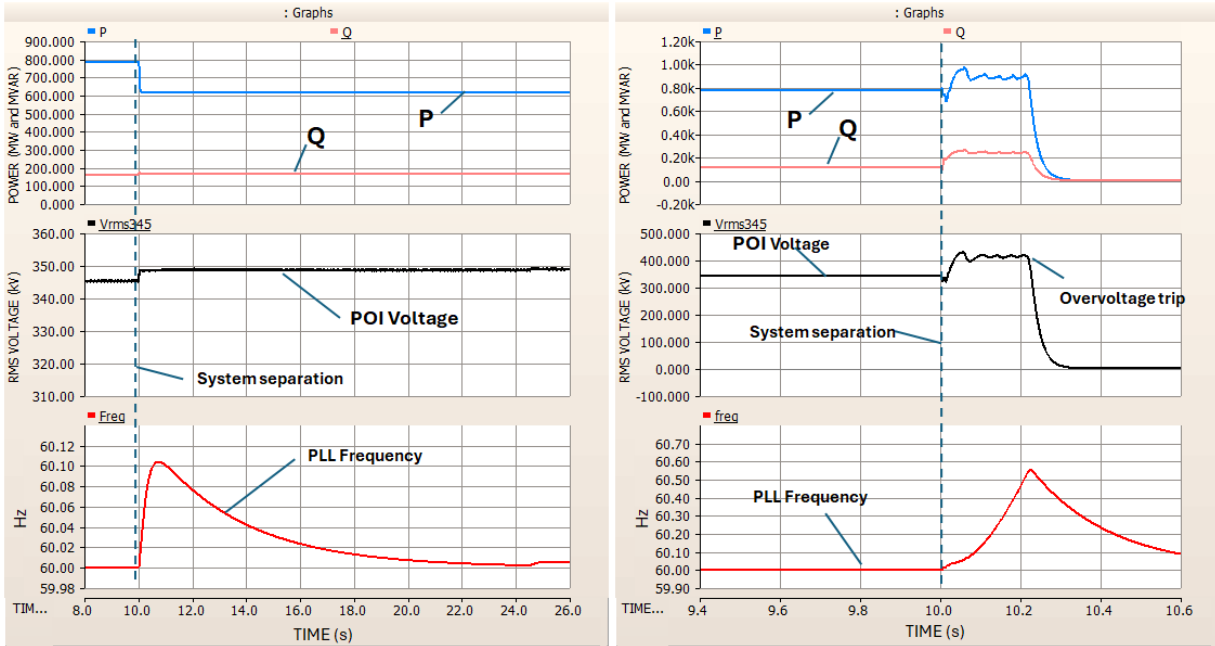


Figure 88. Transition to islanded operation during system separation (GFM wind plant – left, GFL wind plant – right)

The ability of an offshore GFM WPP to track the load under variable wind speed and load conditions is shown in Figure 89. The wind plant is operating with some curtailment to maintain sufficient headroom for increasing its power if required by the load in islanded mode.

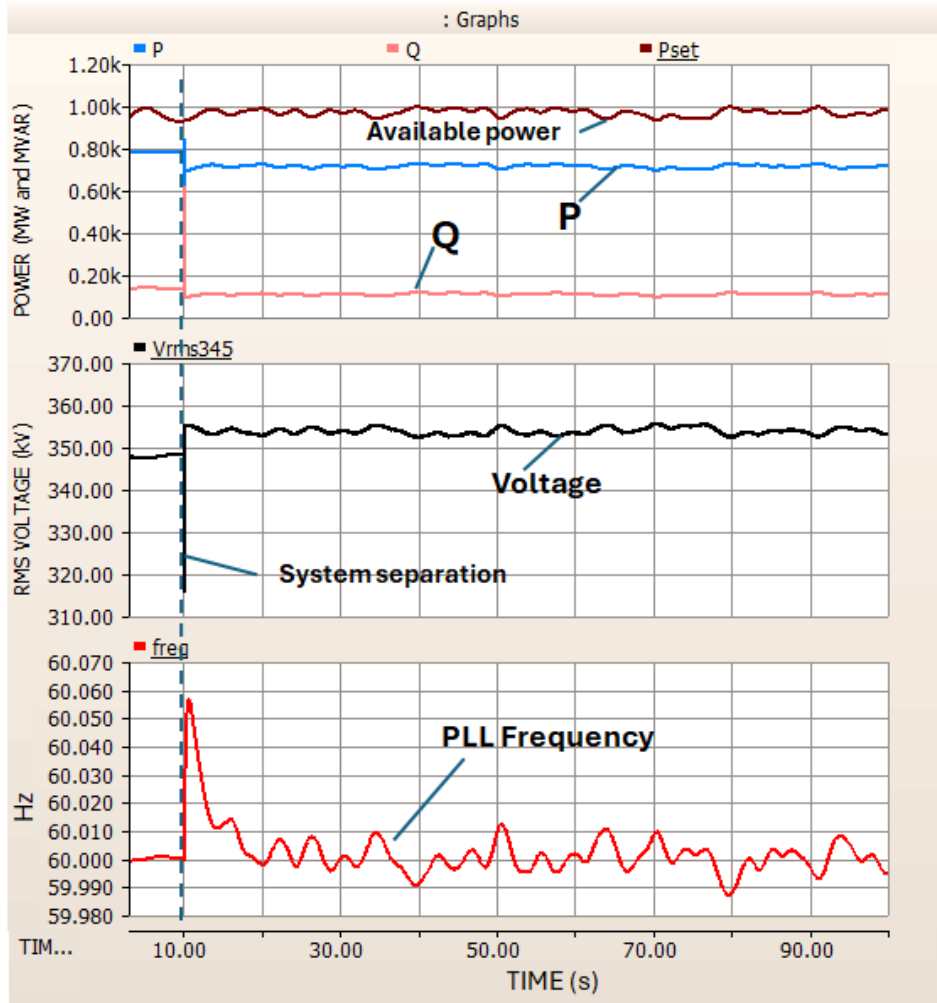


Figure 89. Islanded operation of a GFM wind plant under variable load and wind conditions

7 Testing Results

7.1 Description of Test Site

The purpose of this stage of the project was to demonstrate and validate through testing the controllability aspects of modern utility-scale wind turbine generators that have been studied and modeled in previous tasks of this project. This includes control for HVAC-interconnected WPPs that are directly exposed to all dynamic and transient conditions occurring in the onshore grid, and control for HVDC-interconnected plants that are buffered from grid conditions because of the DC link. For this purpose, we used the 1.5-MW commercial GE wind turbine generator installed at NREL's Flatirons Campus test site (Figure 90). The turbine operates under real variable wind conditions that are extremely turbulent due to the site's proximity to the foothills of Rocky Mountains. Such turbulence conditions are more extreme than what is usually observed in a typical offshore WPP, making it a good testing site. The turbine was fully integrated into the multi-megawatt emulation platform described in the next section.



Figure 90. NREL test site with GE wind turbine and CGI

7.2 Test Platform

The experiment platform is depicted in Figure 91. The GE 1.5-MW wind turbine generator is connected to the 13.2-kV collector system through its pad-mount step-up transformer (690 V to 13.2 kV AC). On the other side of collector system is NREL's 7-MW power electronic grid simulator, or controllable grid interface (CGI). CGI also operates at a medium voltage of 13.2 kV. It is capable of independent voltage control in each of three phases allowing emulation of all types of voltage faults. The CGI can also test turbine responses to fault conditions occurring deep in the power system in some electrical distances from a WPP. CGI is rated for 7 MW of continuous power but can absorb or produce 6 times higher-than-rated current for at least 2 s under fault conditions. In this way, potentially large fault current contributions from the test turbine can be absorbed by the CGI without disturbing the rest of the grid.

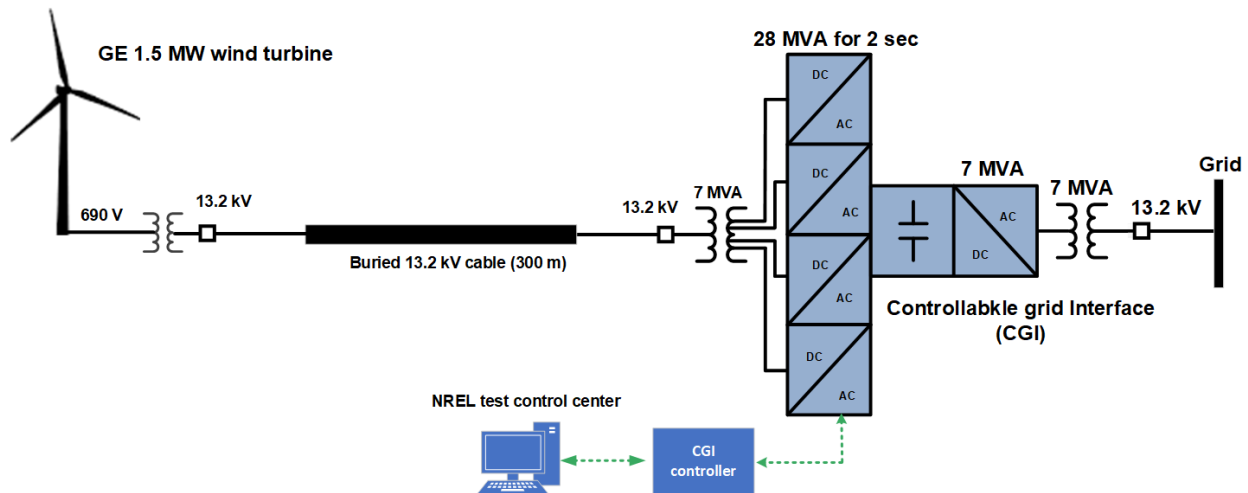


Figure 91. NREL experimental platform

The CGI can also control the frequency of the voltage that the wind turbine sees, enabling testing of frequency responsive controls of the wind turbine. The CGI has also a programmable feature to emulate stronger or weaker POIs at the receiving end of the export cable. Since the CGI is based on power electronics hardware, it has a capability to emulate AC interconnection POIs for wind plants, but also emulate dynamics of HVDC terminals for HVDC-interconnected WPPs.

The power levels and voltage of the experimental platform shown in Figure 91 are lower than the ones used in real offshore WPPs. While the collector systems in modern WPPs are rated at 66 kV, the rated voltage in NREL’s test collector system is only 13.2 kV. However, this type of mismatch does not significantly impact this testing since all control parameters and electrical values were normalized (or per-unitized) by the CGI control to ensure that test conditions are as close as possible to the PSCAD simulation cases described in previous reports.

The wind turbine controls are connected to the GE WPP controller, so it operates as a “WPP of one.” Turbine-level controls such as voltage fault ride-through and inertial response are implemented at the turbine level. Other frequency responsive controls such as primary frequency control (or frequency droop control) and operation with reserves are implemented in the power plant controller. This is a normal division of control functions implemented in many commercial WPPs worldwide.

The following tests were conducted under Task 6 of this project:

- Low-voltage ride-through and zero-voltage ride-through tests of the wind turbine when connected to the AC grid
- Operation of the wind turbine under frequency excursions introduced by the CGI to demonstrate inertial and primary frequency control by wind power.

The results of these experiments are described in the sections below.

7.3 Voltage Fault Tests

The wind turbine was tested under different fault conditions (including fault depth and duration). The depths of voltage faults were emulated by the CGI for up to 100% level (zero-voltage faults) with durations up to 1 s. The purpose of this test was to validate the general findings of PSCAD simulations conducted under previous tasks. The purpose was not to verify turbine compliance to different standards and not to re-tune turbine parameters to change the performance. Changing turbine parameters is outside of NREL capabilities since it involves liability and requires full participation by the vendor (GE) in this project. Results of testing

under this task are sufficient to demonstrate turbine’s ability to respond to voltage faults under different fault parameters and POI SCRs represented by the CGI.

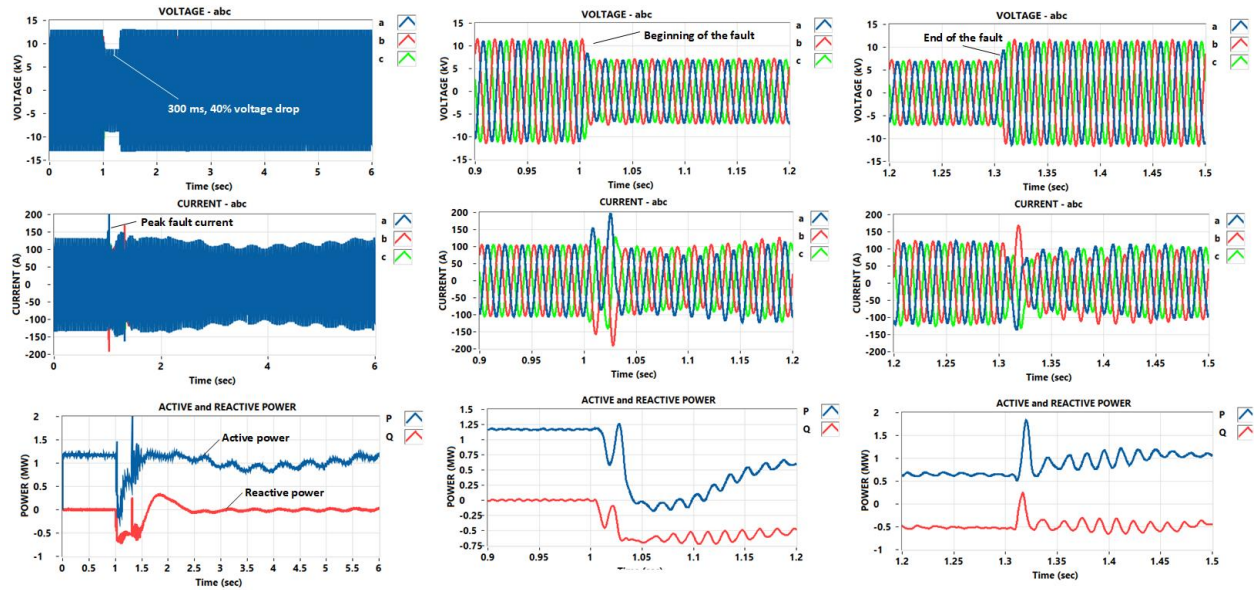


Figure 92. Turbine ride-through during a 300-ms, 40% voltage fault (5% SCR)

Figure 92 shows results of a 300-ms, 40% three-phase voltage fault (as measured on the turbine’s 13.2 kV terminal). The CGI emulated the rectangular voltage dip with depth that is 40% below turbine rated voltage. The turbine demonstrated successful ride-through during this fault and restored its power production shortly after the voltage was recovered (left column of plots in Figure 92). The turbine’s short-circuit current contribution can also be observed in these plots. Middle and right columns in Figure 92 show zoomed recorded traces for voltage, current, and power during the start and end of the fault, respectively. This is an example of a successful voltage fault ride-through that was simulated under previous PSCAD modeling tasks.

Another example of a successful ride-through is shown in Figure 93 for a deeper (50%) fault of the same 300 ms duration. As in the previous case, the turbine demonstrates robust performance and restores its production shortly after the voltage is restored to its nominal level.

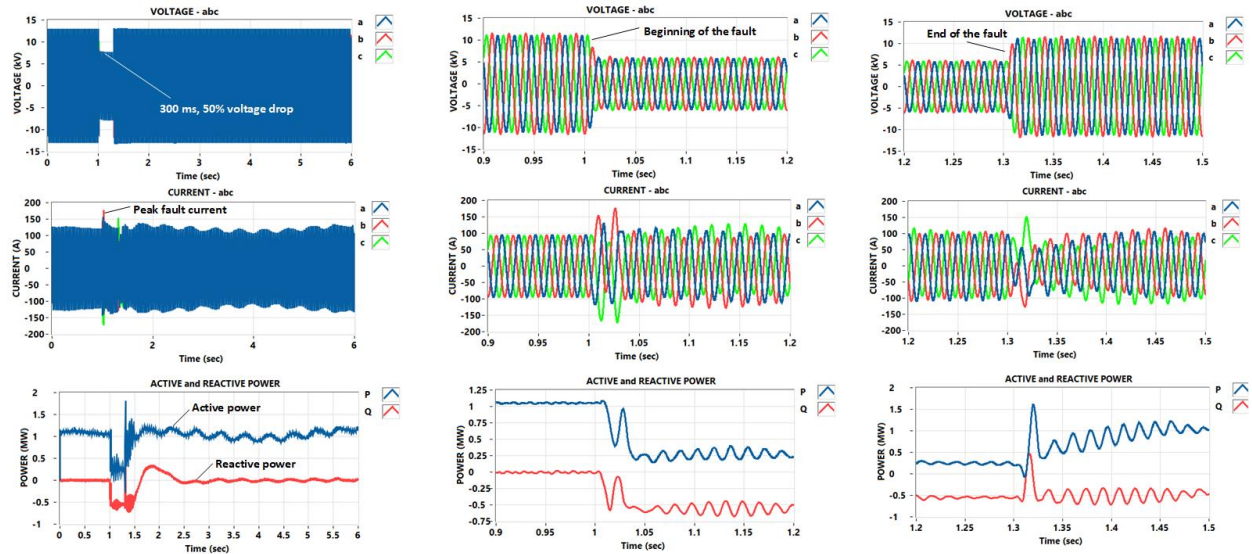


Figure 93. Turbine ride-through during a 300-ms, 50% voltage fault

In both cases, some active and reactive power oscillations can be observed during recovery. If these oscillations become excessive, they may cause dangerous vibrations in turbine components and cause protection tripping to avoid physical damage to the turbine. Examples of such unsuccessful ride-through tests are shown below in Figure 94, Figure 95, and Figure 96. In these cases, the turbine was exposed to the longer and deeper voltage faults of different shapes.

In Figure 94, the turbine was exposed to a 625-ms voltage fault with long post-fault voltage recovery. The turbine was able to ride through the fault. However, turbine protection tripped the turbine shortly after recovery because of excessive vibrations observed in turbine components. A similar situation can be observed in Figure 95 for a 90%, 625-ms fault. In this case as well, the turbine protection disconnects the turbine shortly after the fault to protect it. An extreme ride-through condition is shown in Figure 96 when the turbine was exposed to a 1-s, zero-voltage fault. In this case, the turbine tripped off immediately due to a combination of high currents and excessive vibration.

These examples demonstrate clearly that ride-through performance of utility-scale wind turbines needs to be studied thoroughly for each type of wind turbine used in offshore projects. The testing conducted under this task demonstrated that successful voltage fault ride-through performance of wind turbines depends on several critical factors:

- Standards implemented in turbine ride-through controls
- Parameters and settings of turbine ride-through controller
- Depth, duration, and profile of a fault
- Plant POI characteristics (SCR, strength)

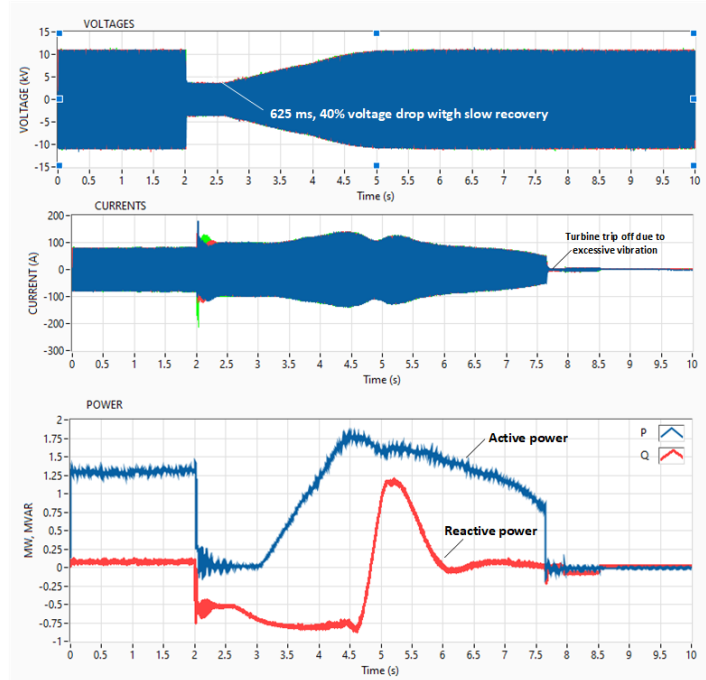


Figure 94. Turbine ride-through during the 40%, 625-ms long-recovery fault and subsequent turbine trip

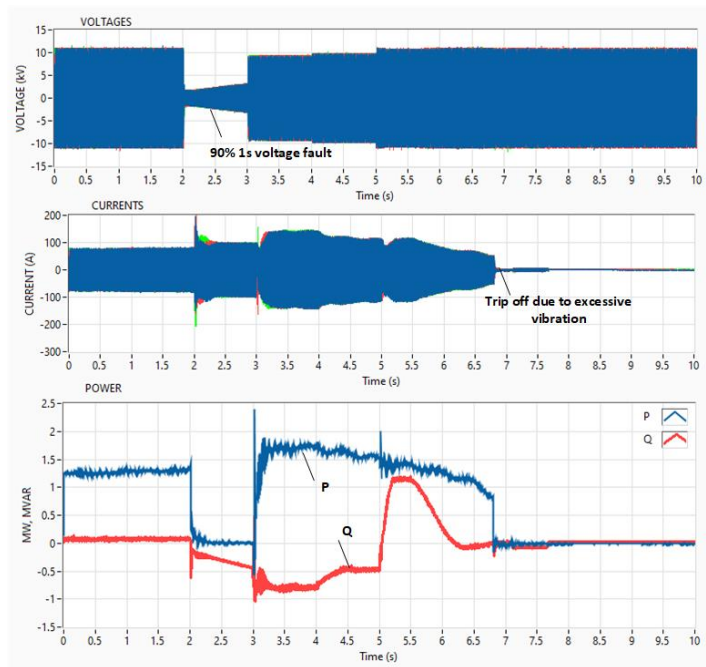


Figure 95. Turbine ride-through during the 90%, 1-s rectangular fault and subsequent turbine trip

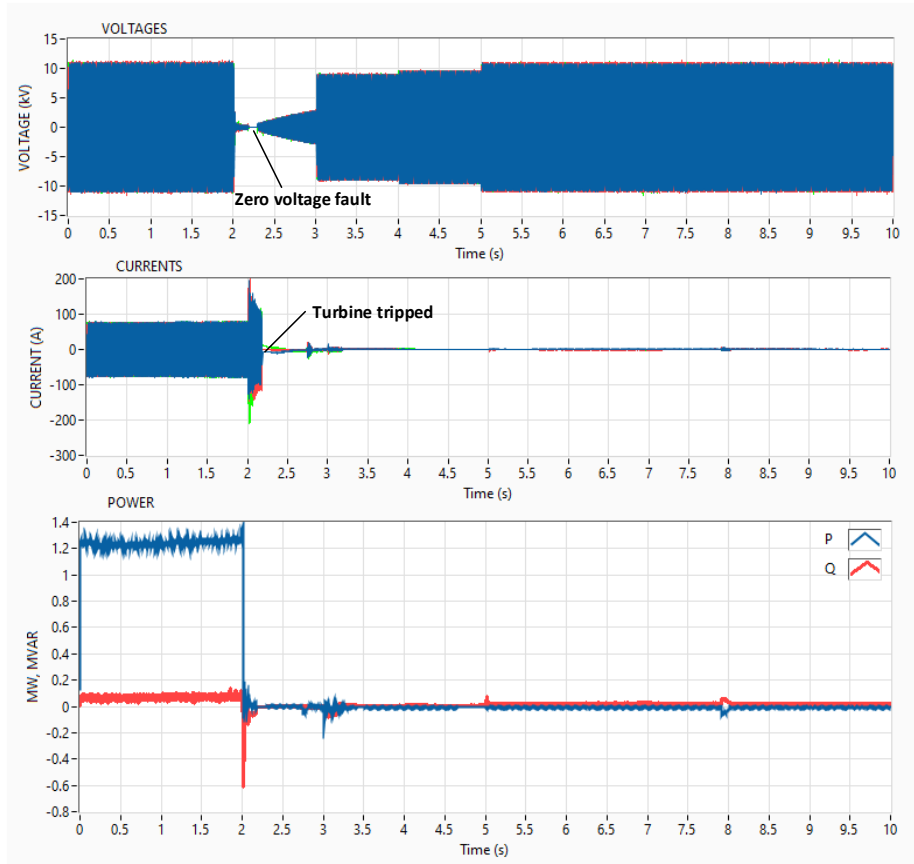


Figure 96. Turbine inability to ride-through zero-voltage fault

7.4 Turbine Response to Frequency Variations

As described in the Task 4 report, HVAC-interconnected onshore WPPs already have controls available to provide all types of reliability services to the grid, including many forms of active and reactive power control for frequency response, frequency regulation, and voltage support. Some subsets of these controls are used by utilities and system operators depending on locations and markets. HVAC-interconnected offshore wind plants can also provide similar types of services. However, for HVDC-interconnected plants, services related to plant response to frequency and voltage conditions at the POI cannot be provided in a traditional way since the DC link introduces full isolation between the offshore plant collector system and the onshore grid. NREL-modeled controls allow HVDC-interconnected offshore plants to provide two frequency responsive services: inertial response and primary frequency response (frequency droop response). In normal operation, the frequency of an offshore HVDC converter is not changing, so controllers of an offshore WPP are unaware of a frequency event that may be happening in the onshore grid. To overcome this limitation, we developed and simulated two types of controls as shown in Figure 97:

- Option 1: Grid frequency is measured at the onshore POI and communicated to the offshore HVDC converter controller in real time. If a grid frequency event is detected (based on frequency deviation from scheduled frequency and rate of change of frequency), the offshore terminal controller will command the offshore AC frequency to change proportionally to the onshore grid frequency. In

this way, the WPP will be exposed to a real frequency event that is the same as the frequency at the POI (with some communication delay).

- Option 2: There is no real physical change of frequency in the offshore collector system. Instead, the measured POI frequency signal is communicated to the offshore WPP controller, which interprets it as a real frequency change and sends set points to individual WPPs. Normally, the inertial response is turbine-level control, so individual turbine controllers will respond to the rate of change of frequency. Primary frequency control is plant-level control, so active power set points proportional to frequency are sent to individual wind turbines.

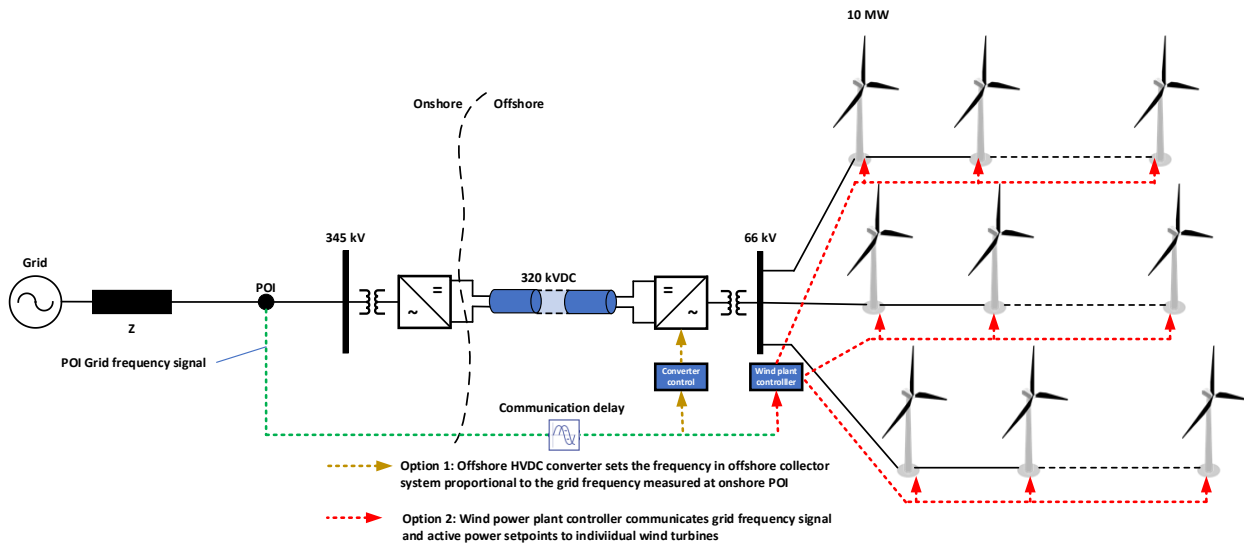


Figure 97. Provision of frequency responsive services by an HVDC-interconnected offshore plant

Examples of tests validating the Option 1 method are shown in Figure 98 and Figure 99 for two cases:

- Wind turbine provides only inertial response (this is a response proportional to the rate of change of frequency)
- Wind turbine provides inertial and primary frequency response (response proportional to the magnitude of frequency fluctuation)

It can be observed in Figure 98 that the turbine’s power increase is proportional to the rate of change of frequency (aggressive low-inertia case is tested at 3 Hz/s rate of change of frequency). The test was conducted at different wind speeds. Frequency steps were emulated by the CGI. After each frequency down-step, the turbine injects extra power to the grid by extracting the inertial energy storage in the wind rotor. This causes the wind turbine rotor to slow down. As a result, there are short periods of small underproduction after each event. This is the “price to pay” for provision of inertial response. It is important to note that inertial response does not require turbine curtailment.

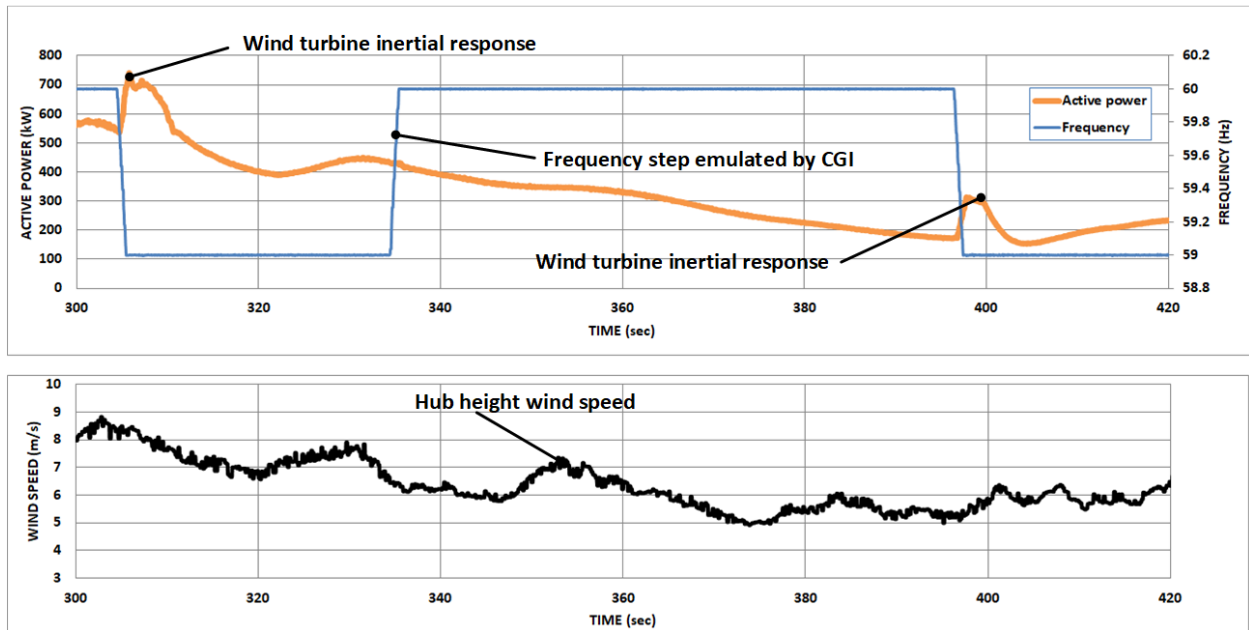


Figure 98. Turbine response: inertial control only

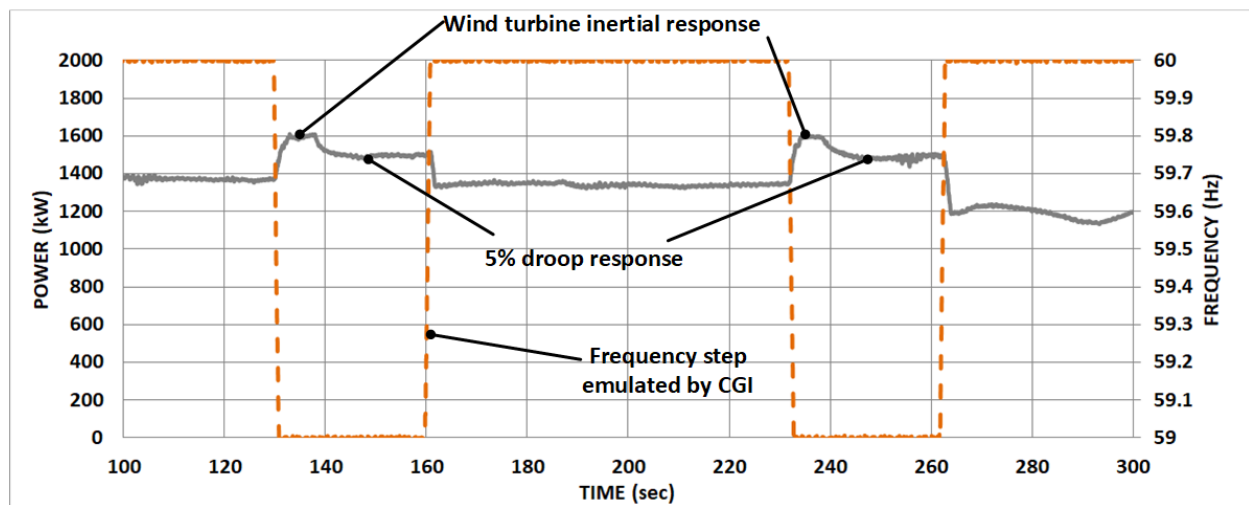


Figure 99. Turbine response: combination of inertial and primary frequency response

Figure 99 shows a more complicated case where the turbine provides both inertial and 5% frequency droop response. In this case, the turbine was operating in curtailed mode with 10% headroom, and the response of the turbine after each frequency drop can be divided into two different stages:

- Inertial response as in previous case (based on ROCOF)
- Droop response: the turbine deploys its reserve power based on 5% droop. After frequency returns to the nominal 60-Hz level, the turbine goes back to a curtailed mode with enough reserves to provide response during next event.

These are unique experiments that can be conducted only at NREL (because of the availability of the CGI). This may have been the first time such experiments have demonstrated that a wind turbine generator isolated from the grid by a power electronics HVDC converter terminal can provide the same type of frequency

response as turbines connected to the grid via an HVAC export line.

7.5 Emulation of HVDC Terminal

NREL developed a real-time model of MMC-HVDC converters and conducted testing on a real-time digital simulator (RTDS) system to demonstrate transient performance of onshore and offshore HVDC converters. RTDS provides an effective measure for the design of HVDC system configuration and engineering commissioning of control/relay devices. All of the major control system manufacturers use the RTDS to test their HVDC and FACTS controls during factory systems testing. The interoperability of devices from different vendors can also be validated using real-time simulation and HVDC replica controls via hardware-in-the-loop testing. At early stages of projects, such replicas are not available and prevent real-time simulation testing from taking place. Systems successfully tested include line commutated converter- and voltage source converter-based HVDC, MMCs, network and industrial STATCOMs, dynamic voltage regulators, and power flow controllers.

This section describes NREL’s efforts on real-time modeling and simulation of HVDC systems at the component level. To achieve the high-fidelity of the HVDC model, three Giga Transceiver System on a Chip (GTSOC) parallel computing units are used. Specifically, the first GTSOC works as the complete converter station with 1024 submodules at each phase, and the second and third GTSOCs work as the converter controller for sending out firing pulses. In this way, we achieved the detailed two-terminal monopole HVDC simulation. Figure 100 shows the simulation setup using RTDS with GTSOC parallel computing units. Due to hardware limits of hardware, one terminal (MMC terminal 1) of HVDC link is simulated in detail and the other terminal (MMC terminal 2) is simulated with average model. Both terminals are simulated with 1024 submodules.

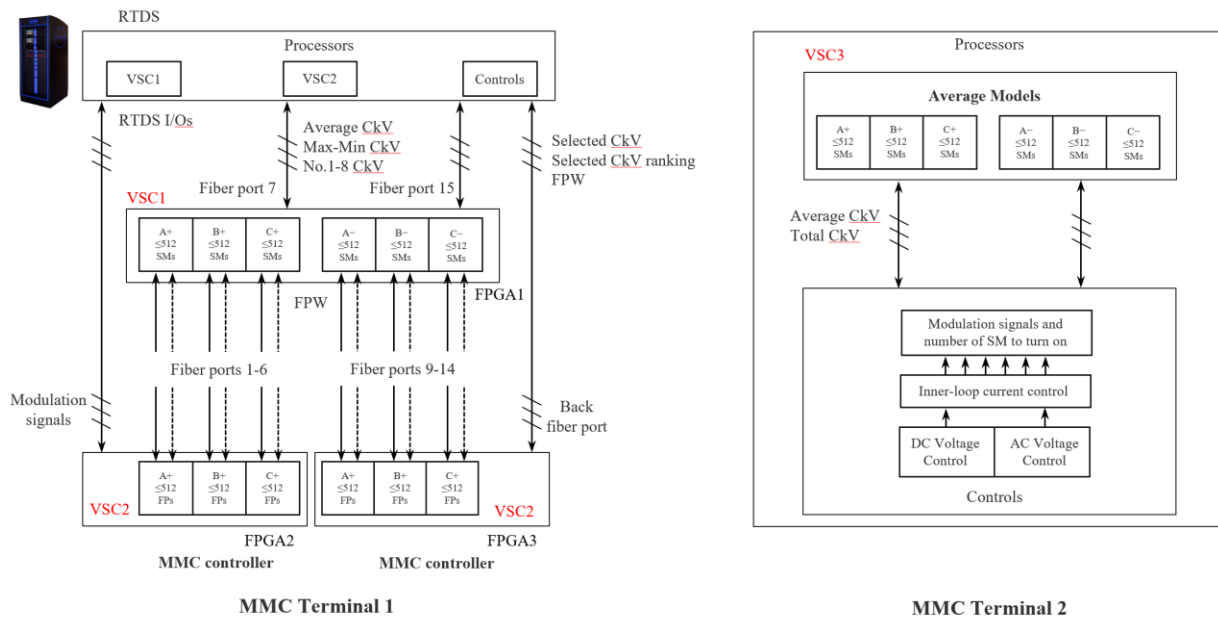


Figure 100. Diagram of MMC-HVDC real-time simulation

The use of GTSOC units enables a more detailed HVDC terminal simulation, where individual capacitor voltage can be selected and monitored in real-time. Firing pulses are generated from GTSOC2 (FPGA2) and GTSOC3 (FPGA3) to feed GTSOC1 (FPGA1) through 12 fiber optic cables, with GTSOC1 working as a converter circuit model. On the other hand, the average MMC model (MMC terminal 2) can only monitor the average capacitor voltage and the total capacitor voltage of all capacitors. The system-level control, including DC/AC voltage control, power flow control, inner-loop current control, is modeled

Figure 102 presents the real-time simulation result when one of the HVDC terminals is exposed to 100 ms of 0pu 3ph AC fault. The model with GTSOC simulation shows the detailed behavior of individual capacitors in the converter valve. In this case, we intend to demonstrate the difference between the detailed real-time model and the average option.

Figure 103 gives the DC voltages during an AC fault at both terminal stations, where the blue trace shows the processor-based average MMC model, and the red trace shows the GTSOC-based detailed MMC model. There is no significant difference regarding DC voltages since the capacitance at the converter station acts as a high pass filter. DC voltage presents slow dynamics; hence, little difference can be observed between detailed and average models in real-time simulation.

Figure 104, on the other hand, shows the difference between the measurable variables in detailed and average model. As discussed, the detailed model can simulate and monitor individual capacitor voltage. This is critical in controller validation and understanding the fault behavior of a MMC-HVDC converter station. The average model simulated in the RTDS processor can only calculate and monitor the average and total voltage of capacitors. Hence, it has limited capability to be used in system fault and transient analysis. The RTDS system at NREL Flatirons Campus for MMC-HVDC real-time simulation is shown in Figure 105.

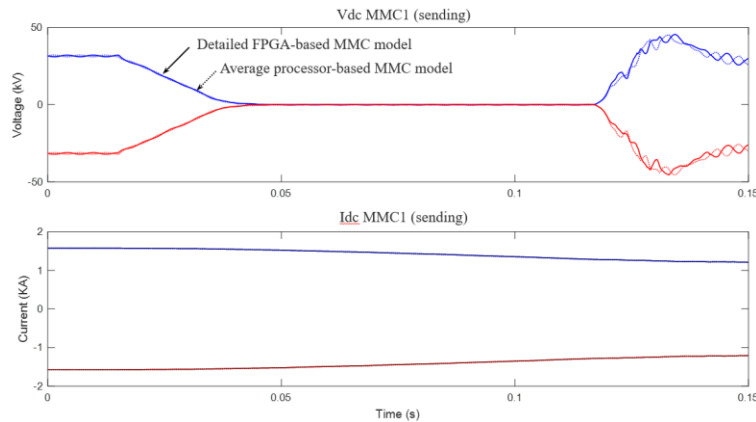


Figure 103. Real-time simulation of MMC-HVDC with AC fault at MMC terminal 1

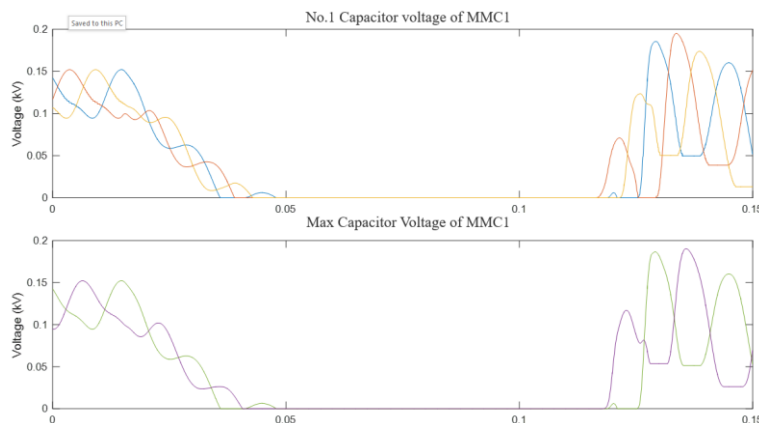


Figure 104. Monitoring of converter capacitor voltages

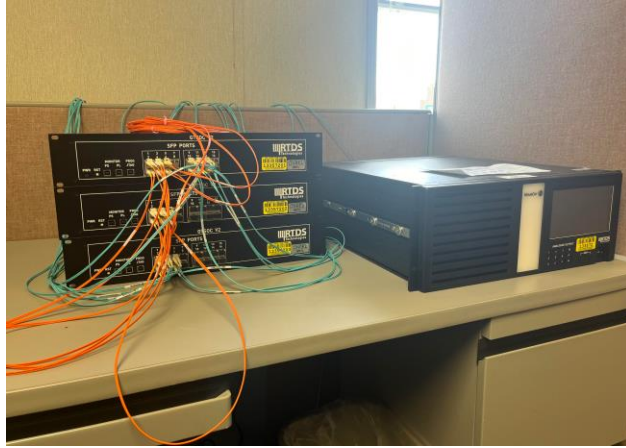


Figure 105. RTDS system at NREL Flatirons Campus for MMC-HVDC real-time simulation

8 Summary and Conclusions

During this project, we developed advanced modeling, control, stability monitoring, and protection methods for the analysis and mitigation of dynamic stability problems in offshore WPPs interconnected with onshore power systems via HVAC or HVDC submarine transmission connected to strong and weak POIs in onshore power grids. The PSS/E-PSCAD co-simulation platform for offshore wind power analysis combined with NREL's GIST platform is instrumental for removing barriers to the reliable integration of large levels of offshore wind power. The tool application was demonstrated for various use cases using offshore WPP POIs in three different interconnections: PJM, NYISO, and ISO-NE. The tool can be used for HVDC- and HVAC-interconnected offshore WPPs and allows for evaluating transient and dynamic behavior.

The NREL team developed a co-simulation platform that combines:

- PSS/E – positive-sequence transmission planning and analysis software by Siemens
- PSCAD – EMT simulation software
- E-TRAN – a software tool to interface positive-sequence phasor models in PSS/E of a large power system, such as the Eastern Interconnection, with the EMT models in PSCAD of power electronics generators, such as offshore WPP with HVAC or HVDC transmission to the grid
- GIST – (PSCAD-based) developed by NREL.

The platform combines the strengths of three commercial software tools (PSS/E, PSCAD, and E-TRAN) and the NREL-developed GIST to accurately represent small-signal stability, dynamic and transient behavior, and instabilities and control interactions that can exist in offshore WPPs, between several WPPs, and between offshore WPPs and the onshore grid. The use of the platform was demonstrated in several cases for three ISOs using models of offshore WPPs with HVAC and HVDC interconnection. POIs with low SCR were selected for the model testing to demonstrate possible instabilities. Simulations conducted in this project are for demonstrating the capabilities of the co-simulation platform only and are not classified as integration studies. The platform can be used later by any stakeholder to conduct detailed integration studies for any offshore project or for studies to identify system-level reliability impacts of clusters of offshore WPPs using different transmission configurations.

The NREL team conducted testing on a utility-scale wind turbine generator installed at NREL's Flatirons Campus to demonstrate the feasibility of some of the controls and transient characteristics that were modeled using the co-simulation platform. The testing was conducted under controlled grid conditions using NREL's multi-megawatt, medium-voltage power electronic grid simulators, also known as the CGI. NREL also developed a model and tested controls of MMC-HVDC converters used in HVDC-interconnected offshore WPPs.

9 References

- [1] P. Denholm, et al. 2024. *Maintaining Grid Reliability: Lessons from Renewable Integration Studies*. Golden, CO: National Renewable Energy Laboratory. NREL/TP-5C00-89166. <https://www.nrel.gov/docs/fy24osti/89166.pdf>.
- [2] A. Bloom, et al. "The Value of Increased HVDC Capacity Between Eastern and Western U.S. Grids: The Interconnections Seam Study." *IEEE Transactions on Power Systems* 37(3): 1760–1769.
- [3] A. Bloom et al. 2016. *Eastern Renewable Generation Integration Study*. Golden, CO: National Renewable Energy Laboratory. NREL/TP-6A20-64472. <https://www.nrel.gov/docs/fy16osti/64472.pdf>.
- [4] V. Gevorgian, Y. Zhang, and E. Ela, "Investigating the Impacts of Wind Generation Participation in Interconnection Frequency Response." *IEEE Transactions on Sustainable Energy* 6 (3): 1004-1012, July 2015.
- [5] N.Y. Department of Public Service, NYSERDA, The Brattle Group, and Pterra Consulting. 2021. *New York Power Grid Study*.
- [6] B. Kroposki et al., "Achieving a 100% Renewable Grid: Operating Electric Power Systems with Extremely High Levels of Variable Renewable Energy." *IEEE Power and Energy Magazine* 15 (2): 61-73, March-April 2017.
- [7] S. Shah. "Small and large signal impedance modeling for stability analysis grid-connected voltage source converters." PhD Thesis, RPI, April 2018.
- [8] S. Shah. "Grid Impedance Scan Tool (GIST)." Presentation at EPRI Subsynchronous Oscillations Workshop, April 2023. <https://www.nrel.gov/docs/fy23osti/86112.pdf>.
- [9] U.S. Department of Energy. *Atlantic Offshore Wind Transmission Study*, March 2024.
- [10] S. Shah, P. Koralewicz, V. Gevorgian, H. Liu, and J. Fu. "Impedance methods for analyzing the stability impacts of inverter-based resources – stability analysis tools for modern power systems." *IEEE Electrification Magazine*, Mar. 2021.
- [11] L. Kocewiak et. al. "Instability mitigation methods in modern converter-based power systems." 20th International Wind Integration Workshop, 29-30 September, Berlin, Germany.
- [12] C. Loutan, V. Gevorgian et al. 2020. *Avangrid renewables Tule Wind Farm: Demonstration of capability to provide essential grid services*." Report by California ISO, Avangrid Renewables, GE, and National Renewable Energy Laboratory, March 2020. <https://www.esig.energy/download/avangrid-renewables-tule-wind-farm-demonstration-of-capability-to-provide-essential-grid-services-march-2020/>.
- [13] J. Peralta, H. Saad, S. Denetiere, J. Mahseredjian, and S. Nguefeu, "Detailed and Averaged Models for a 401-Level MMC–HVDC System." *IEEE Transactions on Power Delivery* 27 (3): 1501-1508, July 2012.
- [14] W. Du et al. "A Comparative Study of Two Widely Used Grid-Forming Droop Controls on Microgrid Small-Signal Stability." *IEEE Journal of Emerging and Selected Topics in Power Electronics* 8 (2): 963-975, June 2020.
- [15] Y. Liu and Z. Chen, "A Flexible Power Control Method of VSC-HVDC Link for the Enhancement of Effective Short-Circuit Ratio in a Hybrid Multi-Infeed HVDC System." *IEEE Transactions on Power Systems* 28 (2): 1568-1581, May 2013. <https://ieeexplore.ieee.org/document/6341872>
- [16] PSCAD Knowledge Base: CIGRE B4-57 working group developed models.
- [17] Q. Tu and Z. Xu. 2010. "Impact of Sampling Frequency on Harmonic Distortion for Modular Multilevel Converter." *IEEE Transactions on Power Delivery* 26 (1): 298-306, <https://ieeexplore.ieee.org/document/5673482>.